Master's Thesis

석사 학위논문

Fabrication and characterization of 2 dimensional biodegradable microrobot with 5 Fluorouracil for targeted drug delivery

Sanghun Jeon (전 상 훈 田 尙 焄)

Department of

Robotics Engineering

DGIST

2017

Master's Thesis

석사 학위논문

Fabrication and characterization of 2 dimensional biodegradable microrobot with 5 Fluorouracil for targeted drug delivery

Sanghun Jeon (전 상 훈 田 尙 焄)

Department of

Robotics Engineering

DGIST

2017

Fabrication and characterization of 2 dimensional biodegradable microrobot with 5 Fluorouracil for targeted drug delivery

Advisor: Professor Hongsoo Choi

Co-advisor: Professor Jae Eun Jang

by

Sanghun Jeon

Department of Robotics Engineering

DGIST

A thesis submitted to the faculty of DGIST in partial fulfillment of the requirements for the degree of Master of Science in the Department of Robotics Engineering. The study was conducted in accordance with Code of Research Ethics[1]

01. 06. 2017

Approved by

Professor Hongsoo Choi (Signature)
(Advisor)

Professor Jae Eun Jang (Signature)
(Co-Advisor)

[1] Declaration of Ethical Conduct in Research**:** I, as a graduate student of DGIST, hereby declare that I have not committed any acts that may damage the credibility of my research. These include, but are not limited to: falsification, thesis written by someone else, distortion of research findings or plagiarism. I affirm that my thesis contains honest conclusions based on my own careful research under the guidance of my thesis advisor.

Fabrication and characterization of 2 dimensional biodegradable microrobot with 5 Fluorouracil for targeted drug delivery

Sanghun Jeon

Accepted in partial fulfillment of the requirements for the degree of

Master of Science.

11. 28. 2016

Head of Committee Prof. Hongsoo Choi (인)

Committee Member Prof. Jae Eun Jang (인)

Committee Member Prof. Jonghyun Kim (인)

MS/RT

201523007

전 상 훈. Sanghun Jeon. Fabrication and characterization of 2 dimensional biodegradable microrobot with 5 Fluorouracil for targeted drug delivery. Department of Robotics Engineering. 2017. 110p. Advisors Prof. Choi, Hongsoo, Co-Advisors Prof. Jang, Jae Eun.

ABSTRACT

Microrobots for biomedical applications have various advantages such as minimally invasive surgery, targeted delivery of drug or biological compounds to specific area, as well as transportation energies, for example, thermal energy by hyperthermia treatment in comparison to a conventional invasive surgery. For such targeted therapeutics with microrobots, it is crucial not only to accurately control them but also to make them biocompatible to use in an *in-vivo* environment. In terms of the biocompatibility, biodegradable material has emerged as a promising material because it naturally biodegrades into harmless substances in aqueous environment therefore the microrobot does not need to be retrieved from the body.

In this thesis, we developed 2 dimensional biodegradable microrobot for targeted drug delivery that consists of poly (D,L-lactide-co-glycolide acid) (PLGA), magnetic particles (Fe particles) (average size < 10 μm) and a drug compound, 5 Fluorouracil (5-FU). The microrobot was fabricated with various 2 dimensional shapes of water-dissoluble PVA templates cut by using UV laser micro machining. Most biomedical microrobots that uses

photo-curable reagent to polymerize and form microrobot structure under UV require post-process to load drugs because drugs can be denatured by UV. In contrast, the developed biodegradable microrobot allows simultaneous encapsulation of anticancer drug (5-FU) without additional drug loading procedure, forming a microrobot structure in PLGA/Fe/5-FU solution.

Translational and rotational motion of the developed 2 dimensional biodegradable microrobot were remotely and accurately controlled by external magnetic field (constant magnetic field (**B**) to Z axis and magnetic field gradient (∇**B**) to X axis) manipulated using an electromagnetic actuation (EMA) system. The fastest translational velocity of fabricated microrobot with 60 % (w/v) of magnetic particles was approximately 2.8 mm/s (≈1/5 body length per second). They have successfully loaded and released approximately 0.013 μg/microrobot of anticancer drug (5-FU) in aqueous environment (around pH 7, 37 ˚C) by biodegrading itself for 6 weeks.

In conclusion, the facile fabrication was developed to form 2 dimensional biodegradable microrobot with various shapes using UV laser micro machining, encapsulating drugs into the microrobot simultaneously. The 2 dimensional biodegradable microrobot was successfully controlled by using electromagnetic actuation (EMA) system and released drugs for 6 weeks by biodegrading itself.

Keywords: Targeted drug delivery, Biodegradable microrobot, Electromagnetic actuation system, UV Laser micro machining, Poly (D,L-lactic-co-glycolic acid)

CONTENTS

List of figures

List of tables

1. INTRODUCTION

1.1 Background

In the last decade, advances in the development of medical science and technology have increased the human lifespan and quality of life. However, increasing the human lifespan and quality of life, several intractable diseases such as tumor increased approximately 10 years from Division of Cancer Control and Population Sciences and National Cancer Institute Figure 1.1. Incurable diseases from stress, less exercise and eating habits could cause the death and aftermath, increasing the cost of treatment and therapy. Therefore, many researchers in medical science and technology have been studying for therapies of the incurable diseases. But exact therapies for healing are still lack and bring low therapeutic efficiency of the existing clinical therapies. As a results of excessive administration of the drug and low therapeutic efficiency from the existing clinical therapies, the situations caused without a solution to overcome issues and expected to remain largely unchanged approximately 10 years Figure 1.2[11, 31, 32, 35-46].

In recent, to overcome this phenomenon, many research groups studying therapies of intractable diseases have gradually been developed to improve the efficiency of therapies and reduce the amount of taking medicine. In addition, therapeutic using functionalized drug delivery mechanism methods have emerged as a promising and outstanding treatment to a tumor, together. The advantages of localized drug delivery system introduced that they can be possible to reduce side or toxic effects to normal cell and transport drug to a specific area such as tumor.

However, in general localized drug delivery mechanisms using micro- and nano-technology, microrobot[3, 4, 22-27, 33, 34, 47-63] or micro- and nano-particles[1, 2, 5-8, 12-21, 28, 30, 56, 63-100], have several considerations that hide practical limitations to be applied in the human body.

Firstly in the case of the microrobot, they are fabricated with photo-sensitive material by photo lithography and deposited by electron beam evaporation or sputtering to cover titanium (Ti) to improve biocompatibility and nickel (Ni) to be controlled by an external magnetic field on the surface[3, 4, 25, 27, 34, 51, 53, 55, 59, 60]. These materials such as photo-sensitive material and nickel (Ni) were known as a toxic property to normal cell and living organisms as well as not biocompatible and biodegradation in vivo. Therefore, these materials and fabrication procedures could cause potential hazards to *in vivo* test to be applied in the human body.

Secondly the micro- and nano-particles are commonly fabricated by emulsion method which is a mixture of liquids of other properties of hydrophilic and hydrophobic, mixing the drug for therapy[2, 14, 64-80, 101]. The fabrications of the micro- and nano-particles by emulsion method are simple and save time in terms of others fabrication procedures for targeted drug delivery. However, although the fabrication has some advantages, they show that the micro- and nano-particles cannot consist of uniform size, which affects drug release time and degradation, and fabricate various shape excluding spherical type due to emulsion property[83]. Also a larger number of spherical shapes can occur low efficiency because of a lot of loss from injecting process and blood circulation after injection. It is difficult to specific and delicate control in the human body under fluid flow condition.

Consequently, exacting technology of the microrobot and small particles shows some issues to be solved to improve the efficiency of therapies. In this thesis, I will introduce the facile fabrication and precise control using an external magnetic field to reduce loss of small particles and solve no degraded issue from the microrobot by applying biodegradable polymer and magnetic particles, together.

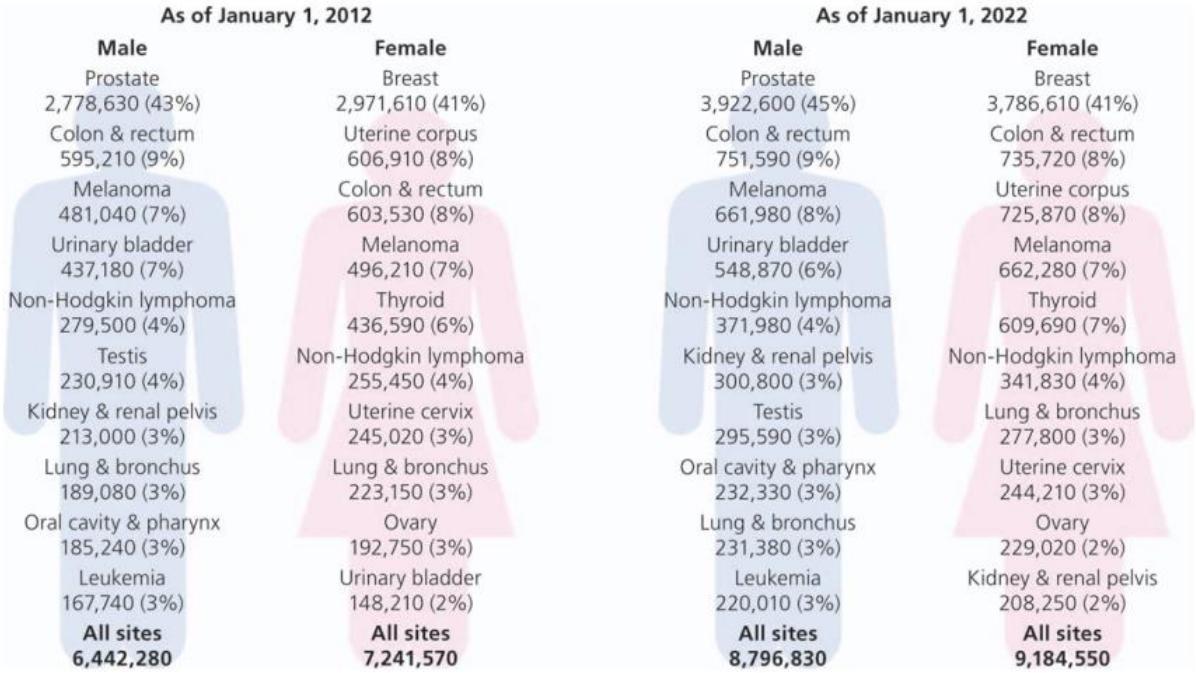

Figure 1.1 Statistics of estimated number of United States cancer survivors by site from Data Modeling Branch, Division of Cancer Control and Population Sciences and National Cancer Institute[32].

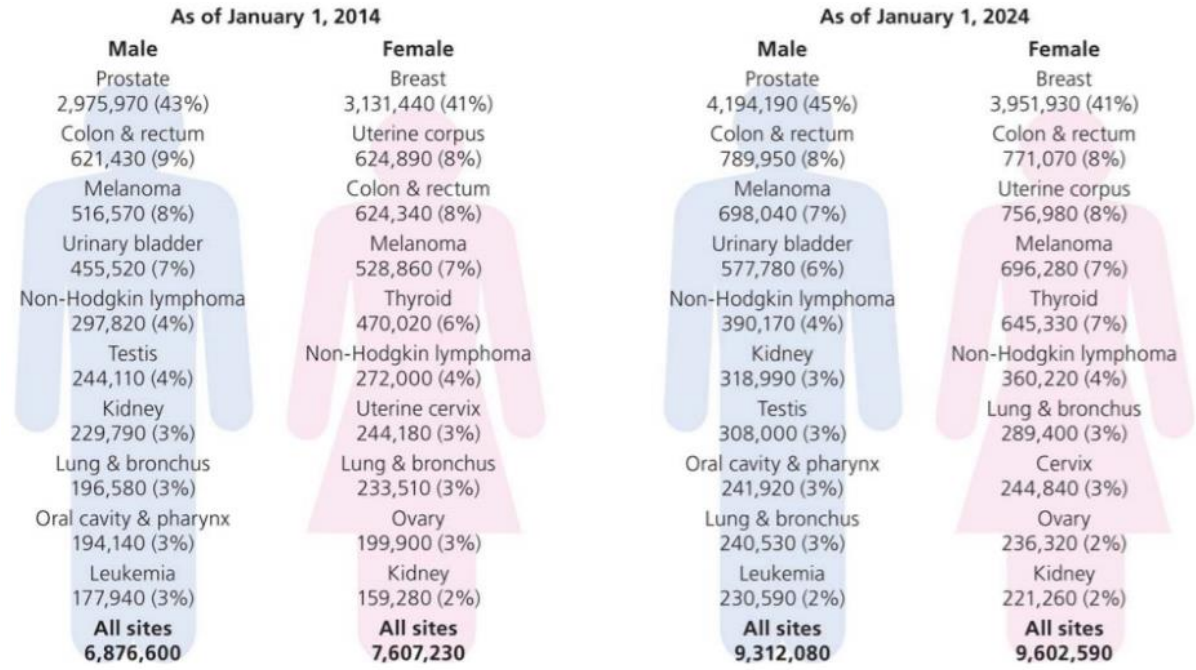

Figure 1.2 Statistics of estimated number of United States cancer survivors by site from Data Modeling Branch, Division of Cancer Control and Population Sciences and National Cancer Institute[31].

1.2 Trend of research for targeted drug delivery

1.2.1 Trend of the microrobot

In recent, the studies to develop magnetically actuated microrobot showed the potential to be used for specific biomedical application such as targeted drug delivery, hyperthermia and sensing to a specific area, also simple diagnosis using minimally invasive therapy to *in vivo*[22, 25, 27, 47-50, 53, 54, 63, 102]. They could be controlled and steered using wirelessly acoustic or external magnetic field which infect harmless to the human body and other living organisms. Therefore, one of the main advantages of the microrobot are that they can be navigated in various aqueous environment such as water or blood having high viscosity. They also are consisted of various biocompatible materials such as titanium (Ti) by deposition to reduce side effects and toxic to normal cell and other living organisms.

1.2.1.1 Bradley J. Nelson group

B. J. Nelson et al. have developed a variety of the functionalized microrobots having different type inspired by mimicking a bacterial flagella or nature for biomedical applications such as targeted drug delivery, single cell delivery and localized therapy[3, 55]. Figure 1.3-(a) shows that the functionalized surface on the microrobot by photo lithography was fabricated for releasing their encapsulated fluorescent materials insisted of drug to single cell, C2C12 cell. The functionalized microrobot was controlled by an external magnetic field using electromagnetic actuation system. They also were particularly used with temperature-sensitive materials, dipalmitoylphosphatidylcholine and 1-myristoyl-2-stearoyl-sn-glycero-3-phosphocholine, to release their encapsulated fluorescent materials insisted of anticancer drug in specific environments when the temperature increase Figure 1.3-(b)[4]. As a result of experiment while increasing the temperature, the functionalized microrobot is feasible to release fluorescent materials, rhodamine B of hydrophilic and calcein disodium of hydrophobic.

The functionalized microrobot also could transport fluorescent materials to single cell, C2C12, using an external magnetic field shown in Figure 1.3-(c). Therefore, this research indicated that they can perform accurate swimming and deliver drug or micro-object in targeted single cell or specific area.

For precise transportation with particles to targeted area, this group also have developed functionalized and schematic design consisting of the micro body and a micro grasping holder by photo lithography Figure 1.3-(a)[34, 51, 53, 56, 60]. A micro grasping holder could grasp micro objects and transport to specific area by an external magnetic field using electromagnetic actuation system. As a result of functionalized design to grasp micro objects, the microrobot has improved functions and high efficiency in terms of transportation Figure 1.3-(b).

In recent to overcome re-collection of the microrobot, this group have demonstrated that the microrobot made of iron oxide magnetite (Fe_3O_4) nanoparticles to control by an external magnetic field and release through metabolic paths such as kidney[62, 63]. A high-stealth poly (ethyleneglycol) diacrylate and pentaerythritol triacrylate could be degraded and indurated [33]. Figure 1.4-(c) shows the biodegradable microrobot consisted of poly (ethyleneglycol) diacrylate and pentaerythritol triacrylate. A poly (ethyleneglycol) diacrylate is possible to decompose in the water and NaOH. Figure 1.4-(d) also shows that the biodegradable microrobot was controlled by an external magnetic field to a targeted pocket.

Consequently, Bradley J. Nelson group have gradually developed the functionalized and special microrobot and design to by mimicking a bacterial flagella or nature for therapies. The microrobot also can be precisely controlled by an external magnetic field using electromagnetic actuation system.

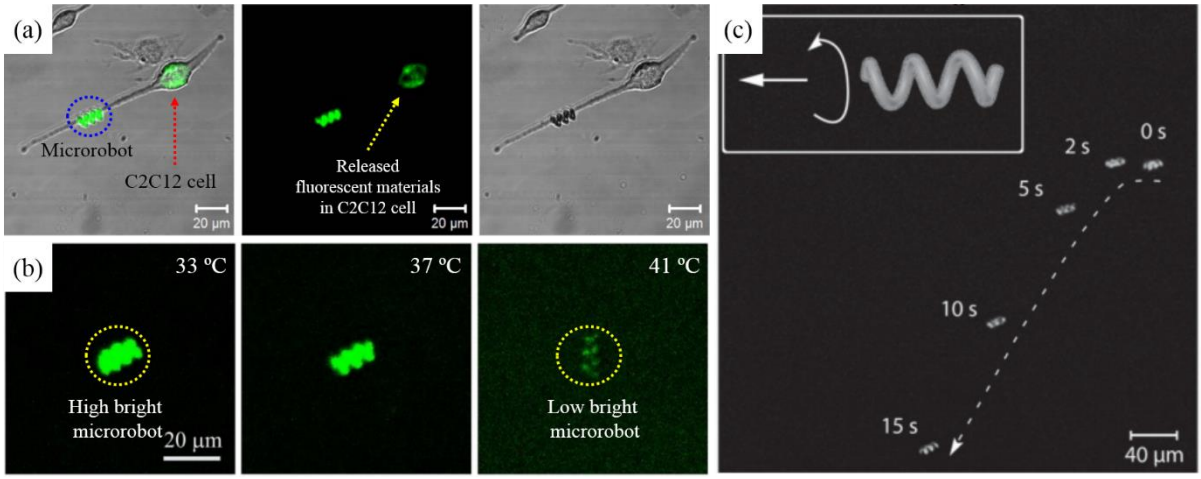

Figure 1.3 Functionalized microrobots of Bradley J. Nelson group[3, 4]. (a) Microrobot by mimicking bacterial flagella to a single cell, C2C12, for targeted drug delivery[3]. (b) Microrobot with temperature-sensitive material for controlled release for targeted drug delivery[4]. (c) Swimming microrobot to single cells, C2C12, by an external magnetic field using electromagnetic actuation system[3].

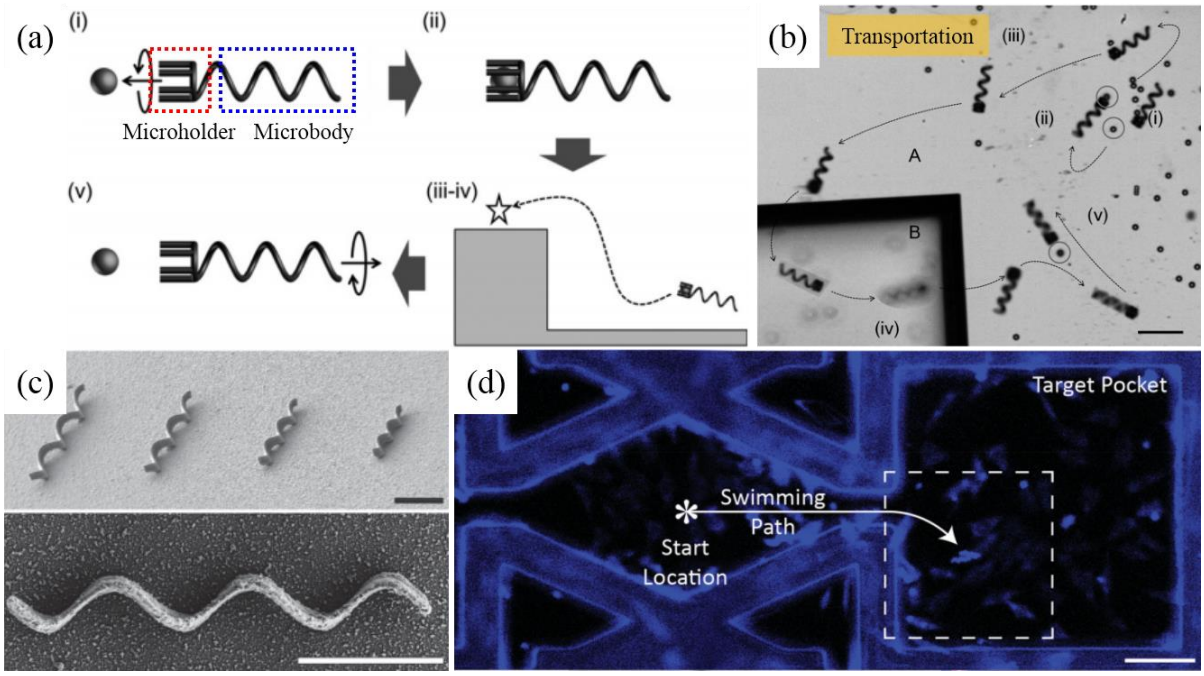

Figure 1.4 Functionalized microrobots of Bradley J. Nelson group[33, 34]. (a) Transportation process by a helical micro grasping holder and micro body[34]. (b) Time-lapsed image of the loading and releasing motion of functionalized microrobot; the scale bar is 50 μm[34]. (c) Scanning electron microscope (SEM) images of helical micro patterns with biodegradable hydrogel ranging from 1.5 and 3.0 μm and lengths ranging from 14 and 28 μm[33]. (d) Fluorescence image of the micro channel to conduct experimental control, the functionalized microrobots are placed in a targeted pocket and control into the container by an external magnetic field using electromagnetic actuation system; the scale bar is 100 μm[33].

1.2.1.2 Joseph Wang group

Joseph Wang group have showed that the helical microswimmers which can be controlled by an external magnetic field using electromagnetic actuation system extracting based on vascular plants from nature described as Figure 1.5-(a)[24, 26]. The microswimmer was fabricated by coating spiral vessel plant fibers Figure 1.5-(d) with a thin magnetic and biocompatible layer, titanium (Ti) and nickel (Ni) to be wirelessly controlled by an external magnetic field Figure 1.5-(c). They were moved by external magnetic field using three orthogonal Helmholtz coils system which can create translational and rotational motion in aqueous environments. According to the frequency from the three orthogonal Helmholtz coils system, the microswimmers could be moved such as a wobbling, rotating and translational motion Figure 1.5-(d). In contrast of Bradley J. Nelson group, Joseph Wang group has demonstrated the microswimmer by mimicking spiral vessel plant fibers form nature.

This group also has demonstrated artificial functionalized microfish with iron oxide and platinum nanoparticles using 3 dimensional (3D) optical printing process which can be easily applied to biomimetic microrobot with optimized and designed functions described as Figure 1.6-(a). They were composed of poly (ethylene glycol) diacrylate (PEGDA) based hydrogels and diverse functional nanoparticles with iron oxide (Fe3O4) for magnetic actuation, platinum (Pt) nanoparticles for mediated propulsion and PDA nanoparticles to reduce toxicity. Figure 1.6-(b) shows scanning electron microscope (SEM) image of diverse artificial microfish shapes. Figure 1.6-(c) has demonstrated artificial microfish motion encapsulated Pt nanoparticle to improve efficient propulsion. Consequently, it is feasible to fabricate various microrobot by mimicking vessel plant fibers and fish from nature to be applied for biomedical applications.

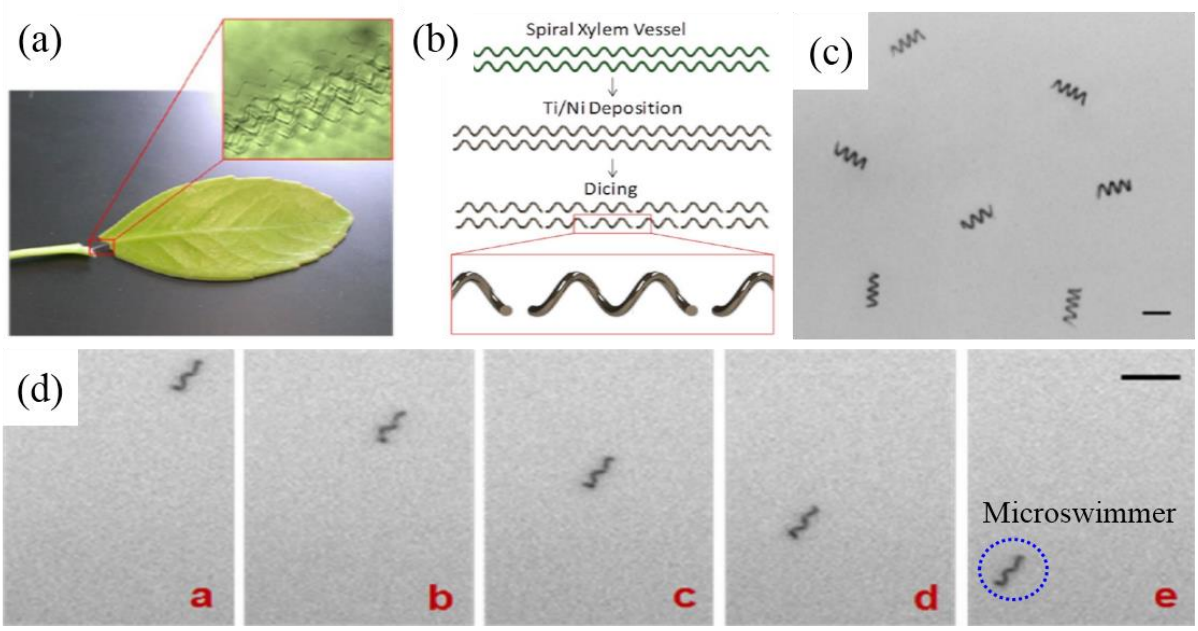

Figure 1.5 Microswimmer of Joseph Wang group[24]. (a) Image by mimicking vessel plant fibers. (b) Fabrication procedure of microswimmer from vessel plant fibers[24]. (c) Optical microscope image of microswimmer; Scale bar, 50 μm[24]. (d) Motion of microswimmer using an external magnetic field, this scale. bar is 50 μm[24].

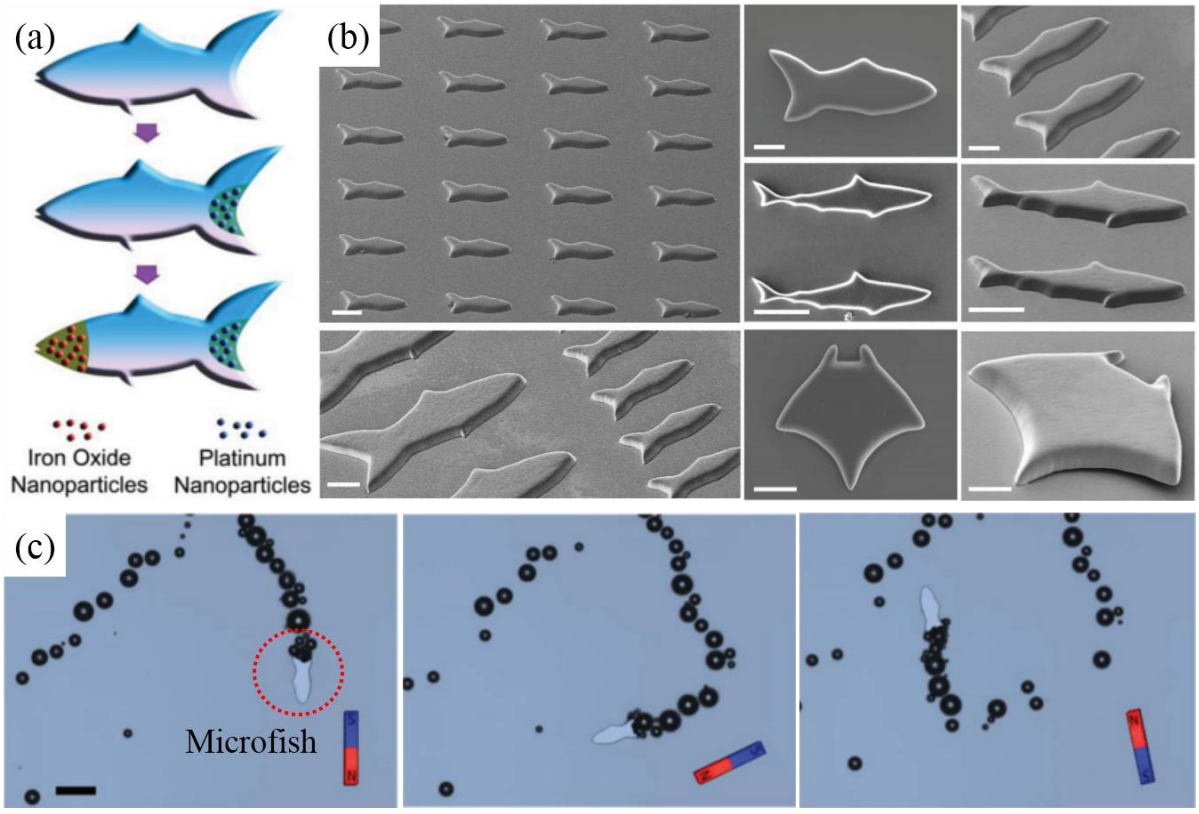

Figure 1.6 Artificial microfish of Joseph Wang group[26]. (a) Schematic design of the artificial functionalized microfish with iron oxide and platinum nanoparticles[26]. (b) Scanning electron microscope (SEM) images of uniform array of the artificial functionalized microfish; Scale bar, 50 μm[26]. (d) Time-lapsed images of the artificial functionalized microfish movement by rotating a nearby magnet[26].

1.2.1.3 Jong-Oh Park group

From Jong-Oh Park group, the 2 dimensional (2D) soft microrobot based on pH-responsive hydrogel, 2-hydroxyethyl methacrylate and poly (ethylene glycol) acrylate and iron oxide nanoparticles (Fe3O4), have been developed by UV light. The developed soft microrobot could change shape such as folding and unfolding motions from changed pH environments and then the soft microrobot of changed shape was controlled by an external magnetic field using electromagnetic actuation system such as schematic design, loading anticancer drug Figure 1.7-(a). It is feasible to grasp and transport microbead loading anticancer drug from changed pH environments Figure 1.7-(b). Figure 1.7-(c) shows that the soft microrobt loading microbead was controlled by electromagnetic actuation system in the micro chamber and then the microbead was released from the soft microrobot when degree of pH increase Figure 1.7-(c).

This group also have demonstrated macrophage based on microrobot to attack a tumor. The fabricated microrobot was consisted of iron oxide (Fe_3O_4) NPs with docetaxel (DTX) encapsulated poly (lactic-co-glycolic acid) (PLGA) nanoparticles. The PLGA-DTX-Fe_3O_4 nanoparticles were fabricated using a single emulsion method with an average size of 300 nm. Figure 1.8-(a) shows the fabricated macrophages (green) loading PLGA-DTX-Fe_3O_4 nanoparticles under a confocal microscope. And then the fabricated macrophages was evaluated using electromagnetic actuation system in chamber Figure 1.8-(b).

Consequently, Jong-Oh Park group have developed responsive microrobot from changed pH and functionalized nanoparticles with anticancer drug, docetaxel, by using macrophage to attack a tumor. As a result of these researches, this group shows possibility of therapies to a specific area[22, 23, 48].

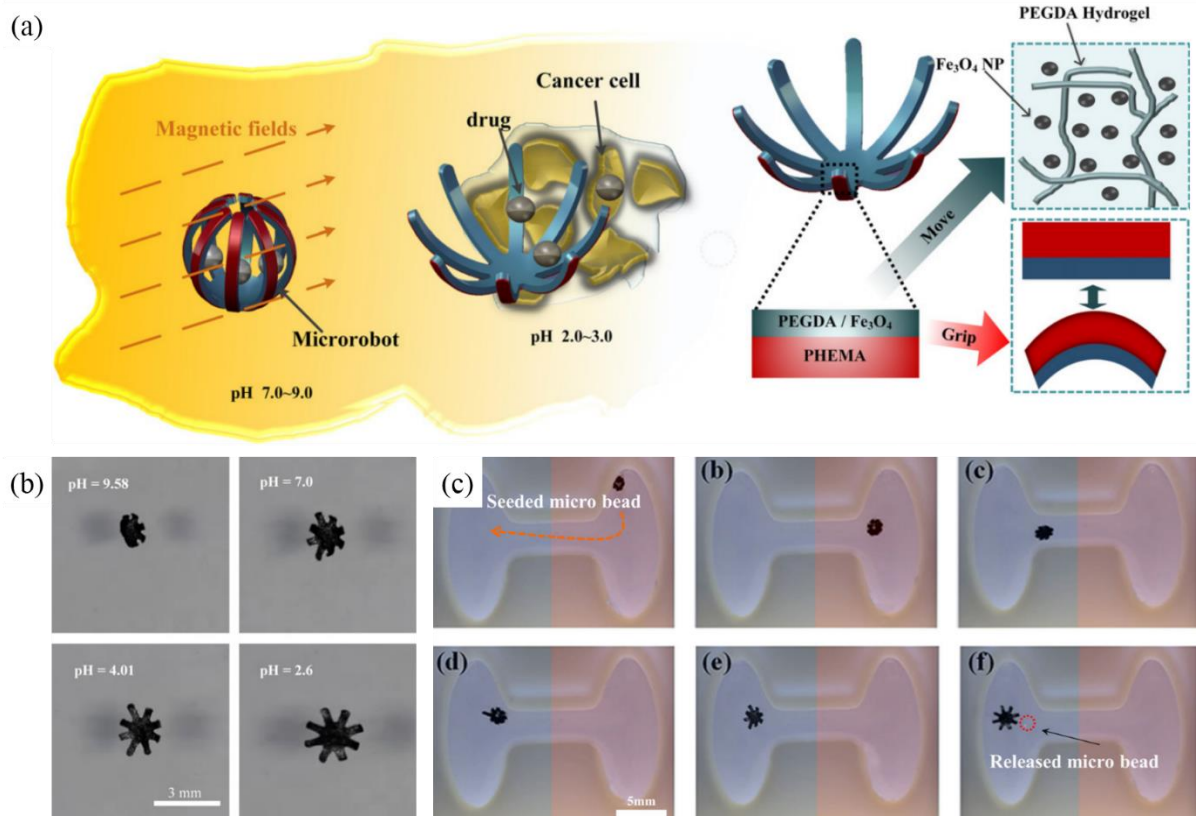

Figure 1.7 Microrobot of Jong-Oh Park group[23]. (a) Schematic design of soft microrobot grasping microbead of anticancer drug based on pH-responsive[23]. (b) Folding and unfolding motions of the microrobot from changed pH, Scale bar; 3.0 mm[23]. (c) Experiment for movement of the pH-sensitive soft microrobot, Blue color is low pH and red color is high pH[23].

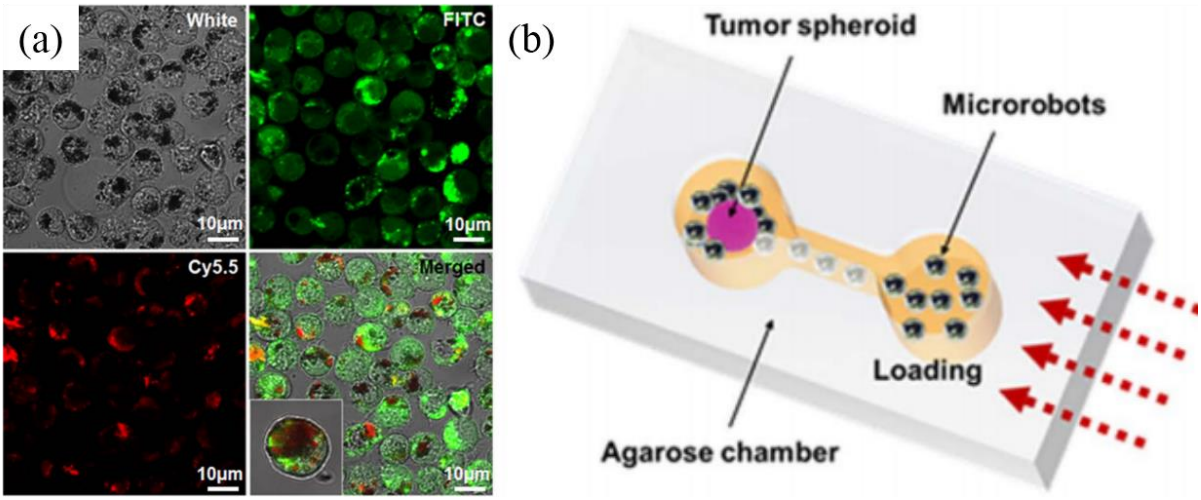

Figure 1.8 Microrobot of Jong-Oh Park group[22]. (a) Intracellular fluorescence from macrophages loading PLGA-DTX-Fe_3O_4 nanoparticles by confocal microscopy, Scale bar; 10 μm[22]. (b) Chamber to conduct imitating experiment of using macrophage loading PLGA-DTX-Fe_3O_4 nanoparticles[22].

1.2.1.4 My group

For targeted drug delivery or 3 dimensional cell culture from the microrobot of scaffold type, Hongsoo Choi group have demonstrated a diverse scaffold-types of magnetically actuated 3 dimensional (3D) microrobot Figure 1.9-(a). The magnetically actuated 3 dimensional (3D) microrobot was fabricated with photo-sensitive material to make microstructure by photo lithography, titanium (Ti) layer to improve biocompatibility and Nickel (Ni) layer for magnetic actuation. It can culture cell from 3 dimensional (3D) microstructure of scaffold and then transport cultured cell to a specific area such as Figure 1.9-(b). Figure 1.9-(c) and (f) show translational and rotational motions of 3 dimensional (3D) microrobot by an external magnetic field using electromagnetic actuation system.

In recent magnetically actuated microrobots from Hongsoo Choi group inspired by nonreciprocal ciliary motion of paramecium also were developed to improve transportation of microobjects described as Figure 1.10-(a) (top view) and (b) (side view). It showed feasible that the cilia microrobot by mimicking paramecium can improve efficiency of transportation micro-objects to a specific area for biomedical applications Figure 1.10-(c) and (f). The result shows that the cilia microrobot was faster translational velocity than 3 dimensional (3D) microrobot in aqueous environments.

Consequently, as described above four groups, the studies to develop the microrobot have many advantages for promptly targeted drug delivery to a specific area, closely 3 dimensional (3D) cell culture and minimally invasive therapies to *in vivo*. In addition functional smart material was used to be applied to develop the functionalized microrobot[25, 27, 58, 102].

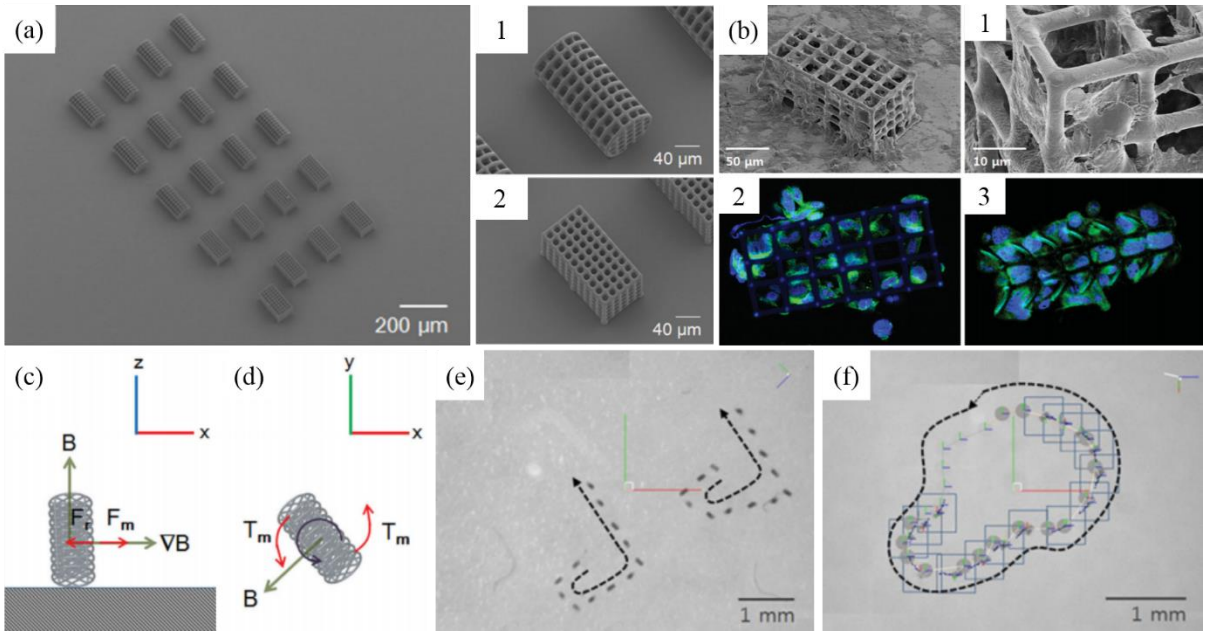

Figure 1.9 Microrobots of Hongsoo Choi group[27]. (a) Scanning electron microscopy image of the scaffold type microrobots. (a-1) a cylindrical-type microrobot[27]. (a-2) a hexahedral-type microrobot[27]. (b, b-1) Scanning electron microscopy image of cylindrical and hexahedral-type microrobot after cell culture[27]. (b-2, b-3) Confocal fluorescence images of cylindrical and hexahedral-type microrobot after cell culture[27]. (c) and (d) Schematic design of Translational and rotational motion from the scaffold type microrobots[27]. (e) and (f) Rolling motion and targeted control motion of the scaffold type microrobots[27].

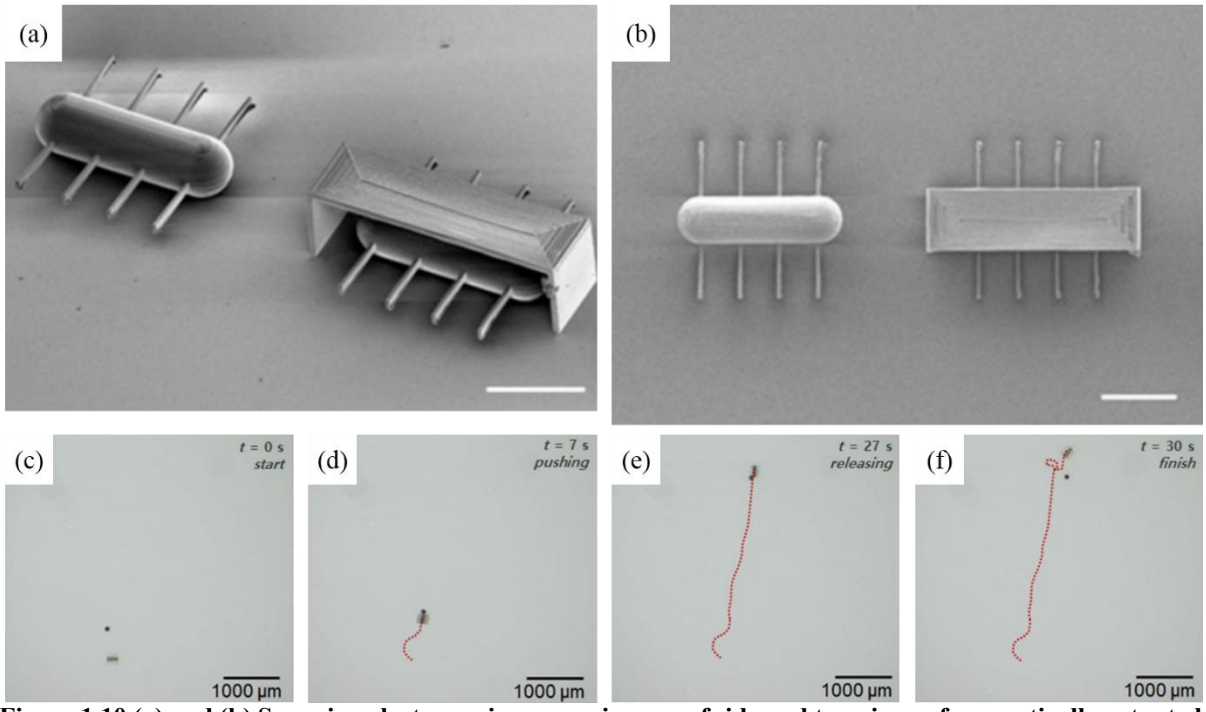

Figure 1.10 (a) and (b) Scanning electron microscopy images of side and top views of magnetically actuated cilia microrobots by mimicking paramecium[25]. (c) The cilia microrobot stared to transport the micro-particles[25]. (d) The cilia microrobot pushed the micro-particles using an external magnetic field[25]. (e) The cilia microrobot transported the micro-particles from (d)[25]. (f) The cilia microrobot released the micro-particles[25].

1.2.2. Trend of the micro- and nano-particle

The researches to develop functional micro- and nano-particles mixed various anticancer drugs have gradually been demonstrated for biomedical application such as specific targeted drug delivery to a tumor[14, 65, 71, 72]. This technology shows one of the many advantages which can attack a targeted tumor, reducing injuries of normal cell and living organisms from extra anticancer drugs. In addition, as another advantages of micro- and nano particles, the functional micro- and nano-particles consisted of biodegradable polymer and anticancer drug can be decomposed and released over time[103-109]. As a results advances in the development from micro- and nano-technology, the targeted drug delivery system has been emerged as a promising therapy for healing of intractable diseases such as tumor[1, 72, 110-127].

In the last decade, the functional micro- and nano-particles were fabricated by general emulsion method[1, 2, 14, 28, 83, 91]. It is feasible to make micro- and nano-particles with various drugs from others properties, hydrophobic and hydrophilic property[28, 73, 77, 128]. This method has been widely used to overcome several issues, released time of drug, half-life of the drugs and degradation time of polymer. In order to improve efficiency with release time and half-life of drug, multiple layers have been devised with anticancer drug using multiple emulsion methods Figure 1.11.

However, in recent, the methods to make functional micro- and nano-particles occurred consistently some issues, uniform size, and low efficiency from loss of small particles in the injecting process and precise control from a lot of small particles in flow fluid. From issues, to improve efficiency of uniform particles in fabricating process by emulsion method, the hydrogel template process with gelatin and degraded material was developed from other groups. It was feasible to fabricate uniform micro- and nano-particles from the hydrogel template process on the silicon wafer or polydimethylsiloxane molds[74]. The hydrogel template process

could be decomposed in the warm water for a short time and not affect the micro- and nano-particles Figure 1.12. Using hydrogel template process has some advantages which can improve the high efficiency of uniform particles and various shape. However, using hydrogel template process still cannot overcome loss of small particles in inserting process.

To minimize loss of small particles in inserting process, another group has developed functional polymer by applying phase-transformation of the micro- and nano-particles in mouse Figure 1.13-(a). Figure 1.13-(b) and (c) showed that the polymer with transformed-responsive polymer could be agglomerated and then collect the micro- and nano-particles to a tumor in the mouse body. Using phase-transformation could improve efficiency of the micro- and nano-particles because loss of small particles was reduced.

Consequently, as described above trend of the micro- and nano-particles like the microrobot, the studies to develop the functional drug delivery shows possibility for targeted drug delivery of biomedical application. This chapter introduces recent trends such as functional microrobot and small particles and then advantages and disadvantages to be applied for targeted drug delivery of biomedical application.

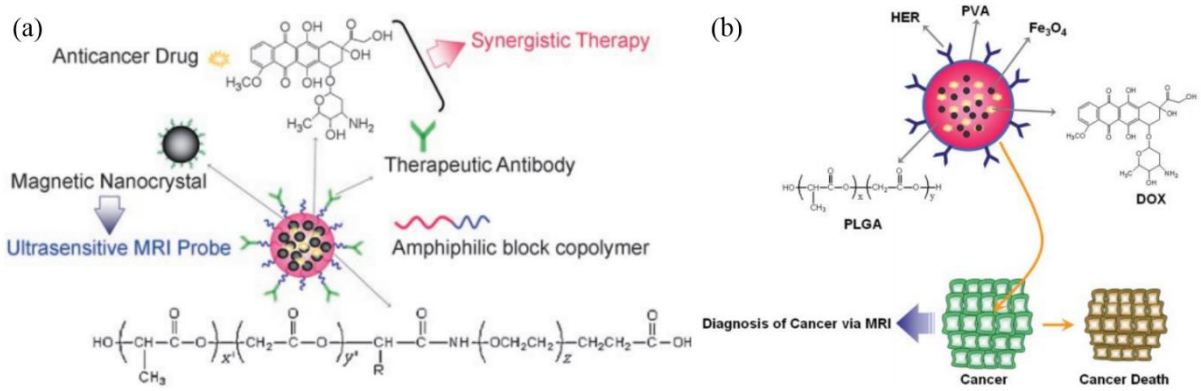

Figure 1.11 Multifunctional layer for targeted drug delivery[1, 2]. (a) Schematic design for fabrication and chemical structure of multifunctional magneto polymeric nanoohybrids[1]. (b) Schematic design of magnetic PLGA nanoparticles for therapy of tumor[2].

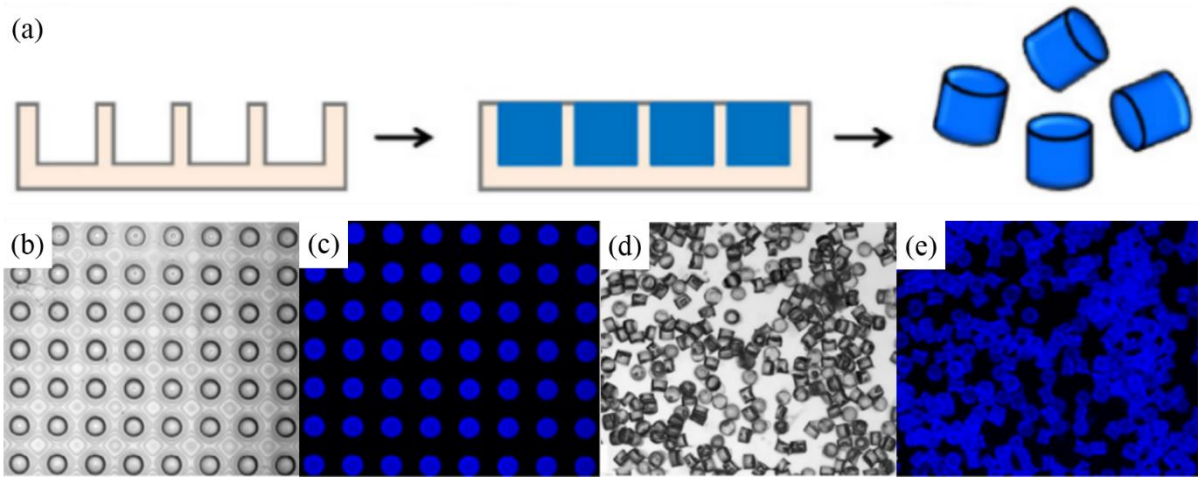

Figure 1.12 (a) Schematic procedure of the hydrogel template process of homogeneous micro particles loading anticancer drug [28] (b) Bright field image of a template with gelatin such as (a) (c) Fluorescence image of the gelatin template poured with polymer and anticancer drug (d) and (e) Bright and fluorescence images obtained micro particles after by dissolving the gelatin template in the water

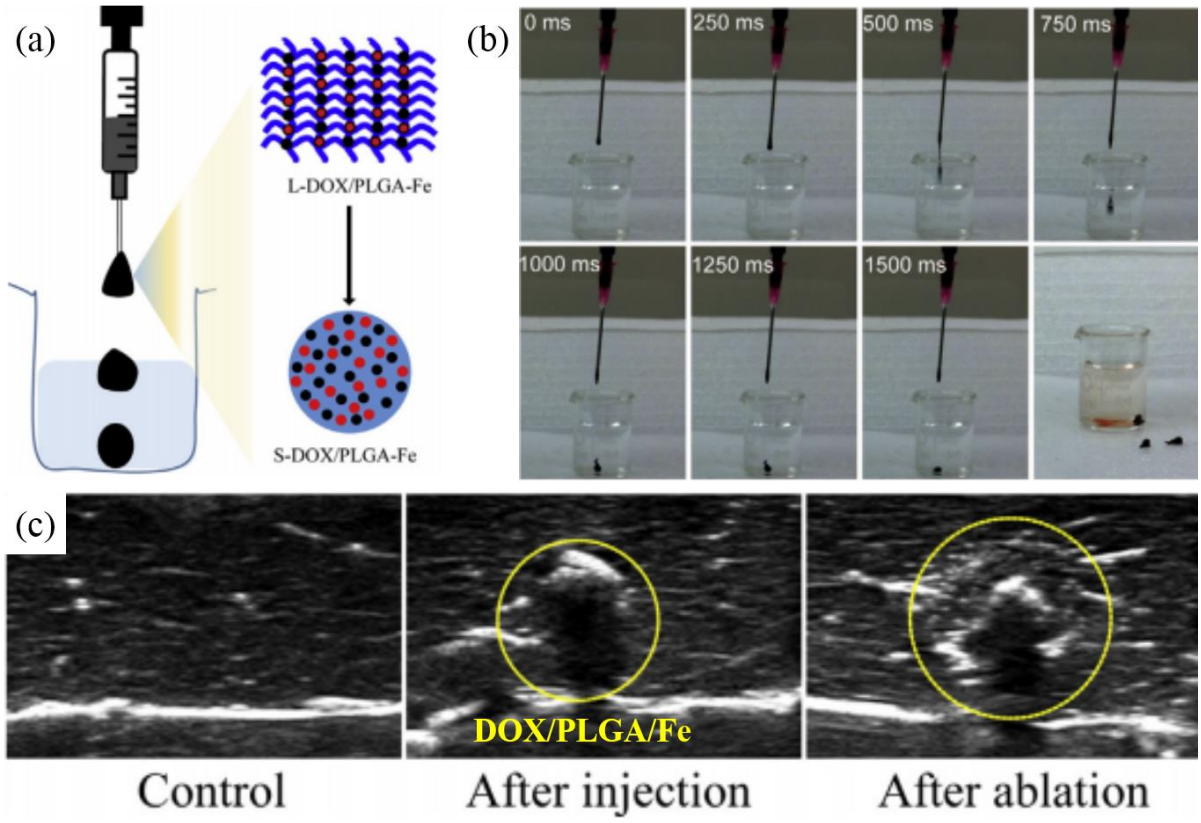

Figure 1.13 (a) and (b) Schematic procedure and time-lapsed images of liquid- solid phase transformation of the micro particles with polymer and drug contacting with water[30]. (c) The ultrasound images of *in vivo* bovine liver before and after injection of liquid- solid phase transformation with biodegradable polymer and drugs (DOX/PLGA/Fe) for therapy such as a tumor.

1.3 Aims of this research

The chapter 1.2 introduced trends and related researches of therapies using the microrobot and small particles to a specific area such as a tumor[30, 35, 49, 69, 81, 93]. From the chapter 1.2.1, using the functionalized microrobots showed many advantages which can be accurately and promptly controlled and deliver drug and objects to a targeted area and single cell[3, 4]. The chapter 1.2.2 introduced that the functional micro- and nano-particles can fabricate uniform product by hydrogel template method, improve efficiency of the amount of drug and reduce loss of small particles by phase-transformation to be applied for biomedical applications[30, 74, 81].

However, they have still several limitations that are material for degradation, various shape to control drug release time, control for targeted delivery and drug encapsulation. One of the several considerations is material which can affect biocompatibility and biodegradation in the body[28, 73, 77, 90, 129]. In general, the introduced microrobots were fabricated with photo-sensitive material for 3 dimensional (3D) structure using a light such as UV or laser and then thin magnetic metals layer such as titanium (Ti) and nickel (Ni) to improve propulsion and biocompatibility of surface on the microrobot[3, 4, 25, 27, 34, 59]. The photo-sensitive material such as SU-8 for microrobot could not be decomposed, released and difficult to re-collection from the body because the photo-sensitive materials were firmed up from light and small size approximately 100 to 500 μm. They also could not easily encapsulate drugs in the fabricating process due to transmutation of drug by light. Another one of the following important limitations is loss and low efficiency of small particles in the inserting process to a targeted area, having flow fluid. A lot of small particles could not be easily controlled and re-collected because blood circulation in the body is repetitively fast. Therefore, to overcome following focused issues, the small particles should be used larger quantity or thickness of particles than existing conditions. However, the using large quantity and thickness of small particles can

cause not only slow degradation but also inaccurate control and high side effects because of more drugs and more time, when the quantity and thickness of small particles increase.

Consequently, this study aims firstly to overcome issues of uniform shape and mass product with anticancer drug unlike hydrogel template methods, the microrobots were simply and easily fabricated by using a UV laser micro machine for a short time with biodegradable polymer for degradation and magnetic particles for magnetic actuation to be controlled by an external magnetic field. Secondly for biodegradation and drug delivery, they also are consisted of biodegradable polymer, which can be decomposed such as water and carbon dioxide, and anticancer drug to attack a tumor. Finally, to conduct accurate control for targeted drug delivery, the microrobots are controlled by an external magnetic field using electromagnetic coils system. Figure 1.14-(a) shows a conceptual schematic about targeted drug delivery using the developed microrobot and the structure of the anti-cancer drug containing biodegradable microrobot. As depicted in Figure 1.14-(b), the anticancer drug is released from the microrobot to tumor, biodegrading itself.

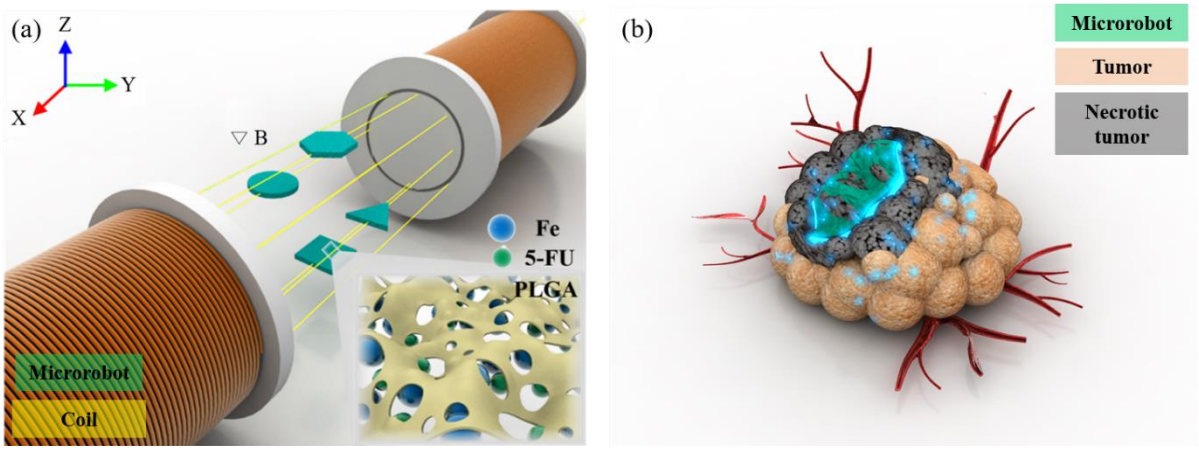

Figure 1.14 Conceptual schematic for targeted drug delivery using the developed microrobot (a) Translational motion and chemical structure of the fabricated microrobot (b) After degraded the microrobot, regression of a tumor.

2. MATERIAL AND FABRICATION

2.1 Material

The fabricated microrobots are consisted of biodegradable polymer (poly (D,L-lactide-co-glycolide acid) (PLGA)), magnetic particles (iron particles (average size < 10 μm)) and anticancer drug (5 Fluorouracil (5-FU)). In this chapter 2.1 introduces various biodegradable polymer and anticancer drug for targeted drug delivery to a specific area[12-21]. Briefly, biodegradation process also is showed from Figure 2.1.

In general, the biodegradable polymers such as poly (lactic acid) (PLA), poly (glycolic acid) (PGA) and poly (D,L-lactide-co-glycolide acid) (PLGA) are decomposed by hydrolysis in biological environment[1, 21, 86, 130]. To explain biodegradation process, when the high molecular weight of polymer is sufficiently hydrolyzed from biological environment, the polymer chains are converted to low molecular weight compounds (Primary Degradation Process). After primary degradation process in biological environment, low molecular weight compounds are absorbed through several microorganisms' metabolic pathways and products such as water (H_2O), carbon dioxide (CO_2) and methane (CH_4) Figure 2.1[5-8, 94].

In recently, a growing number of biodegradable polymers such as poly (lactic acid) (PLA), poly (glycolic acid) (PGA) and poly (D,L-lactide-co-glycolide acid) (PLGA) are used to develop drug delivery system, cardiovascular applications (stents), orthopedic devices (ligaments, pins and screws), wound management (surgical meshes, structures and staples) and tissue engineering for therapy and treatment to a specific area Figure 2.2. Consequently, in this study the 2 dimensional biodegradable microrobot encapsulated anticancer drug will be fabricated with biodegradable polymer and anticancer drug for targeted drug delivery.

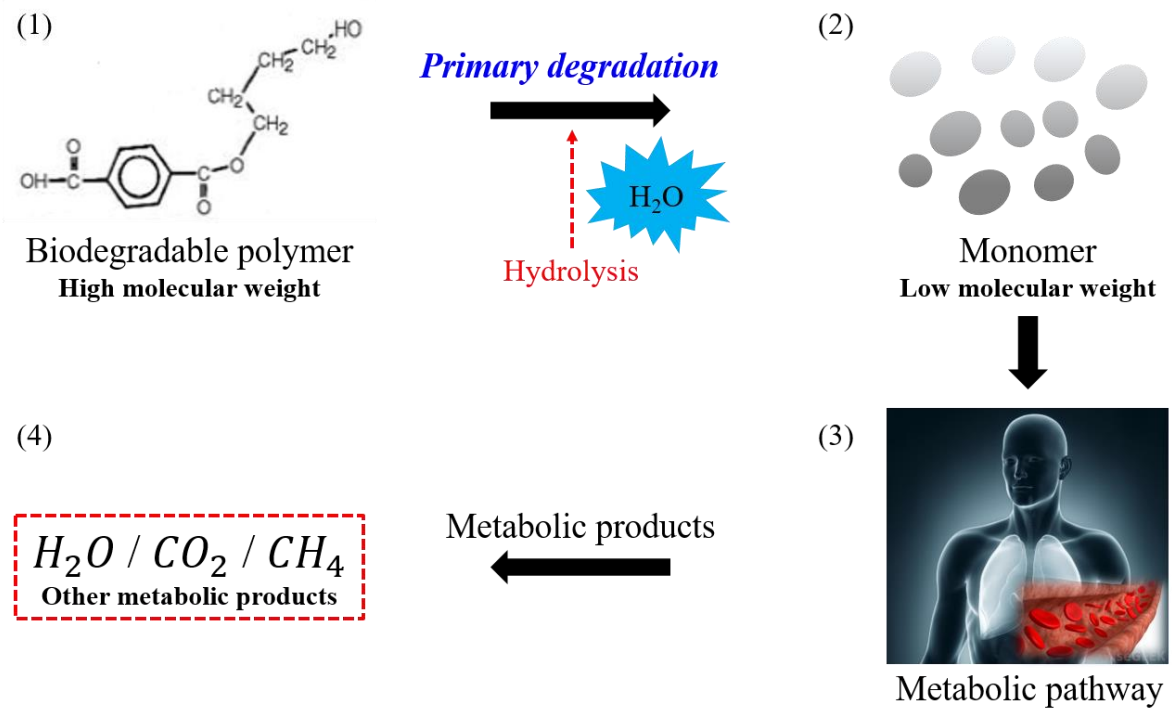

Figure 2.1 Schematic diagram of mechanism for biodegradation process[5-8].

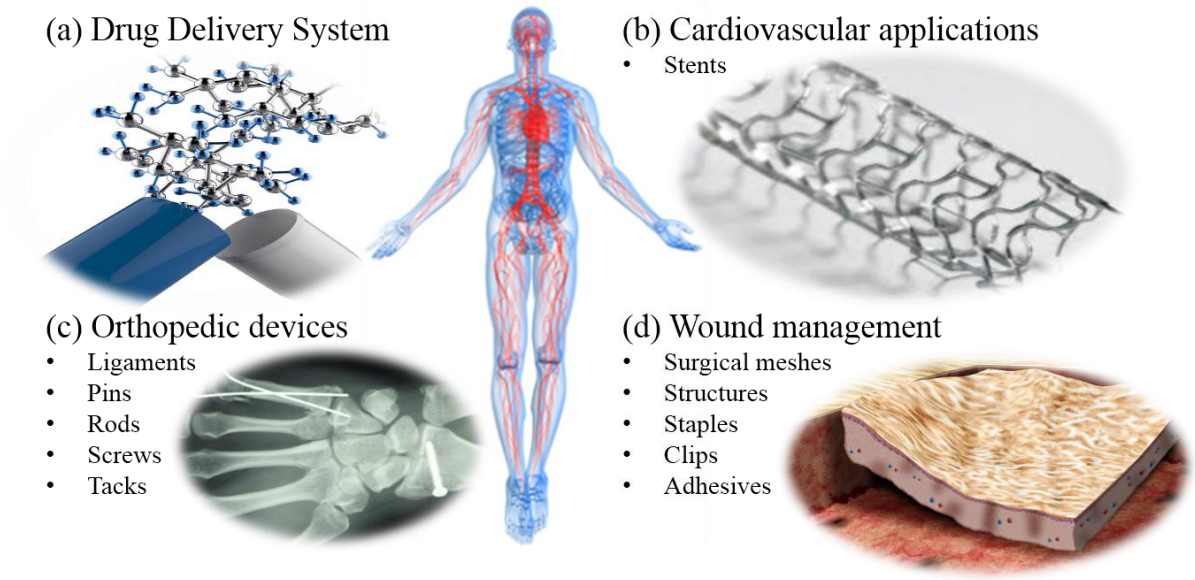

Figure 2.2 Biomedical applications such as drug delivery system, cardiovascular applications, and orthopedic devices and wound management of biodegradable polymers[12, 14, 15, 17, 20].

2.1.1 Biodegradable polymers

Poly (glycolide) (PGA) has general linear aliphatic polyester Figure 2.3-(a). It is composed by ring opening polymerization of a cyclic lactone and glycolide. It is not soluble in most organic solvent because of highly crystalline with a crystallinity of 45-55% and has higher melting point (220-225 ˚C) than normal polymers. It also has a glass transition temperature ranging from 35 to 40 ˚C Table 2.1. Therefore poly (glycolide) (PGA) polymer is limited for biomedical applications due to low solubility and slow degradation[12, 15].

Poly (lactide) (PLA) is generally obtained from polycondensation of D- or L- lactic acid Figure 2.3-(b). It has a hydrophobic property with -CH_3 side group which are more resistant to hydrolysis than poly (glycolide) (PGA) and poly (D,L-lactide-co-glycolide acid) (PLGA) due to the steric shielding effect. It has glass transition temperature of 55-60 ˚C and lower melting points (170-180 ˚C) than poly (glycolide) (PGA) Table 2.1. Therefore poly (lactide) (PLA) has low brittleness and thermal stability[15].

Poly (D,L-lactide-co-glycolide acid) (PLGA) is consisted with poly (glycolide) (PGA) and poly (lactide) (PLA) Figure 2.3-(c). It has different glass transition temperature and degradation time according to the ratio of poly (glycolide) (PGA) and poly (lactide) (PLA). Therefore when the ratio of poly (lactide) (PLA) increase from poly (D,L-lactide-co-glycolide acid) (PLGA), the degradation time is increase because the -CH_3 side groups of poly (lactide) (PLA) are resistant to hydrolysis Table 2.1, 2.2. Consequently in this experiment to develop the 2 dimensional biodegradable microrobot for targeted drug delivery, they are fabricated with poly (D,L-lactide-co-glycolide acid) (PLGA; 50:50) to control decomposed time according to the concentrations of magnetic particles with anticancer drug in biological environments for 6 weeks[12, 15-17, 19, 131, 132].

Polymer product	Melting point (˚C)	Glass transition temperature (˚C)	Degradation Time (months)
Poly (glycolide)	220 – 225	35 – 40	6 – 12
Poly (lactic acid)	170 – 180	55 – 60	12 – 16
Poly (D,L lactide-co-glycolide)	Amorphous	45 – 55	1 – 2

Table 2.1 Melting points (˚C), glass transition temperature (˚C) and degradation time (months) of biodegradable polymers such as Poly (glycolide), Poly (lactic acid) and Poly (D,L-lactide-co-glycolide acid)[12-14, 16, 17, 19, 20].

Polymer product	Ratio (%)	Melting Point (˚C)	Glass transition Temperature (˚C)	Degradation Time (months)
Poly (D,L-lactide-co-glycolide)	85:15	Amorphous	50 - 55	5 – 6
Poly (D,L-lactide-co-glycolide)	75:25	Amorphous	50 - 55	4 – 5
Poly (D,L-lactide-co-glycolide)	65:35	Amorphous	45 – 50	3 – 4
Poly (D,L-lactide-co-glycolide)	50:50	Amorphous	45 - 50	1 – 2

Table 2.2 Different ratio, melting points (˚C), glass transition temperature (˚C) and degradation Time (months) of poly (D,L-lactide-co-glycolide acid) (PLGA)[12-15, 18-20].

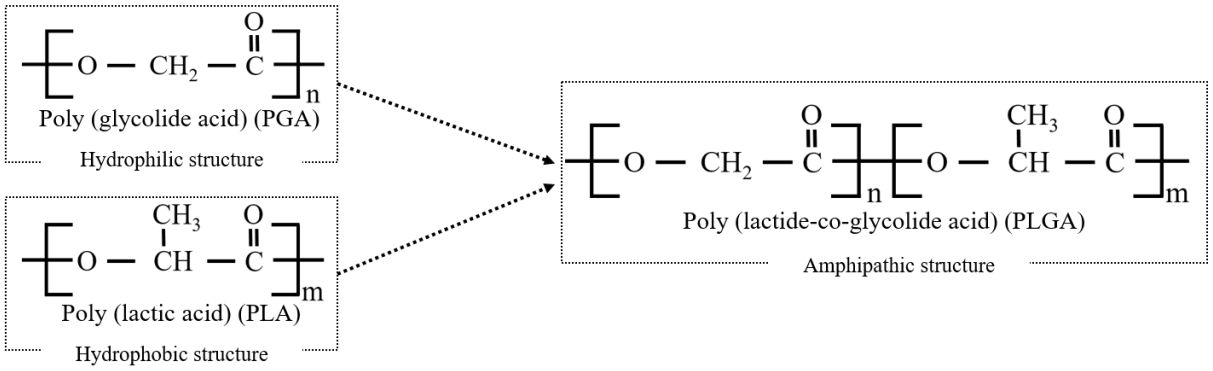

Figure 2.3 Chemical structures of biodegradable polymer (a) Poly (glycolide) (PGA) (b) Poly (lactic acid) (PLA) (c) Poly (lactide-co glycolide)[12-21].

2.1.2 Anticancer drug (5 Fluorouracil)

For targeted drug delivery using the develop microrobot with anticancer drug, the drug type (hydrophilic or hydrophobic) is important to be released and degraded because released drug have been associated with solubility. In this experiment, the 2 dimensional biodegradable microrobot is fabricated with hydrophilic drug (5 Fluorouracil) to have higher the degree of initial burst than hydrophobic drug[133-139].

The 5 Fluorouracil in hydrophilic drug has been widely used in a variety of solid cancers such as stomach, colon, and lung and breast cancer for chemotherapy[10, 11, 140-147]. It prevents nucleic acid synthesis, inhibits DNA synthesis and cell growth from a growing tumor. However, when the 5 Fluorouracil is used for chemotherapy to a tumor, it can cause nausea, vomiting, bone marrow depression, gastrointestinal tract reaction, leucopenia and thrombocytopenia because of adverse effects depending on the person[9, 137, 148-153]. In addition, it is usually injected in vein using intravenously because the 5 Fluorouracil has disadvantages which are short half-life and rapid dispersion in injecting process Figure 2.4. However, in this experiment, the developed 2 dimensional biodegradable microrobot is fabricated to improve efficiency of 5 Fluorouracil.

The 5 Fluorouracil, having 130.1 g/mol of molecular weight is dissolved in the organic solvent such as ethanol, dimethyl sulfoxide, dimethyl formamide which can dissolve approximately 0.8, 53 and 60 mg/ml and phosphate buffered saline (8 mg/ml) solution[154-156]. Therefore, for calibration curve using solubility of 5 Fluorouracil, it is dissolved in the phosphate buffered saline from 50 to 500 μM. Additionally, specific data of calibration curve and conditions can be found to the following chapter 4.3.3 description.

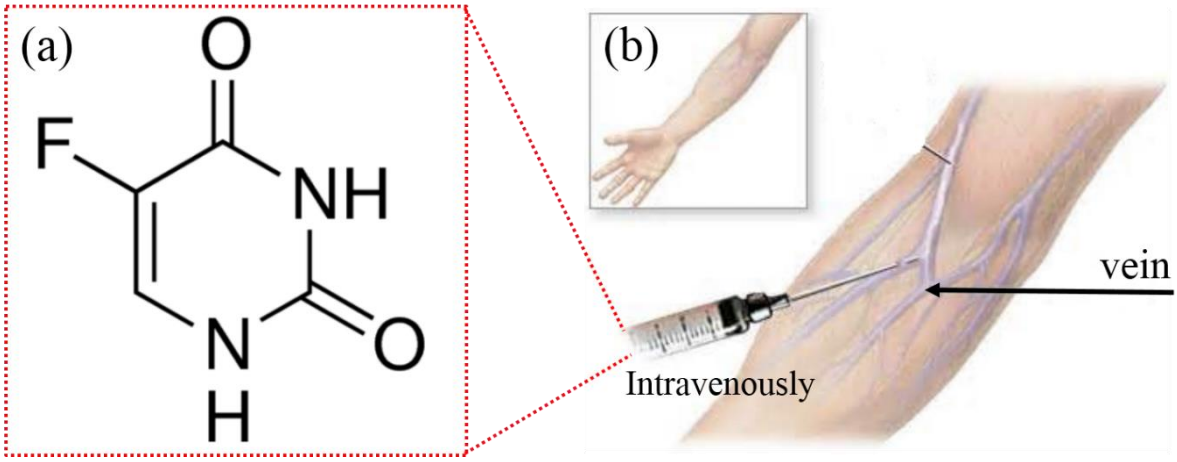

Figure 2.4 (a) Chemical structure of 5 Fluorouracil (b) injecting process using intravenously in vein[9-11].

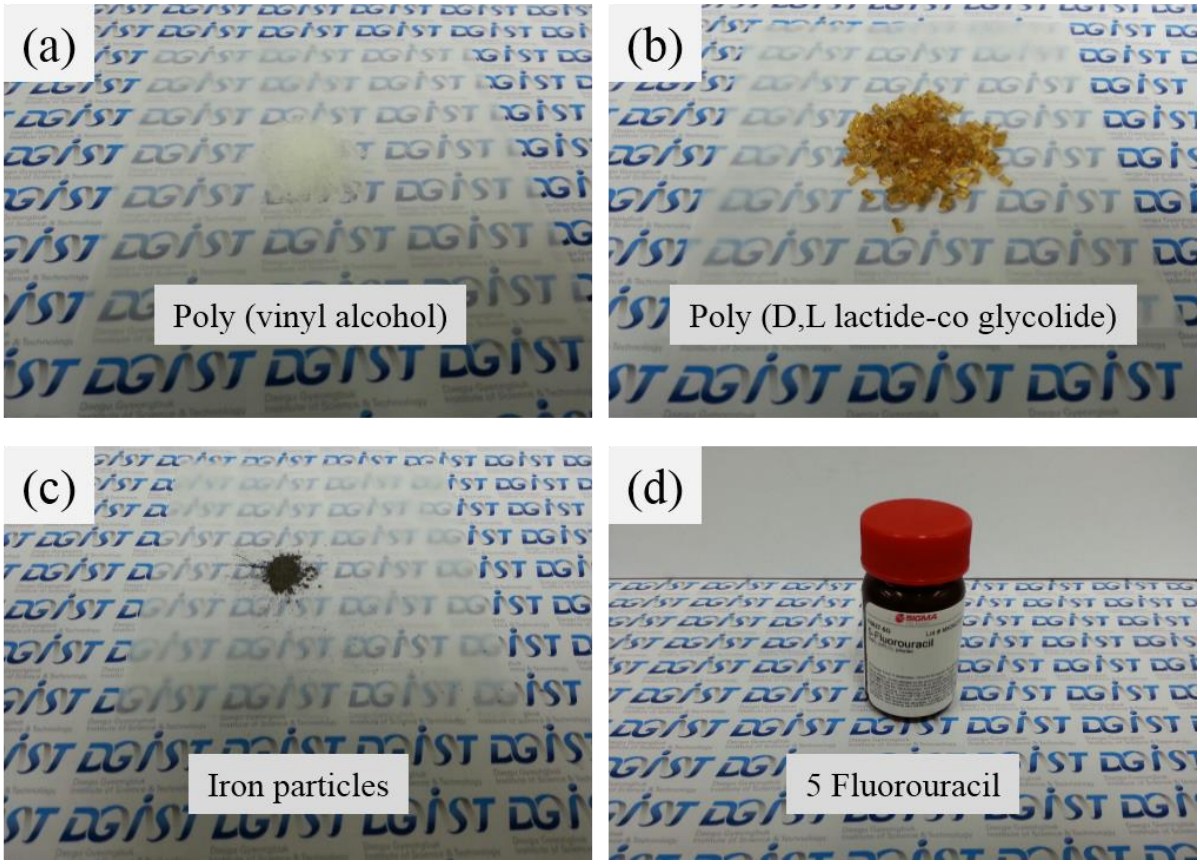

Figure 2.5 (a) Poly (vinyl alcohol) (PVA; 87-89% hydrolyzed) (b) Poly (D,L-lactide-co-glycolide acid) (PLGA; 50:50) (c) magnetic actuation (iron particles (Fe); average size < 10 µm) (d) 5 Fluorouracil.

2.1.3 Others material

Poly (vinyl alcohol) (PVA; 87-89% hydrolyzed, Sigma-Aldrich, Korea) for thin film (thickness: 30 μm), magnetic particles for magnetic actuation (iron particles (Fe); average size < 10 μm, Sigma-Aldrich, Korea), methylene blue solution (Sigma-Aldrich, Korea) to be measured with optical microscope, dichloromethane (DCM; purity > 99.9 %, Sigma-Aldrich, Korea) to dissolve poly (D,L-lactide-co-glycolide acid) (PLGA) and phosphate buffered saline (PBS; 10 mM, around pH 7, Sigma-Aldrich, Korea) were purchased. 5 Fluorouracil (5-FU) for targeted drug delivery was obtained from AppliChem (Korea).

2.2 Fabrication

In this chapter introduce that the microrobot is made using the new and simple fabrication procedures with biodegradable polymer (poly (D,L-lactide-co-glycolide acid) (PLGA; 50:50)) to solve issues of degradation, magnetic particles (iron (Fe) particles; average size < 10 μm) to be controlled by an external magnetic field using electromagnetic actuation system and anticancer drug (5 Fluorouracil (5-FU)) for targeted drug delivery. Figure 2.6 shows that schematic design of simple actual fabrication to develop the 2 dimensional biodegradable microrobot.

Before entering the main fabrication procedure, briefly the thin film was made with poly (vinyl alcohol) (PVA; 87-89% hydrolyzed) which can easily be hydrolyzed in water and methylene blue solution for optical microscope Figure 2.6-(a) and (b). Figure 2.6-(c) and (d) shows that the made thin film was prepared to make various shapes in 2 dimensional micro structure using a UV laser micro machine. Firstly for biodegradation solution having magnetic property, the poly (D,L-lactide-co-glycolide acid) (PLGA; 50:50) powder was dissolved into the dichloromethane (DCM; purity > 99.9 %) and mixed with magnetic particles (iron (Fe) particles; average size < 10 μm). Secondly to have anticancer drug for targeted drug delivery, the anticancer drug (5 Fluorouracil) was mixed with the made Fe/PLGA solution Figure 2.6-(e). From Figure 2.6-(d), the patterned thin template was dipped into the made Fe/PLGA/5-FU solution for a short time to format the template Figure 2.6-(f). The thin template formatted with the Fe/PLGA/5-FU solution was again dipped into the deionized (DI) water to decompose the poly (vinyl alcohol) (PVA) thin template with methylene blue inside of the formatted microrobot on the magnetic broad Figure 2.6-(g). After being decomposed, the 2 dimensional Fe/PLGA/5-FU microrobot was successfully fabricated Figure 2.6-(h). Additionally, specific fabrication procedures and conditions can be found the following detailed description.

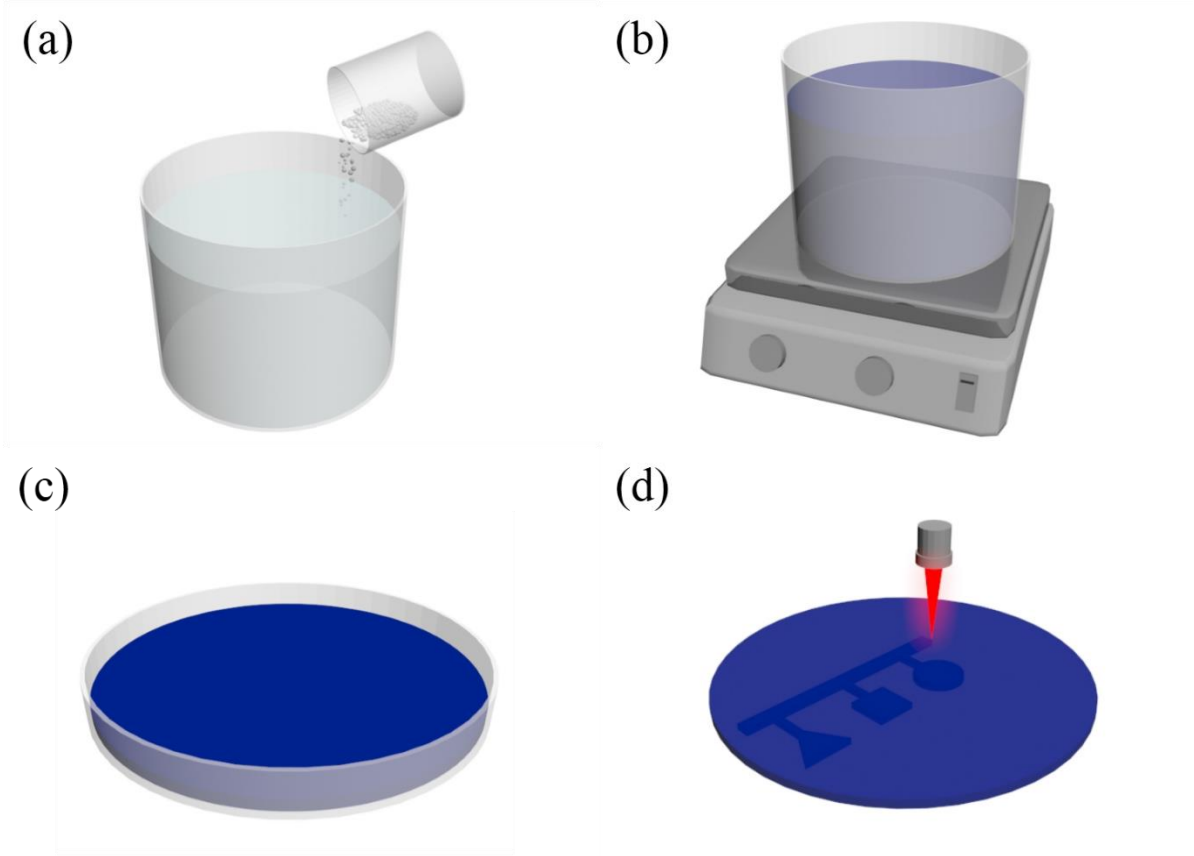

Figure 2.6 Fabrication procedure of the proposed 2 dimensional Fe/PLGA/5-FU microrobot. (a) Preparation of the poly (vinyl alcohol) films, consisting of a poly (vinyl alcohol) powder and in deionized water. (b) Mixture of the poly (vinyl alcohol) solution and methylene blue for visualization, Place beaker containing PVA solution and methylene blue the on hot plate for 1hour. (c) Poly (vinyl alcohol) thin film (Diameter: 100 mm, thickness; 30 μm to prevent tearing). (d) Poly (vinyl alcohol) thin film was peeled off a petri dish and cut by using a UV laser micro machine.

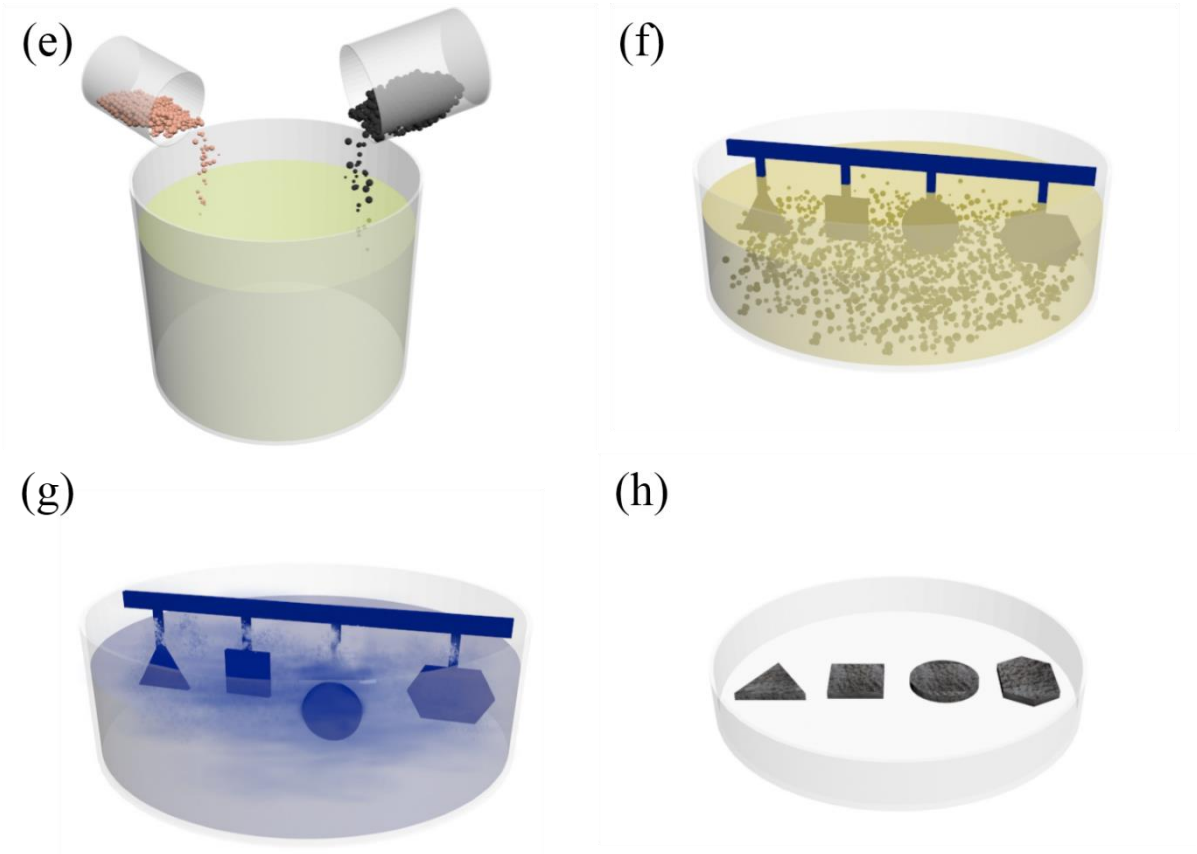

Figure 2.6 Fabrication procedure of the proposed 2 dimensional Fe/PLGA/5-FU microrobot. (e) Preparation of the Fe/PLGA/5-FU solution with magnetic particles (iron (Fe) particles; average size < 10 μm), poly (D,L-lactide-co-glycolide) (PLGA; 50:50) and anticancer drug (5 Fluorouracil). (f) the formatted thin template was dipped into Fe/PLGA/50-FU solution to be formatted. (g) After the thin template formatted with Fe/PLGA/5-FU was dipped in deionized water for short second, the thin template was hydrolyzed inside of the fabricated 2 dimensional Fe/PLGA/5-FU microrobot. (h) Complete the fabrication procedure of the proposed 2 dimensional Fe/PLGA/5-FU microrobot.

2.2.1 Preparation of poly (vinyl alcohol) thin film

To prepare the poly (vinyl alcohol) (PVA) solution (2% (w/v)) for a thin film, the poly (vinyl alcohol) (PVA; 87-89% hydrolyzed) powder (0.6 g) was dissolved in deionized water (30 mL) at around 70 to 80 °C for 2 hour on a hot plate. Figure 2.7 that the poly (vinyl alcohol) solution (30 mL) and methylene blue (30 μL) solution for visualization were mixed using a vortex device and ultrasonic cleaner for 10 minute. The solution mixed with poly (vinyl alcohol) solution and methylene blue solution was poured onto a petri dish and then dried on a hot plate at 40 to 50 °C around 1 hours. After the solution was hardened by increasing temperature, the poly (vinyl alcohol) thin film (thickness: 30 μm) was peeled off a dish and stored in a dry and cool place to prevent transition from high humidity Figure 2.8. The poly (vinyl alcohol) thin film (thickness: 30 μm, width: 100 mm, lengths: 100 mm) was successfully fabricated.

2.2.2 Preparation of the poly (D,L-lactide-co-glycolide) solution with magnetic particles

For the preparation of poly (D,L-lactide-co-glycolide acid) (PLGA; 50:50) solution (10 mL) with magnetic particles (iron (Fe); average size < 10 μm) shown in Figure 2.9, the poly (D,L-lactide-co-glycolide acid) (PLGA; 50:50) powder (0.5 g) was dissolved in 10 mL of dichloromethane (DCM; purity > 99.9 %) at room temperature with vortex for 10 minute. After dissolving poly (D,L-lactide-co-glycolide acid) (PLGA; 50:50) powder, iron particles (1, 2, 3, 4, 5 and 6 g) were dispersed into the poly (D,L-lactide-co-glycolide acid) (PLGA; 50:50) solution (10 mL) for 10, 20, 30, 40, 50, 60 % (w/v). The dispersed solution in poly (D,L-lactide-co-glycolide acid) (PLGA; 50:50) with magnetic particles was mixed by stirring and ultrasonic cleaner for 10 minutes at room temperature. Figure 2.10 shows that the Fe/PLGA solution was successfully made.

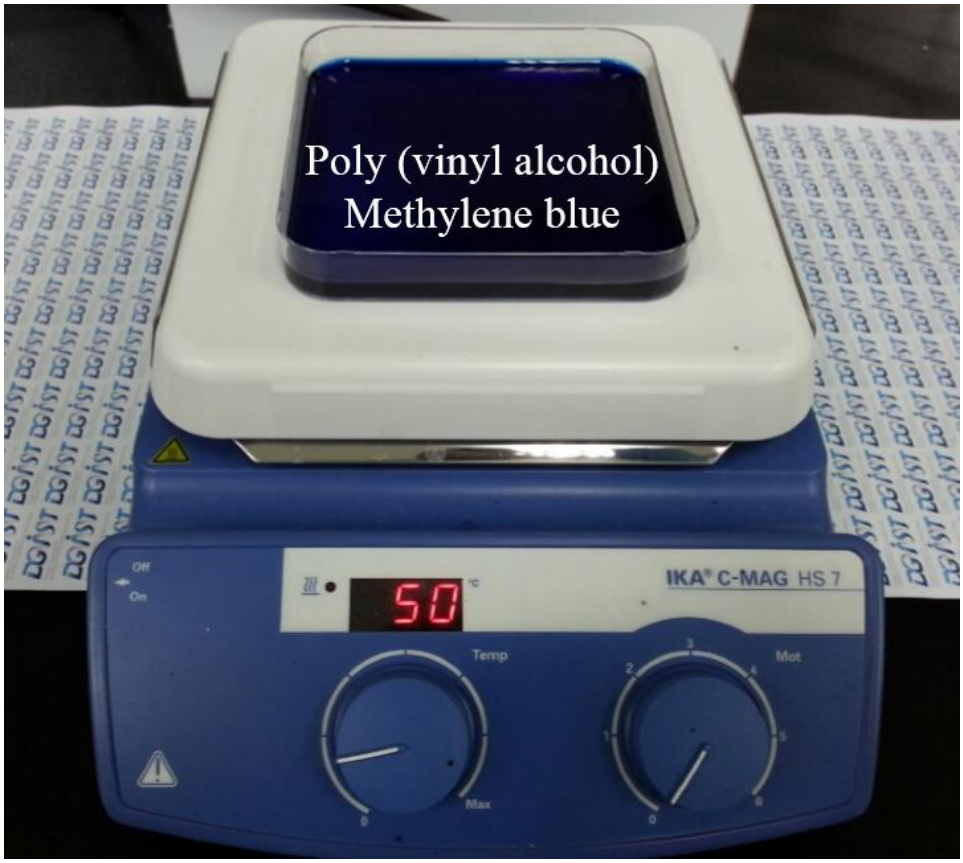

Figure 2.7 Mixture of the poly (vinyl alcohol) solution (30 mL) with methylene blue (30 µL) for visualization.

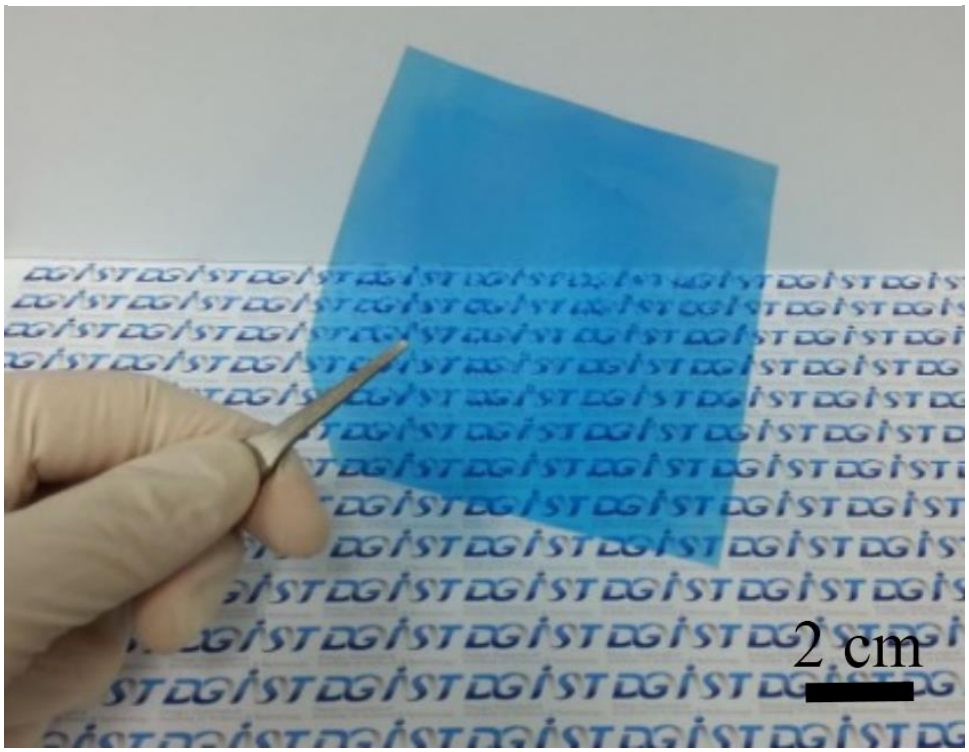

Figure 2.8 Poly (vinyl alcohol) thin film (thickness: 30 µm, width: 100 mm, lengths: 100 mm) with methylene blue.

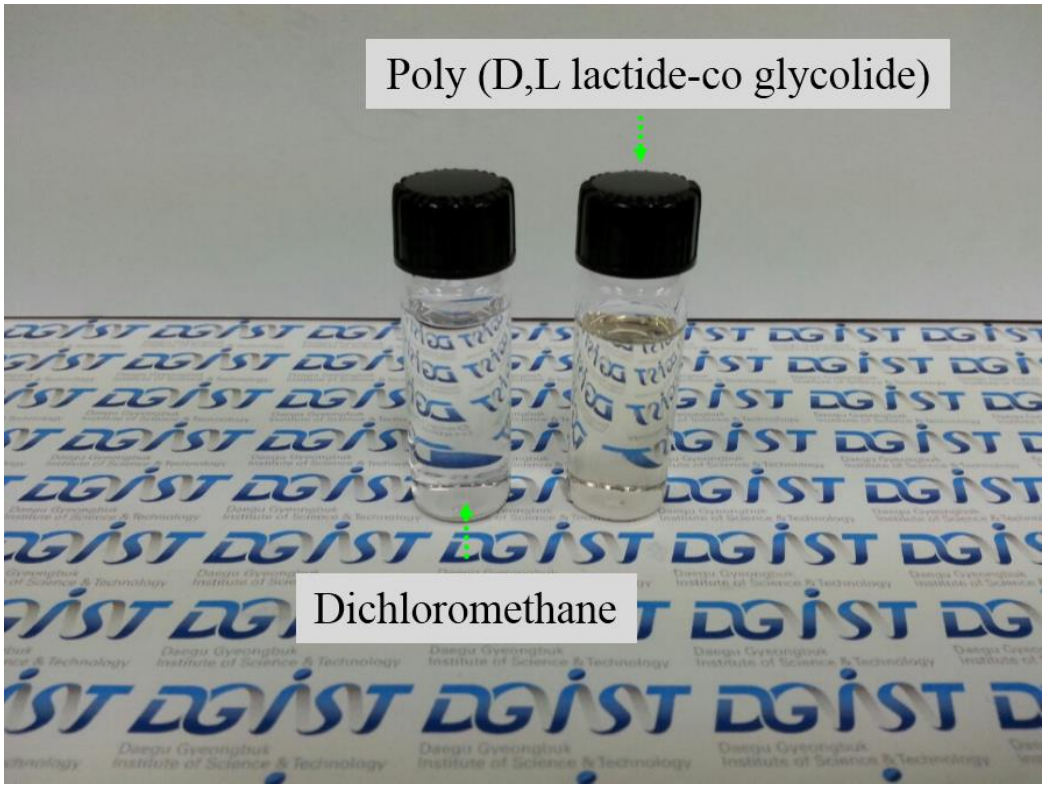

Figure 2.9 Dichloromethane (DCM; purity > 99.9 %) and poly (D,L-lactide-co-glycolide acid) (PLGA; 50:50) solution (10 mL).

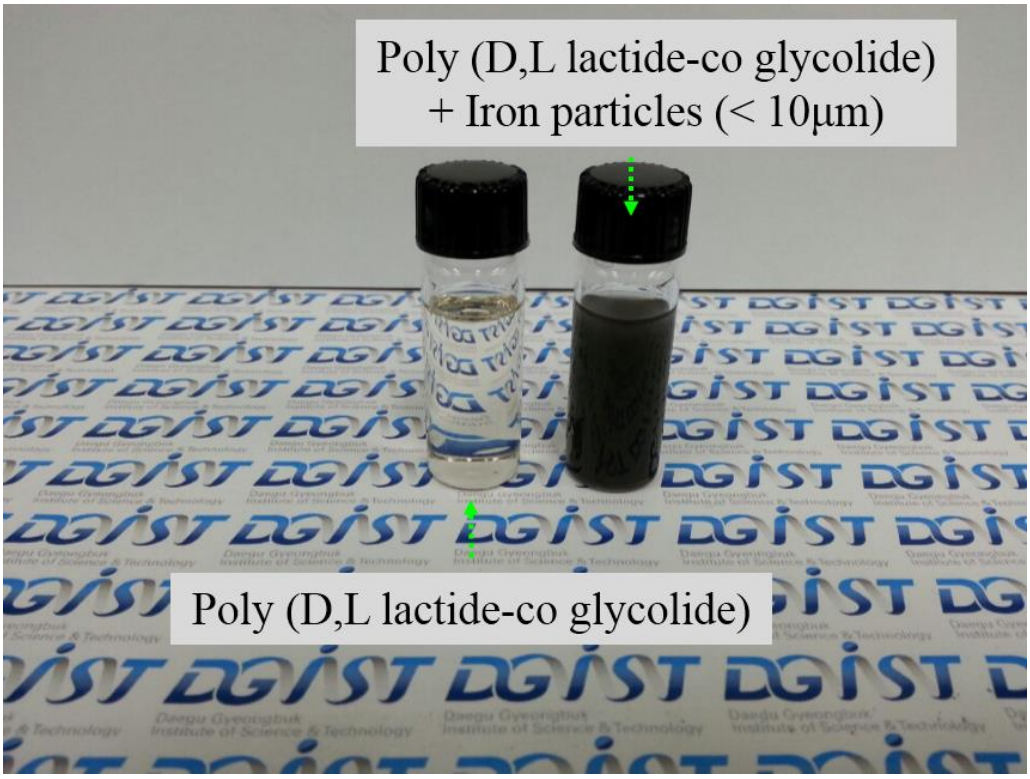

Figure 2.10 Poly (D,L-lactide-co-glycolide acid) (PLGA; 50:50) solution (10 mL) and 60 % (w/v) of Poly (D,L-lactide-co-glycolide acid) (PLGA; 50:50) solution with iron particles (average size < 10 μm).

2.2.3 Fabrication of the 2 dimensional biodegradable microrobots with various shapes for targeted drug delivery

The 2 dimensional biodegradable microrobot with poly (D,L-lactide-co-glycolide acid) (PLGA; 50:50) and iron particles (Fe; average size < 10 μm) was fabricated by using a UV laser micro machine for a short time. The chapter 2.2.1 introduced fabrication procedure of thin film (thickness: 30 μm) with poly (vinyl alcohol) and methylene blue. The thin film was cut by using a UV laser micro machine to make various and uniform shapes shown in Figure 2.11.

The chapter 2.2.2 showed making the Fe/PLGA/5-FU solution with poly (D,L-lactide-co-glycolide acid) (PLGA; 50:50) solution, iron particles (Fe; average size < 10 μm). For targeted drug delivery using the developed microrobot, the anticancer drug (5 Fluorouracil) was dissolved into Fe/PLGA solution (10 mL) in different ratio (50 - 500 μM) and then the patterned thin template was dipped into the Fe/PLGA/5-FU solution for a short second. After dipped into the Fe/PLGA/5-FU solution, the formatted thin template was dried to evaporate dichloromethane at room temperature Figure 2.12. Figure 2.13 shows that the dried formatted thin template was dipped in deionized water on magnetic board to re-collect the fabricated Fe/PLGA/5-FU microrobot at room temperature for 2 minute. After re-collecting the decomposed Fe/PLGA/5-FU microrobot, they were dried at room temperature for 5 minutes.

Consequently, in this chapter the developed Fe/PLGA/5-FU microrobots for targeted drug delivery were successfully obtained shown in Figure 2.14. In flowing chapter, we will introduce an experimental setup and characterizations to analysis chemical structure, movement and degradation of the fabricated Fe/PLGA/5-FU microrobot.

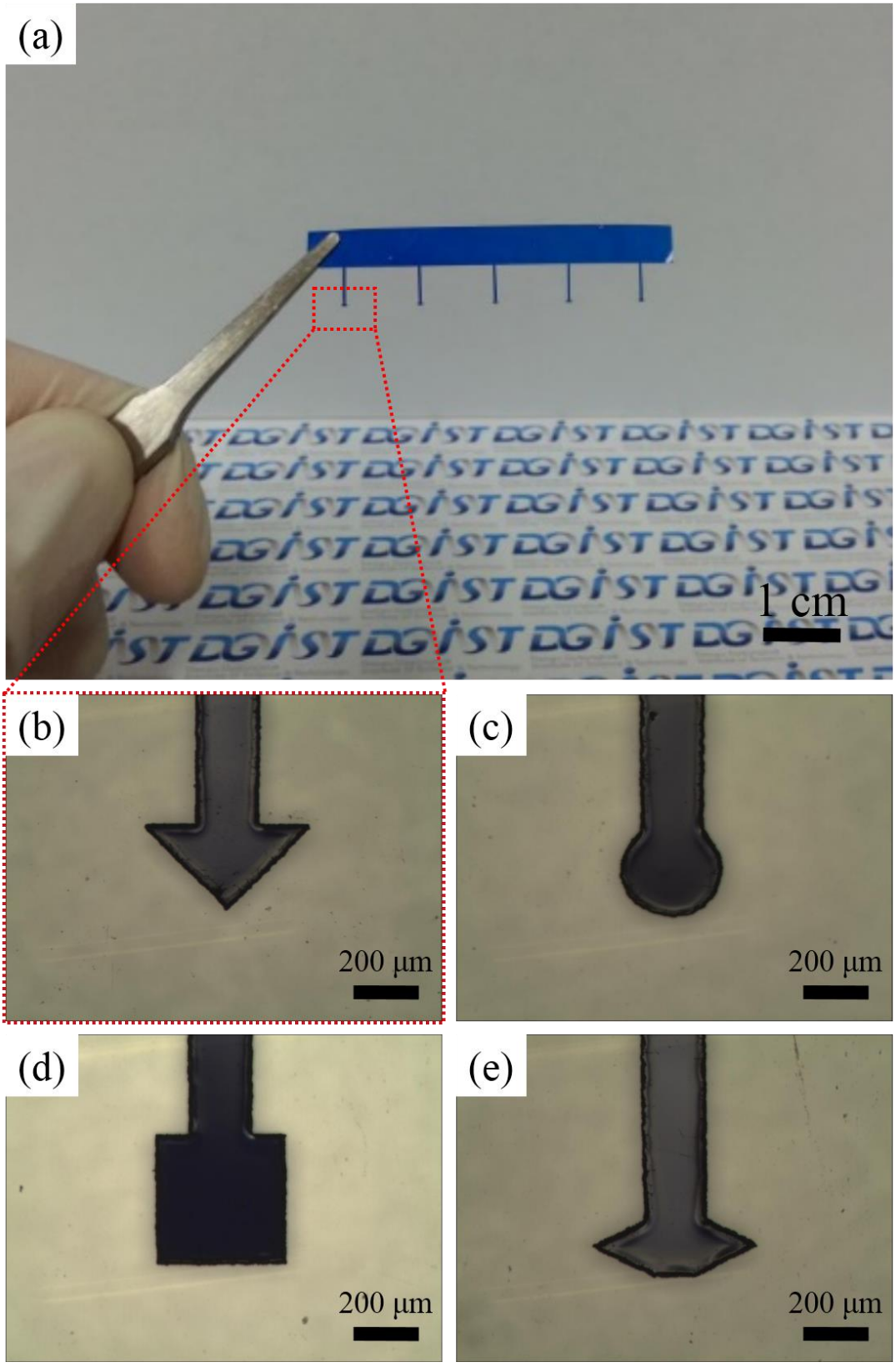

Figure 2.11 (a) Thin template with various and uniform shapes by using a UV laser micro machine (b) triangle type (c) circle type (d) square type (e) rhombus type.

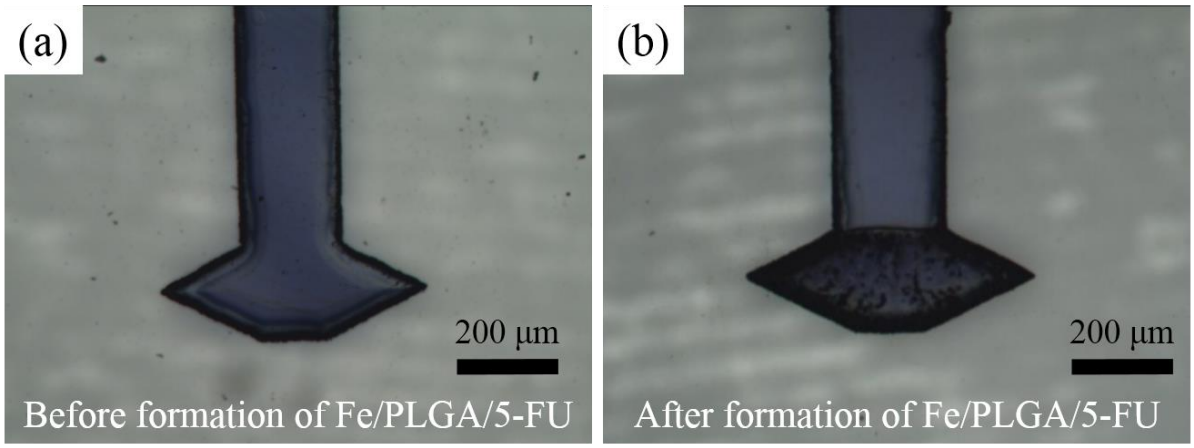

Figure 2.12 (a) Before formation of Fe/PLGA/5-FU solution on thin template. (b) After formation of Fe/PLGA/5-FU solution on thin template.

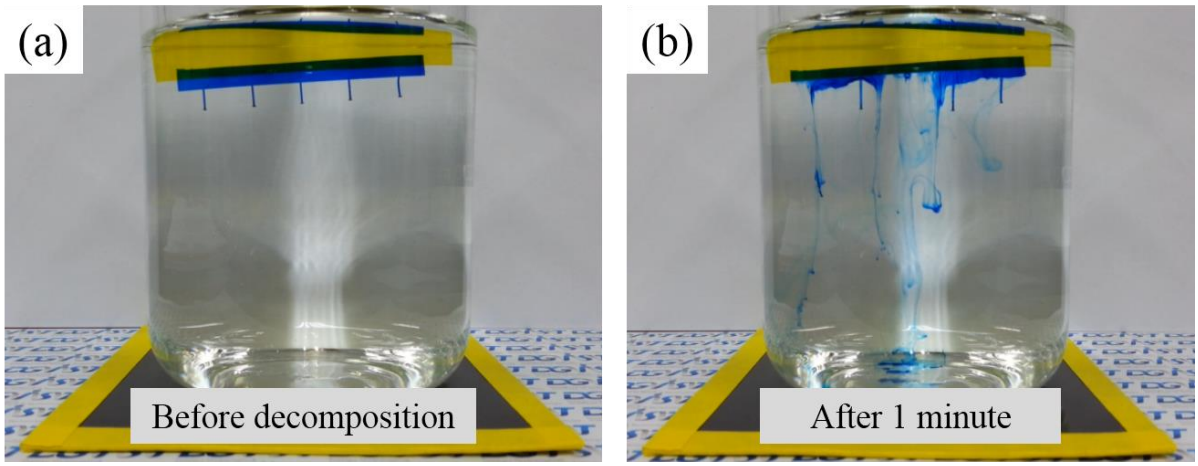

Figure 2.13 (a) Before decomposing the formatted thin template in water. (b) Decomposing the formatted thin template in water for 1 minute.

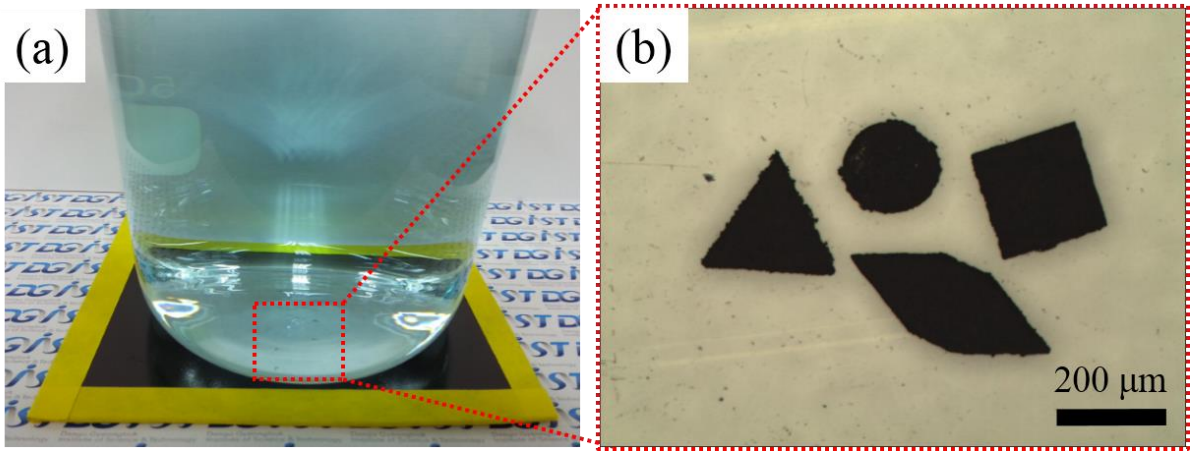

Figure 2.14 (a) After decomposing the formatted thin template in water, the 2 dimensional biodegradable microrobot on magnetic board. (b) Various shape of the dried 2 dimensional biodegradable microrobot.

3. EXPERIMENTAL SETUP

3.1 UV laser micro machine (ALM100; Sejoong Information Technology, Korea)

A UV laser micro machine (ALM100; Sejoong Information Technology, Korea) is used to cut a poly (vinyl alcohol) thin film (thickness: 30 μm) shown in Figure 3.1. Equipment has the beam spot size around 5 to 10 μm and laser source of 355 nm wavelength. It can also be used to cut fine hole and cutting and dicing processing using a laser. In addition a UV laser micro machine can move up to 1000 mm/sec and has position accuracy (<±2 μm) and repeatability (<±1 μm) in the X-axis and Y-axis stage.

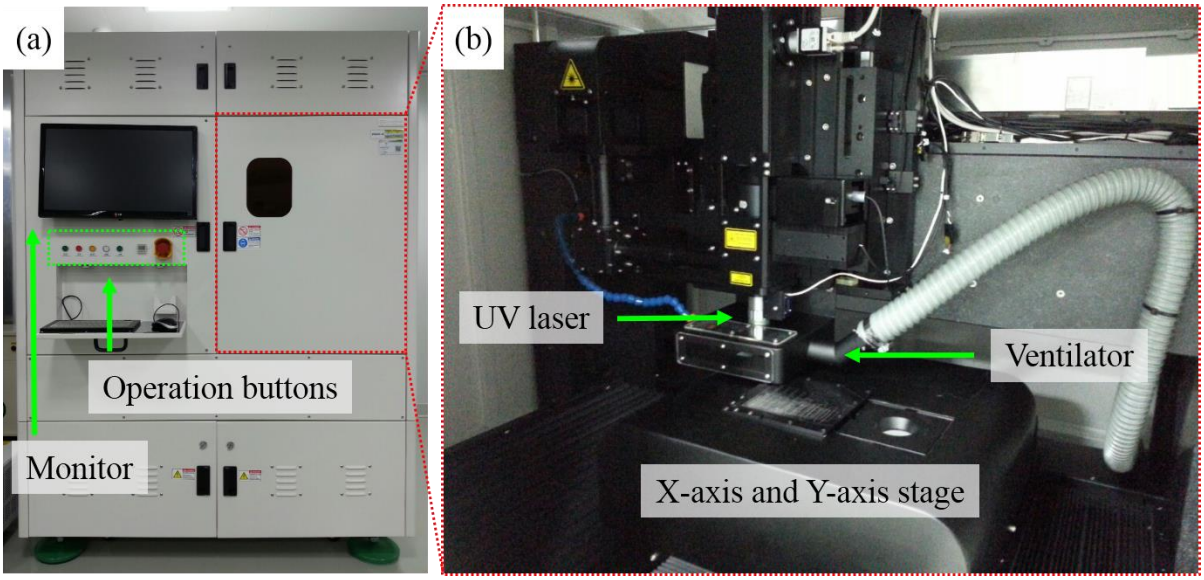

Figure 3.1 Mechanical structure of a UV laser micro machine. (a) Exterior of a UV laser micro machine. (b) Inside of a UV laser micro machine.

Product	ALM 100
Laser source	355 nm wavelength
Beam spot size	5 to 10 μm
Speed	1000 mm/sec
Position accuracy	<±2 μm
Position repeatability	<±1 μm

Table 3.1 Specification of a UV laser micro machine (ALM100; Sejoong Information Technology, Korea).

3.2 Electromagnetic actitation system (Minimag; Aeon Scientific, Switzerland)

The electromagnetic actuation system (Minimag; Aeon Scientific, Switzerland) is used to control the fabricated Fe/PLGA/5-FU microrobot by an external magnetic field. It has five degrees of freedom which include three translational degrees of freedom on X, Y and Z axis and two rotational degrees of freedom X and Z axis. It also can generate magnetic field (20 mT), output field gradient range (2 T/m) and has working space (10 mm^3)[29].

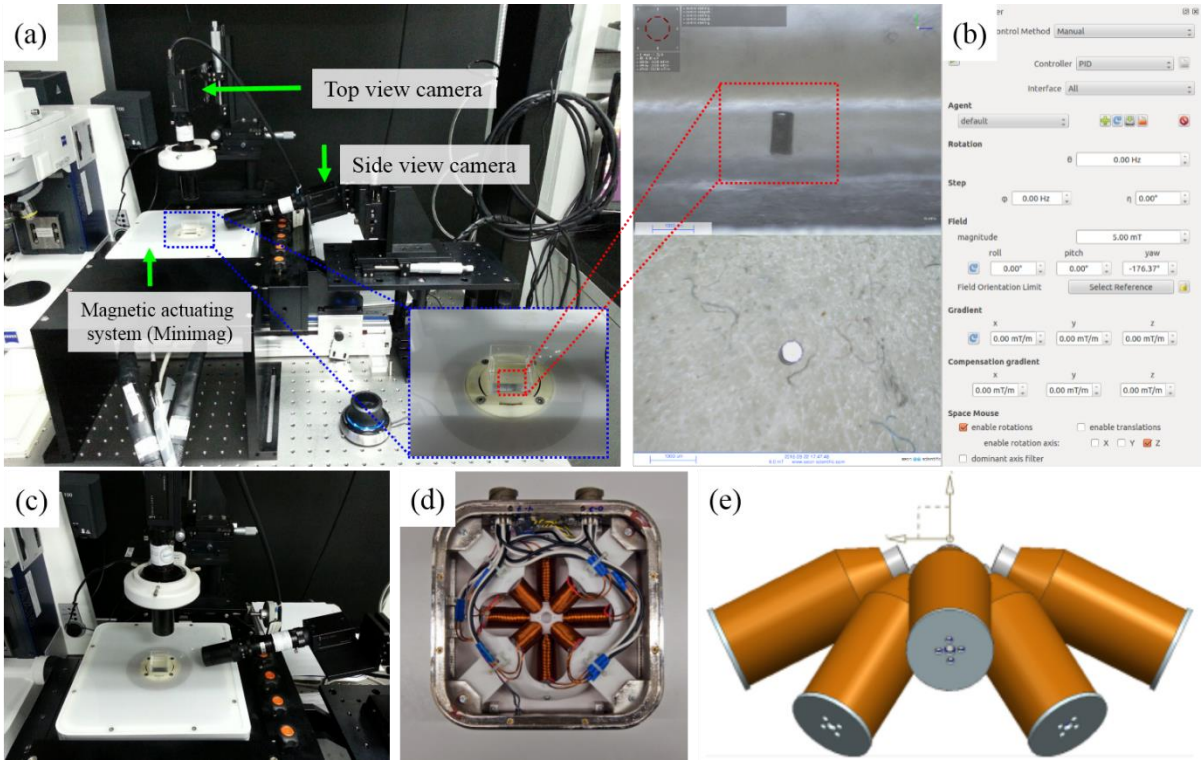

Figure 3.2 (a) Experimental setup to control the fabricated Fe/PLGA/5-FU microrobot. (b) Control GUI (graphical user interface). (c) Electromagnetic actuation system (Minimag; Aeon Scientific, Switzerland). (d) Internal structure of electromagnetic actuation system[29]. (e) Coils structure of inside of electromagnetic actuation system[29].

Product	Minimag
Output field	20 mT
Output field gradient range	2 T/m
Working space	10 mm^3
Field gradient DOF	2 (orientation) & 3 (position)

Table 3.2 Specification of Electromagnetic actuation system (Minimag; Aeon Scientific, Switzerland)

3.3 Optical microscope (BX41M-LED; Olympus, Korea)

The optical microscope (BX41M-LED; Olympus, Korea) is used to measure various shape of the fabricated Fe/PLGA/5-FU microrobots. It uses UIS2 optical system (infinity-corrected system) and 100x, 50x, 20x, 10x and 5x lens, the maximum specimen height is 65 mm (without spacer). It also has stroke (35 mm), fine stroke per rotation (100 μm), and minimum graduation (1 μm).

3.4 Field emission scanning electron microscope (S-4800; Hitachi, Japan)

The field emission scanning electron microscope (S-4800; Hitachi, Japan) is an analyzer component which use the electron beam emitted from the field emission source under a vacuum environment. A lens system is consisted of three stage electromagnetic reduction type and accelerating voltage is from 0.5 to 30 kV (0.1 kV step). This equipment can measure the surface of the fabricated microrobot. To compare before and after formation of the Fe/PLGA/5-FU microrobots, the field emission scanning electron microscope will be used.

3.5 Fourier transform infrared (FTIR) spectroscopy (Continuum; Thermo Scientific, Korea)

The Fourier transform infrared spectroscopy (FT-IR) (Continuum; Thermo Scientific, Korea) is used to measure chemical structure and boding of the microrobot and iron particles. This equipment has spectral range (7,800 – 350 cm-1), resolution (0.09 cm-1), interferometer (graphite material ring for moving mirror) and IR libraries (217,000 libraries).

3.6 UV-VIS-NIR spectrophotometer (CARY5000; Agilent, America)

The UV-VIS-NIR spectrophotometer (CARY5000; Agilent, America) is used to measure the UV values of drug into the Fe/PLGA/5-FU microrobot. It can measure organic solvent and anticancer drug to compare before and after drug release for 6 weeks. This equipment has R928 PMT detectors, limiting resolution (<0.048 nm), wavelength range (175-900 nm).

4. RESULTS AND DISCUSSION

4.1 Characterization of the 2 dimensional biodegradable microrobot

4.1.1 Optical microscope images of the 2 dimensional biodegradable microrobot

The chapter 2 introduced that the 2 dimensional Fe/PLGA/5-FU microrobot consisted of with biodegradable polymer (poly (D,L-lactide-co-glycolide acid) (PLGA)), iron particles (Fe; average size < 10 μm) and anticancer drug (5 Fluorouracil) is fabricated using a UV laser micro machine. Therefore, in this chapter shows that the fabricated microrobot were observed with various shape by optical microscope, after decomposing the formatted thin template.

Figure 4.1-(a) shows the fabricated microrobot of various shapes with formatted Fe/PLGA by optical microscope. Figure 4.1-(b) and -(c) are the surface of before and after formation of the Fe/PLGA microrobot by optical microscope. Before formation of the Fe/PLGA microrobot, the thin film consisted of poly (vinyl alcohol) (PVA) surface is flat and smooth using scanning electron microscope to measure the specific area Figure 4.2-(a). After formation of Fe/PLGA microrobot, they are consisted of porous surface because of quick evaporation of volatile dichloromethane (39 °C) than general organic solvent such as ethanol (78 °C) and acetone (56 °C) Figure 4.2-(b).

Additionally, the Fe/PLGA microrobot was measured for qualitative analysis of atomic ratio by energy-dispersive X-ray (EDX) spectroscopy. Figure 4.3 and 4.4 show the relative amount of the atomic ratio having 10 % (w/v) and 60 % (w/v) of Fe particles. Therefore, according to the relative amount of iron particles, we can see that the relative amount of iron particles increase attached to the Fe/PLGA microrobot. Consequently, it demonstrated that the Fe/PLGA microrobot was successfully fabricated by using a UV laser micro machine and formatted with Fe/PLGA.

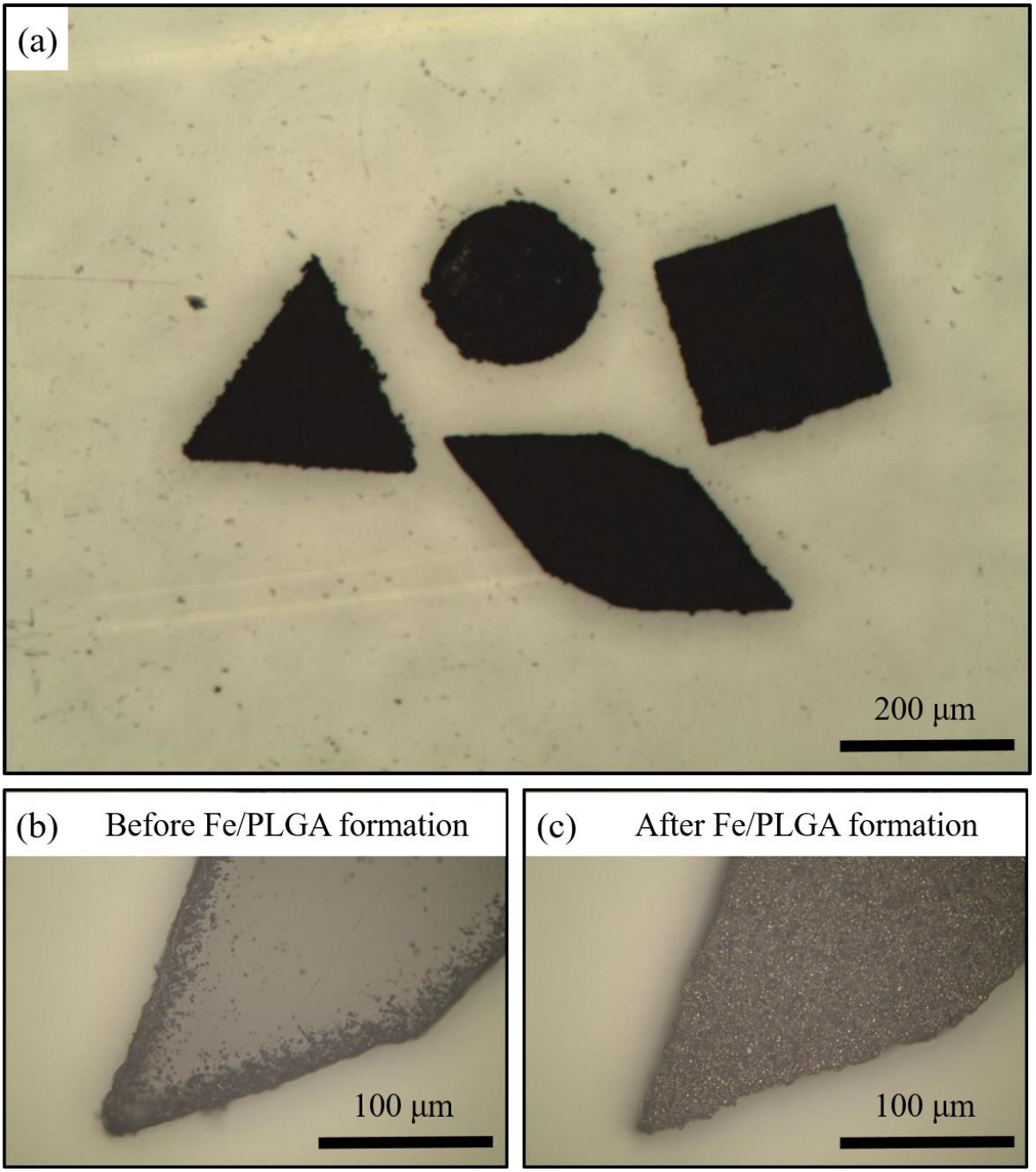

Figure 4.1 (a) Various shape of the fabricated 2 dimensional Fe/PLGA microrobots (square, circle, triangle and rhombus). (b) and (c) are the surfaces of before and after formation of the Fe/PLGA microrobot.

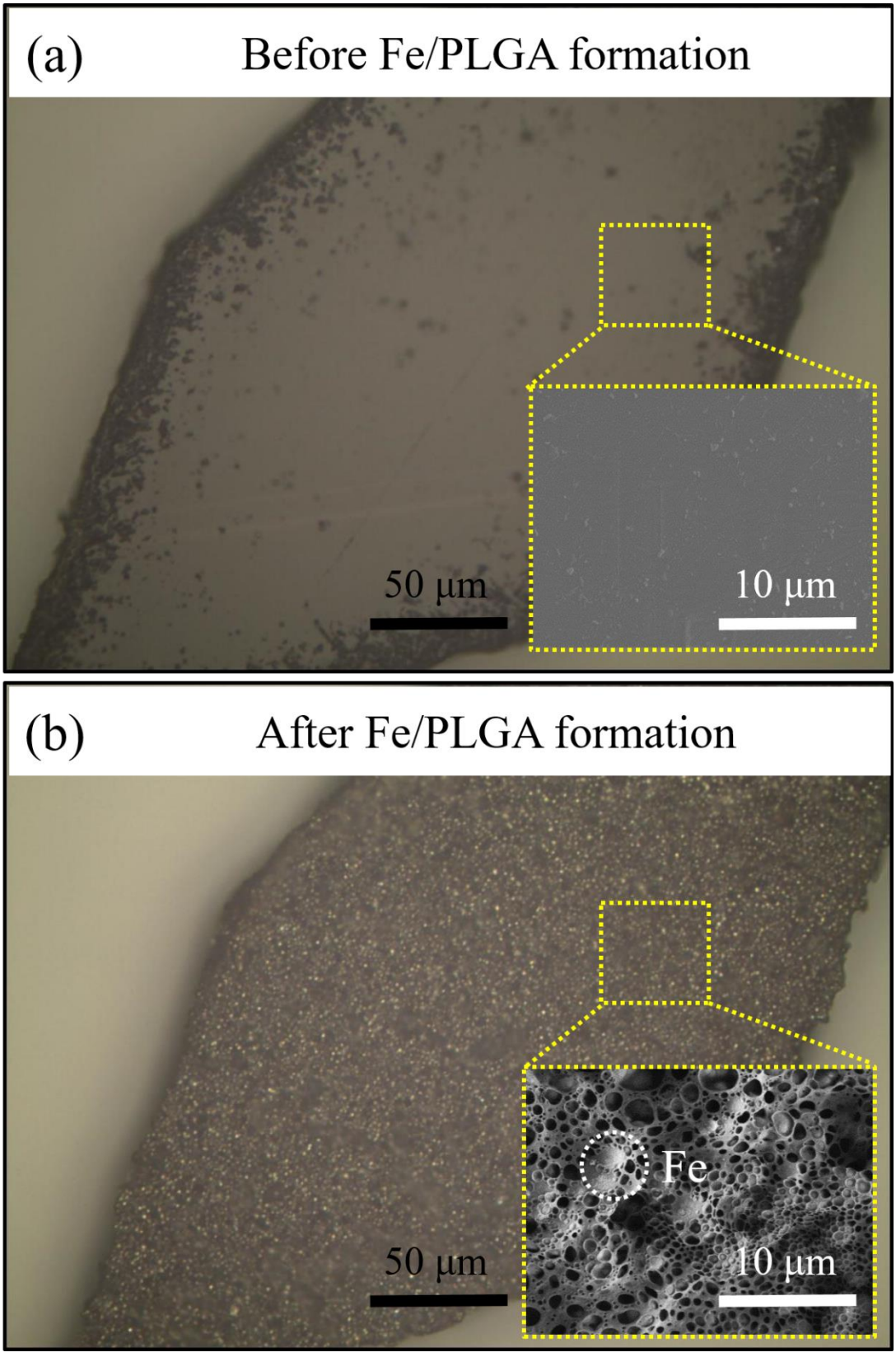

Figure 4.2 Surfaces of the fabricated Fe/PLGA microrobot using optical microscope and scanning electron microscope. (a) and (b) are optical and SEM images of before and after formation of the Fe/PLGA microrobot.

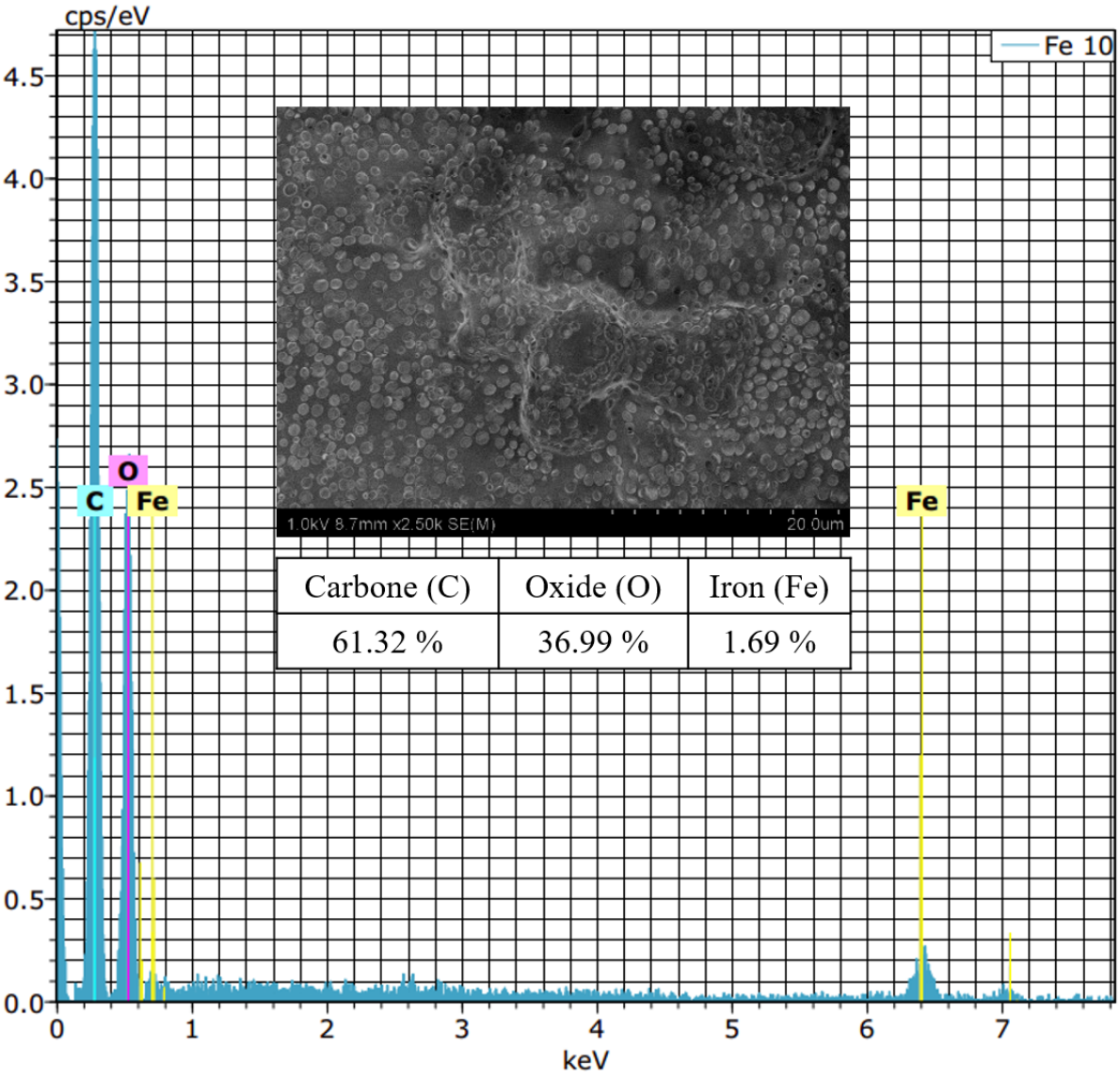

Figure 4.3 Energy-dispersive X-ray spectroscopy (EDX) image of the Fe/PLGA microrobot with 10 % (w/v) iron particles.

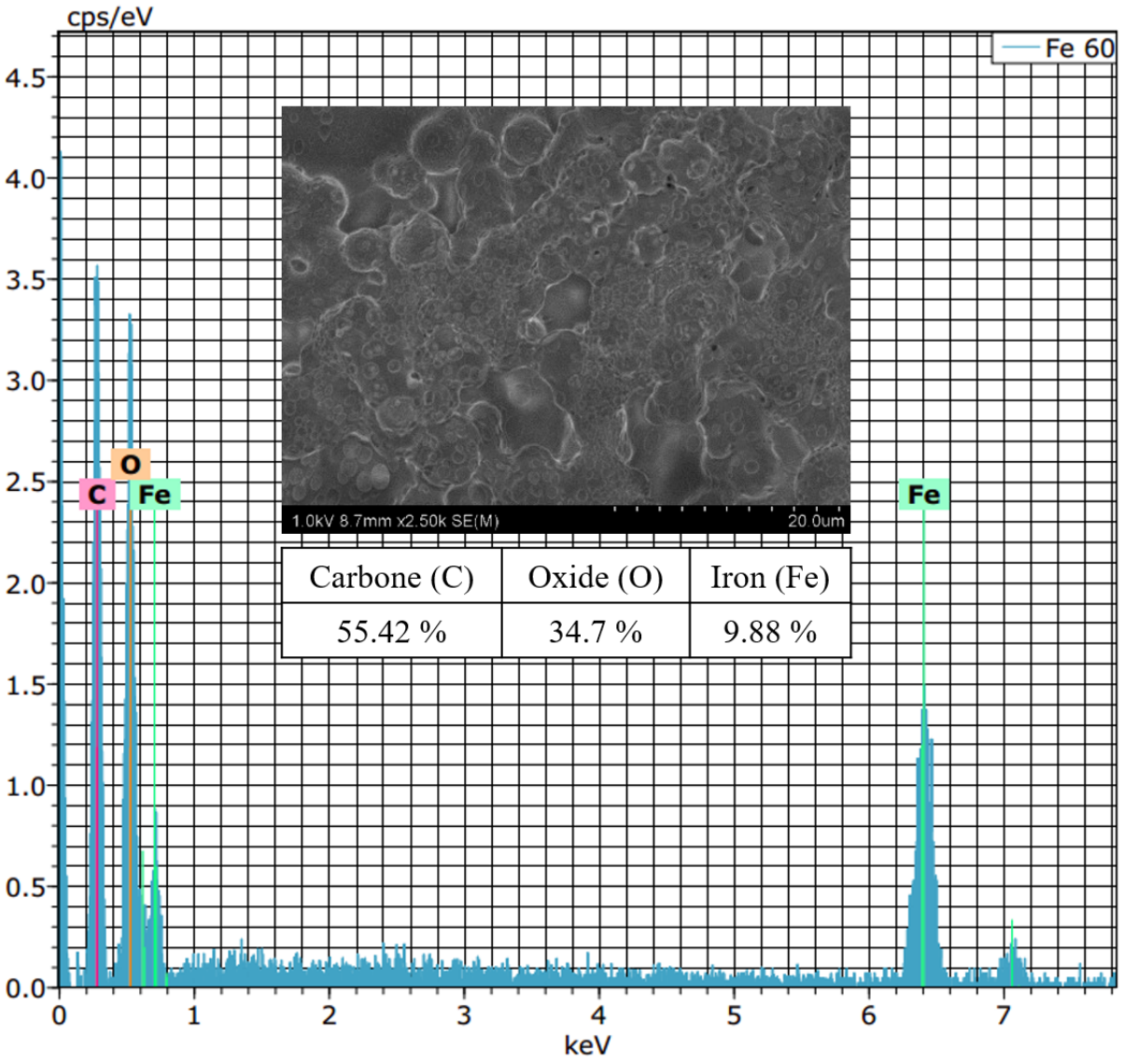

Figure 4.4 Energy-dispersive X-ray spectroscopy (EDX) image of the Fe/PLGA microrobot with 60 % (w/v) iron particles.

4.1.2 Chemical structure of the 2 dimensional biodegradable microrobot

The chapter 2 introduced that the Fe/PLGA microrobot was consisted of poly (D,L-lactide-co-glycolide acid) for biodegradation and iron particles (Fe; average size < 10 μm) for magnetic actuation. In this chapter, to analyze chemical structure from the fabricated Fe/PLGA microrobot, it was conducted using Fourier transform infrared spectroscopy. Figure 4.5 and 4.6 show that Fourier transform infrared spectroscopy was conducted with in three different regions. The first chemical bonding is asymmetric stretching bonding at 1300-1000 cm^{-1}; second and third regions are the aliphatic C-H stretching bonding at 3000-2850 cm^{-1} and the C=O stretching bonding at 1850-1650 cm^{-1} because of the ester group, respectively. Figure 4.6 shows the weak characteristic peak (Fe-O bond) of poly (D,L-lactide-co-glycolide acid) and iron particles at 600-400 cm^{-1}. Therefore we could know that the Fe/PLGA microrobot was consisted of poly (D,L-lactide-co-glycolide acid) and iron (Fe) particles[30, 81, 157-165].

Consequently, from the chemical bonding (Fe-O bond), the Fe/PLGA microrobot can be controlled by an external magnetic field, having translational and rotational motion in an aqueous environment. It also can be degraded with water and carbon dioxide due to poly (D,L-lactide-co-glycolide acid). In this experiment, the Fe/PLGA microrobot was successfully coexisted with poly (D,L-lactide-co-glycolide acid) and iron particles, having chemical bonding of Fe-O bond.

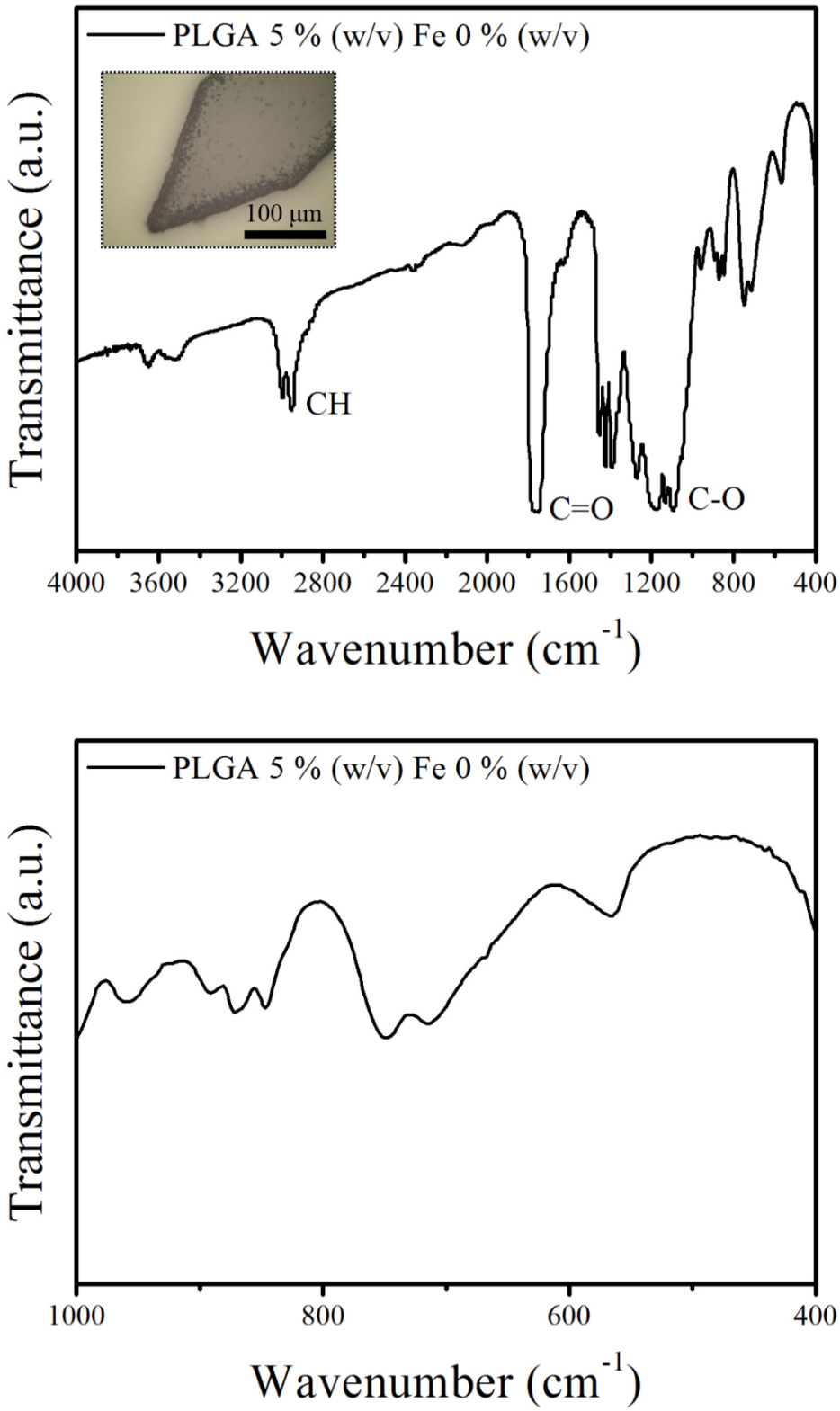

Figure 4.5 Fourier transform infrared (FT-IR) spectroscopy image of before formation of the Fe/PLGA microrobot with iron particles (0 % (w/v)).

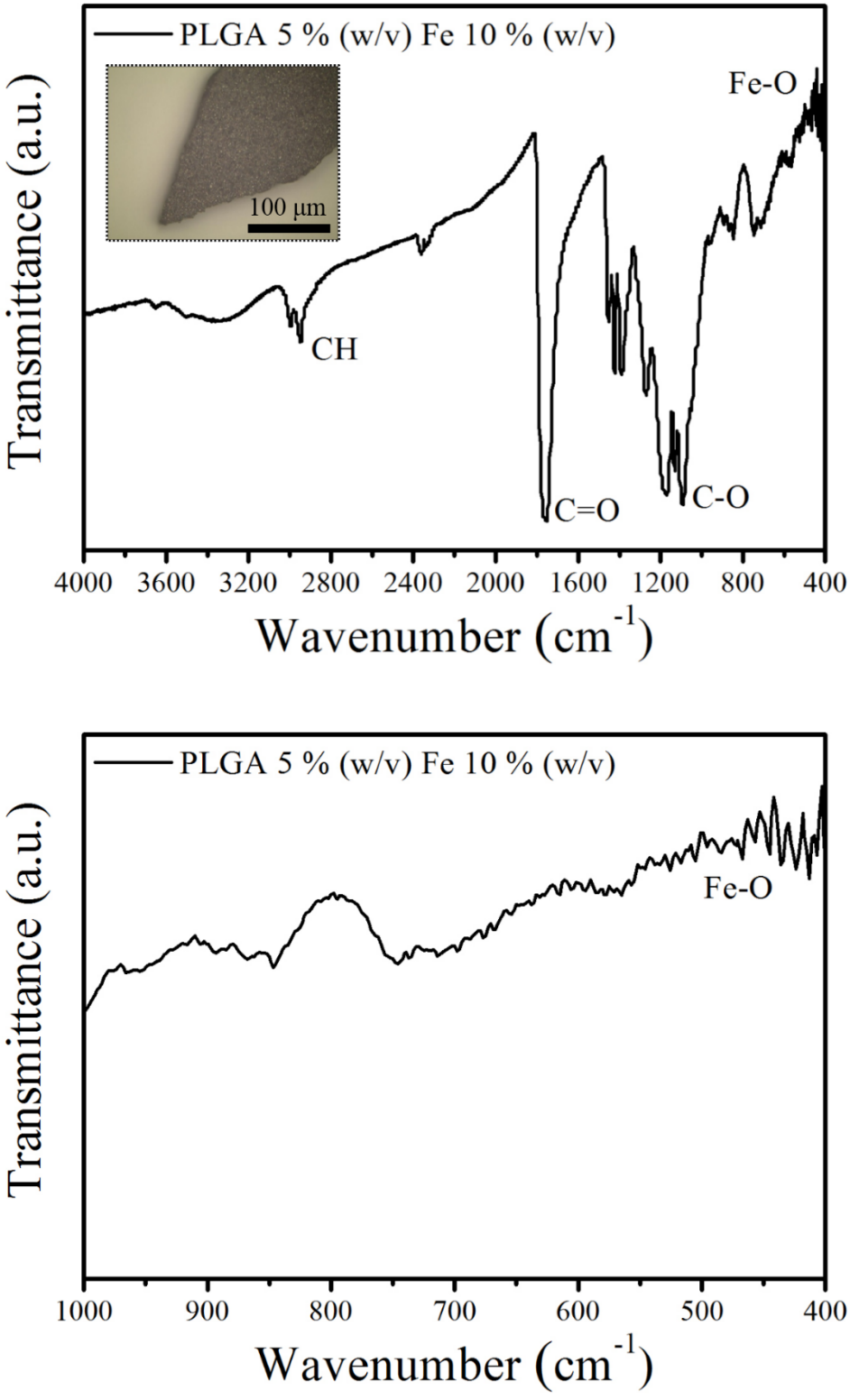

Figure 4.6 Fourier transform infrared (FT-IR) spectroscopy image of after formation of the Fe/PLGA microrobot with iron particles (10 % (w/v)).

4.2 Movement of the 2 dimensional biodegradable microrobot

4.2.1 Principles of translational and rotational motion of the fabricated 2 dimensional biodegradable microrobot

The 2 dimensional biodegradable microrobot for targeted drug delivery is accurately and rapidly controlled using an external magnetic field by electromagnetic actuation system (Minimag; Aeon Scientific, Switzerland). The electromagnetic actuation system of hemispherical type magnetic manipulator is consisted of five degrees of freedom which include three translational degrees of freedom on X, Y and Z axis and two rotational degrees of freedom X and Z axis such as Figure 3.6[27, 29, 102].

For translational by a magnetic force ($\mathbf{F_m}$) and rotational by a magnetic torque ($\mathbf{T_m}$) motion, the 2 dimensional biodegradable microrobot is controlled by applying an external magnetic field Figure 4.7-(a). Firstly, for rotational motion of the 2 dimensional biodegradable microrobot illustrated Figure 4.7-(b-1), after an external magnetic field generates a magnetic torque ($\mathbf{T_m}$), it is aligned to the magnetic field direction such as X axis with volume (**V**) of the magnetized material and a magnetic moment (**M**)

$$\boldsymbol{T_m = VM \times B} \qquad \textbf{(1)}$$

Where $\mathbf{T_m}$, **V**, **M** and **B** are magnetic torque ($\mathbf{T_m}$) from an external magnetic field, volume (**V**) of the magnetized objects, magnetic moment (**M**) and magnetic flux density (**B**). Secondly for translational motion of the 2 dimensional biodegradable microrobot illustrated Figure 4.7-(b-2), the magnetic force ($\mathbf{F_m}$) of the magnetized microrobot is given by

$$\boldsymbol{F_m = V(M \cdot \nabla)B} \qquad \textbf{(2)}$$

Where $\mathbf{F_m}$ and $\boldsymbol{\nabla B}$ are magnetic force ($\mathbf{F_m}$) and magnetic field gradient ($\boldsymbol{\nabla B}$) as follows equation (2). Therefore from following equation (**1**) and (**2**), a magnetic torque ($\mathbf{T_m}$) and

magnetic force ($\mathbf{F_m}$) can control the 2 dimensional biodegradable microrobot such as rotational and translational motion such as Figure 4.7[29, 102].

The 2 dimensional biodegradable microrobot is controlled by three forces which can affect translational velocity in an aqueous environment. Three forces, magnetic force ($\mathbf{F_m}$), resistive force ($\mathbf{F_r}$) with the surface friction and drag force and gravitational force ($\mathbf{F_g}$) is modeled by

$$\boldsymbol{F_m + F_r + F_g = m\frac{dv}{dt}} \quad \textbf{(3)}$$

Equation (3) shows that the magnetic force ($\mathbf{F_m}$) affects the translational velocity of the 2 dimensional biodegradable microrobot in an aqueous environment. To increase translational velocity of the 2 dimensional biodegradable microrobot, the magnetic force ($\mathbf{F_m}$) should be larger than resistive force ($\mathbf{F_r}$) and gravitational force ($\mathbf{F_g}$) in an aqueous environment. The Figure 4.8 shows a schematic design describing model of three forces. Where **m** is the mass and **v** is the translational velocity.

Therefore, from an equation (2) for translational motion and (3) for translational velocity, the 2 dimensional biodegradable microrobot is aligned to Z axis by constant magnetic field (**B**). And then after applying magnetic field to Z axis by constant magnetic field, the driving magnetic force ($\mathbf{F_m}$) from magnetic field gradient ($\boldsymbol{\nabla B}$) is applied to X axis for translational motion of the microrobot. In contrast translational motion, for rotational motion of the microrobot, the driving magnetic torque ($\mathbf{T_m}$) from magnetic flux density is applied such as Figure 4.7-(a). Consequently, the next chapter will show the actual translational and rotional movement of the 2 dimensional biodegradable microrobot based of principles from equation (1), (2) and (3)[27, 29, 102].

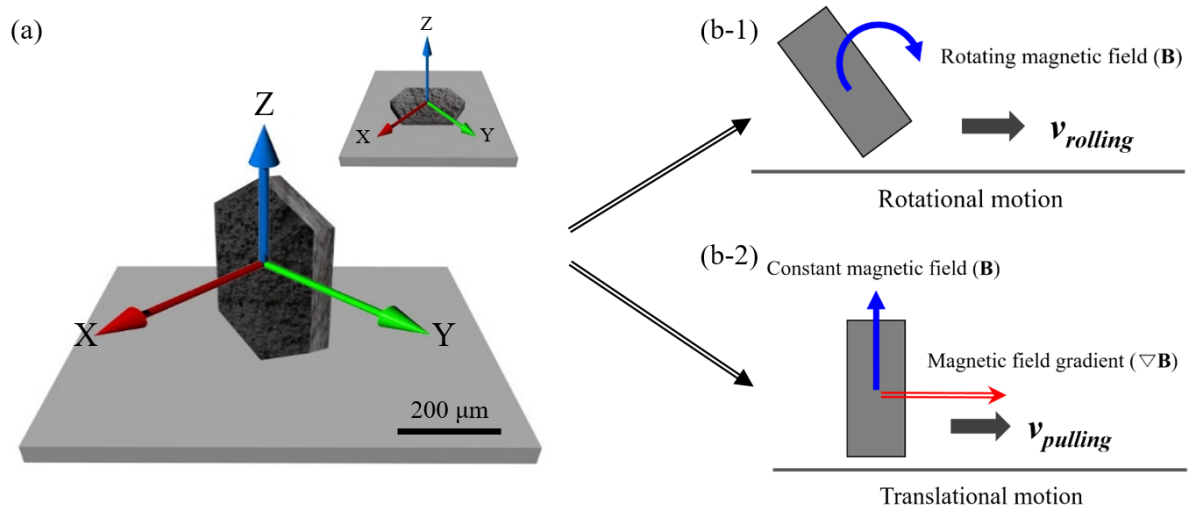

Figure 4.7 Schematic of rotational and translational motion of the 2 dimensional biodegradable microrobot (a) The 2 dimensional microrobot aligned along the Z axis. (b) Translational and rotational motion of microrobot.

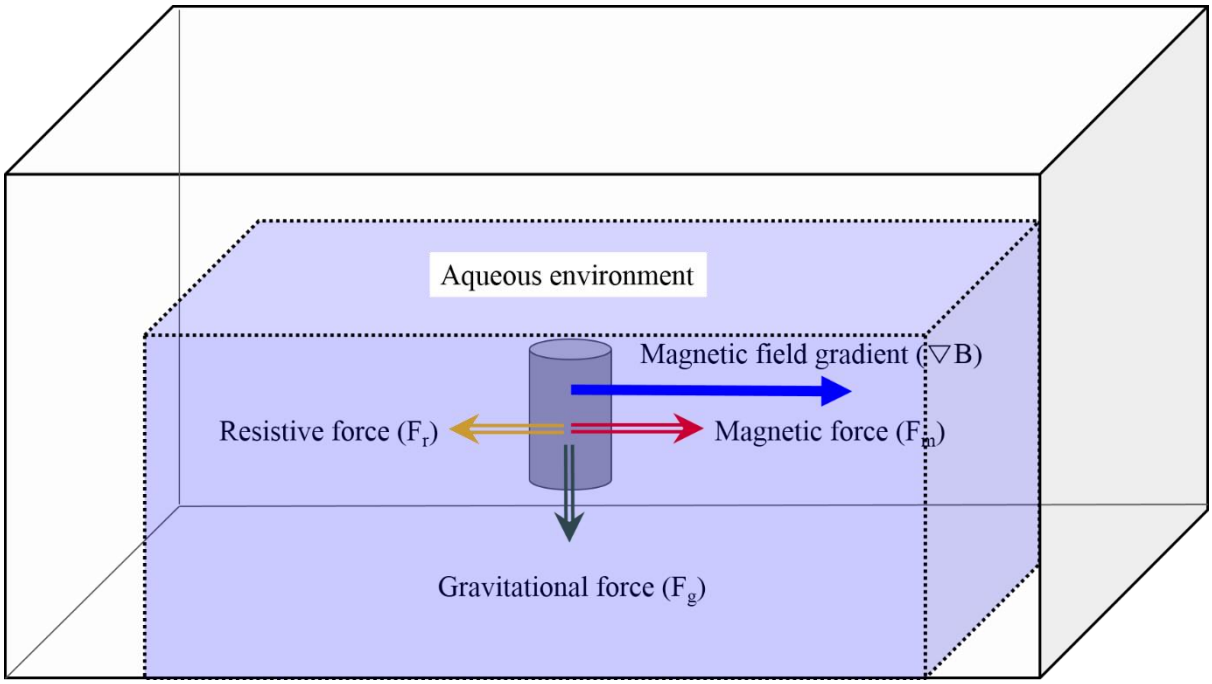

Figure 4.8 A schematic design of three forces with magnetic force (F_m), resistive force (F_r) and gravitational force (F_g) in an aqueous environment.

4.2.2 Time-lapsed image of translational and rotational motion the fabricated 2 dimensional biodegradable microrobot

Figure 4.9 and 11 show time-lapsed images of translational motion of the fabricated 2 dimensional biodegradable microrobot from the chapter 4.1 with square and rhombus type, having 5 % (w/v) of poly (D,L-lactide-co-glycolide acid) and 60 % (w/v) of iron particles. The time-lapsed image illustrated Figure 4.9 shows that before the fabricated 2 dimensional biodegradable microrobot of square type is aligned to Z axis by an external magnetic field. And then after aligned to Z axis, it is controlled by magnetic field gradient (**∇B**) to X axis. Figure 4.10 shows time-lapsed image for rotational motion of the fabricated 2 dimensional biodegradable microrobot of square type. It can be controlled by rotating magnetic field ($\mathbf{T_m}$) by different frequency such as equation (1).

In this paper, the fabricated 2 dimensional microrobot was conducted for translational and rotational motion of square and rhombus type, having 60 % (w/v) of iron particles. We can find that the fabricated 2 dimensional biodegradable microrobot of square type shows slower translational velocity than rhombus type because when the fabricated microrobot was applied by magnetic field gradient (**∇B**) to X axis, the fabricated microrobot of square type was affected by higher surface friction than rhombus type from around ground of square petri dish. Therefore, the fabricated microrobot of rhombus type is faster translational motion than square type. Consequently, we can know that various shapes of the fabricated 2 dimensional biodegradable microrobot affected to translational velocity when it was applied by magnetic field gradient (**∇B**) to X axis in an aqueous environment. The following chapter 4.2.3 will introduce translational velocity of the fabricated 2 dimensional biodegradable microrobot of rhombus type.

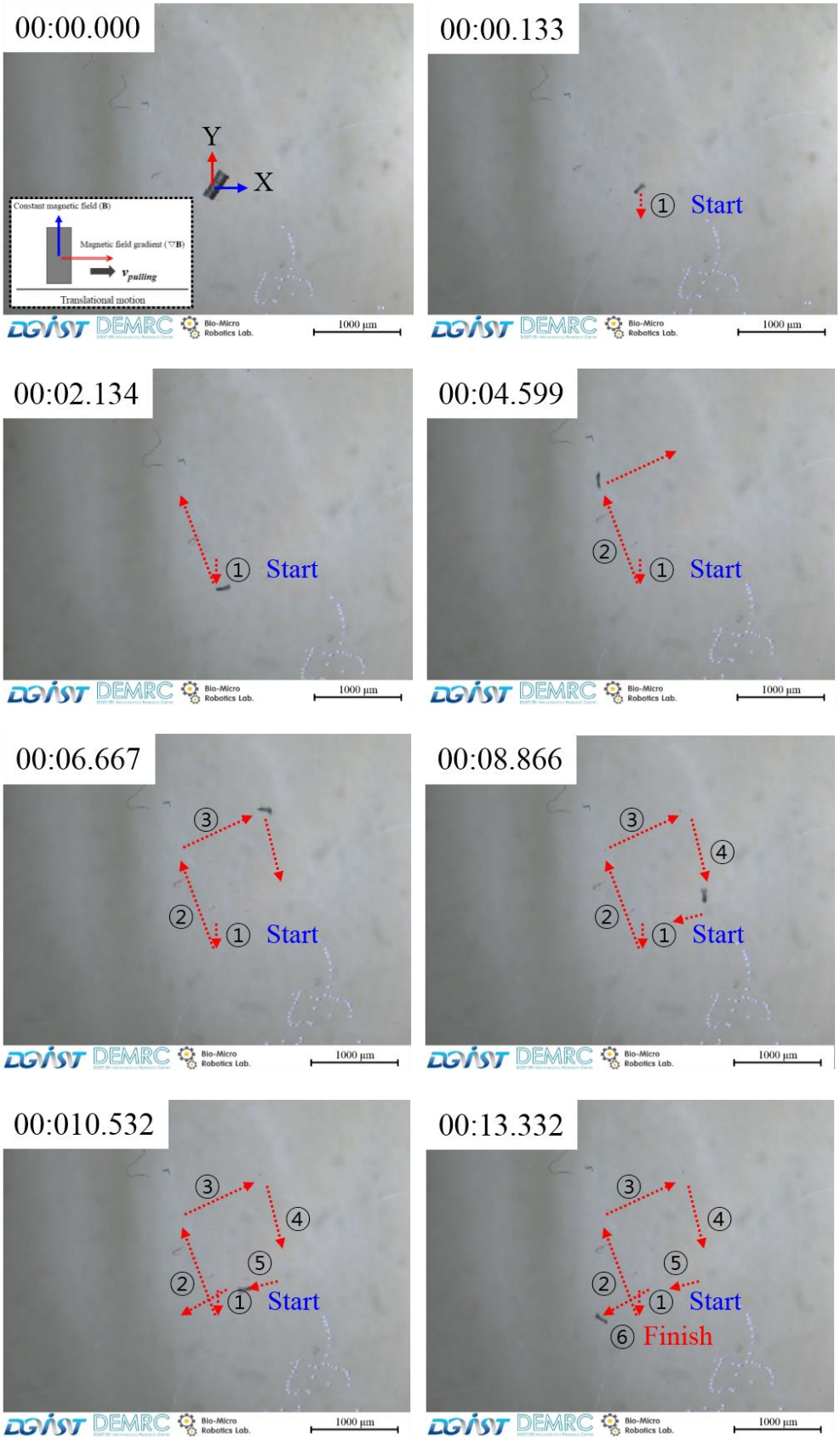

Figure 4.9 Time-lased image of translational motion using square type of the fabricated 2 dimensional biodegradable microrobot by an external magnetic field.

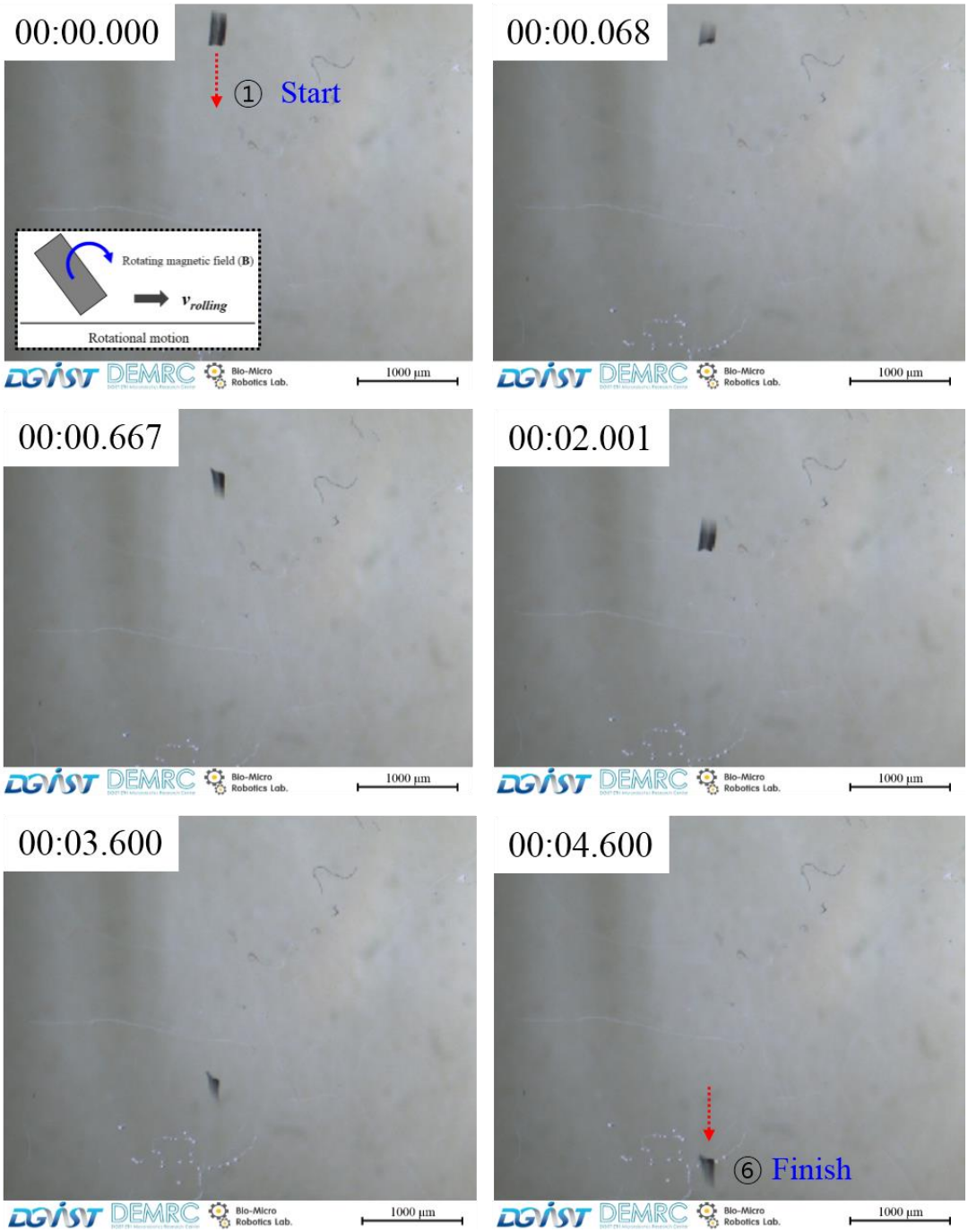

Figure 4.10 Time-lased image of translational motion using square type of the fabricated 2 dimensional biodegradable microrobot by an external magnetic field.

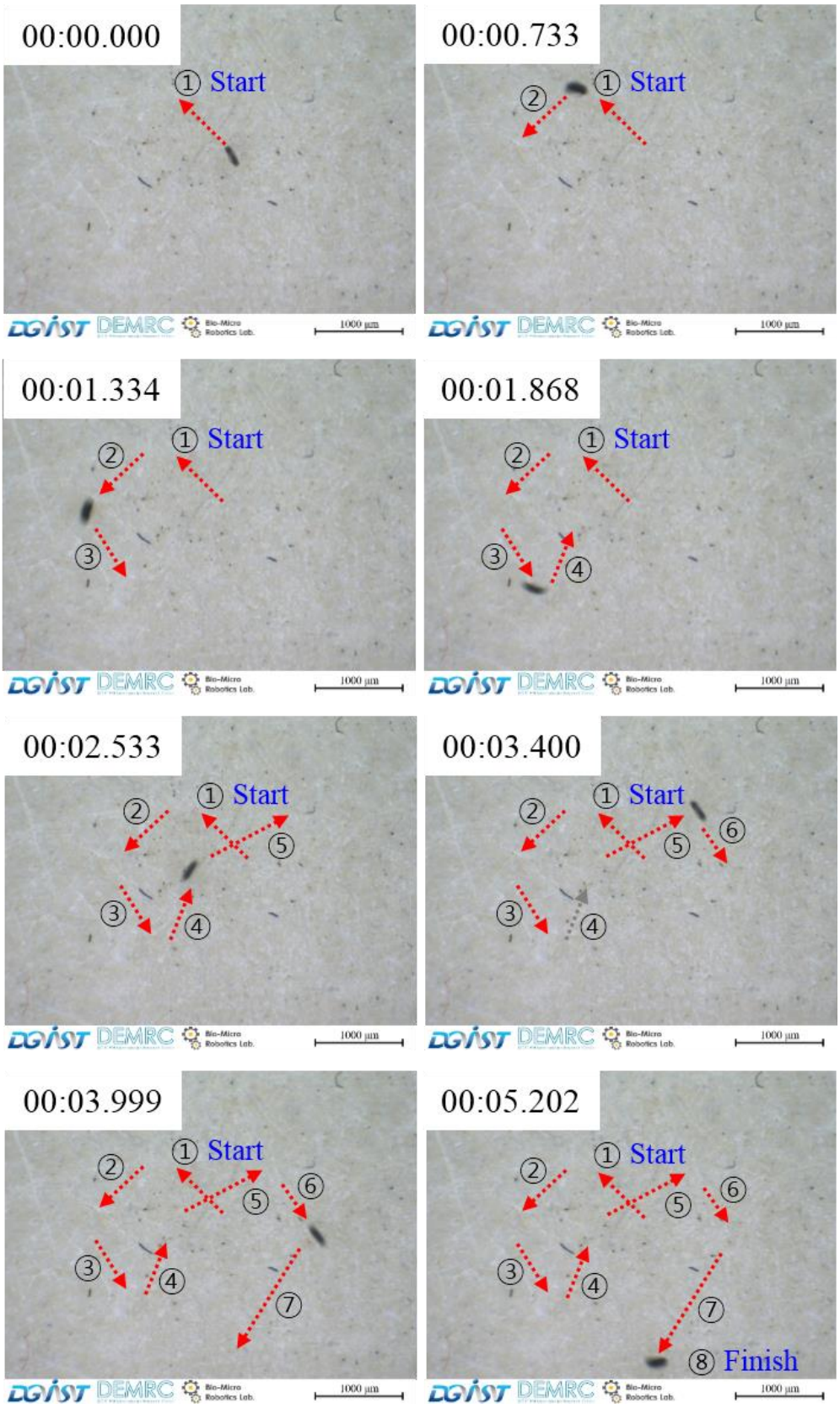

Figure 4.11 Time-lased image of translational motion using rhombus type of the fabricated 2 dimensional biodegradable microrobot by an external magnetic field.

4.2.3 Translational velocity of the fabricated 2 dimensional biodegradable microrobot

The chapter 4.2.2 introduced translation motion of the 2 dimensional biodegradable microrobot using square and rhombus type with 60 % (w/v) of iron particles. As result of the chapter 4.2.2, the 2 dimensional biodegradable microrobot of rhombus type was faster translational velocity than square type due to shape. Therefore in this chapter, we will show increasing translational velocity of rhombus type in different concentration of iron particles and magnetic field gradient ($\nabla \mathbf{B}$) with ranging from 100 to 400 mT/m.

The chapter 4.2.1 also introduced equation (2) for magnetic force ($\mathbf{F_m}$) to be controlled by an external magnetic field using electromagnetic actuation system. In general, the translational velocity of microrobot increase by volume ($\mathbf{V}$) of magnetic material and external magnetic field gradient ($\nabla \mathbf{B}$). In this experiment, we conducted the Figure 4.13 shows translational velocity of the fabricated 2 dimensional biodegradable microrobot with 10, 20, 30, 40, 50, and 60 % (w/v) of iron particles in different magnetic field gradient ($\nabla \mathbf{B}$) on X axis and constant magnetic field ($\mathbf{B}$) to Z axis illustrated Figure 4.12.

We could see that the translational velocity of the fabricated microrobot gradually increase in increasing magnetic field gradient. As a result of experiments, the fabricated 2 dimensional biodegradable microrobot with 10 % (w/v) of iron particles was the slowest approximately 1.8 mm/sec in 400 mT/m of magnetic field gradient ($\nabla \mathbf{B}$). In contrast to 10 % (w/v) of iron particles, the 60 % (w/v) of iron particles was the fastest approximately 2.8 mm/sec in the same magnetic field gradient ($\nabla \mathbf{B}$). Consequently, from experiment of translational velocity using the fabricated 2 dimensional biodegradable microrobot, we can know that the equation (2) coincide the results of the translational velocity. Therefore, the fabricated 2 dimensional biodegradable microrobot with anticancer drug will be possible to be applied for targeted drug delivery to a specific area.

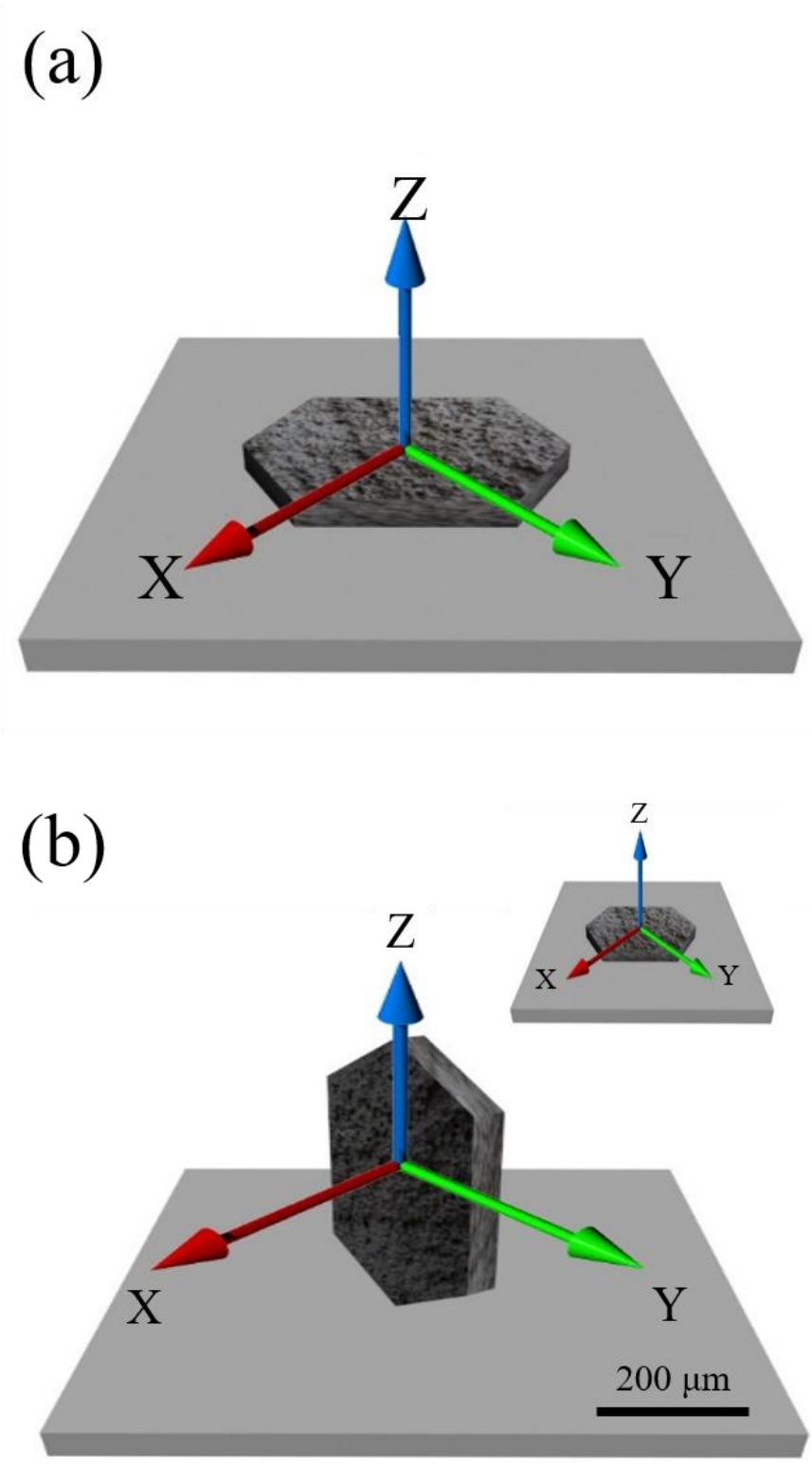

Figure 4.12 Schematic design of translation motion using the fabricated 2 dimensional biodegradable microrobot. (a) before alignment to Z axis by constant magnetic field. (b) After alignment to Z axis by constant magnetic field.

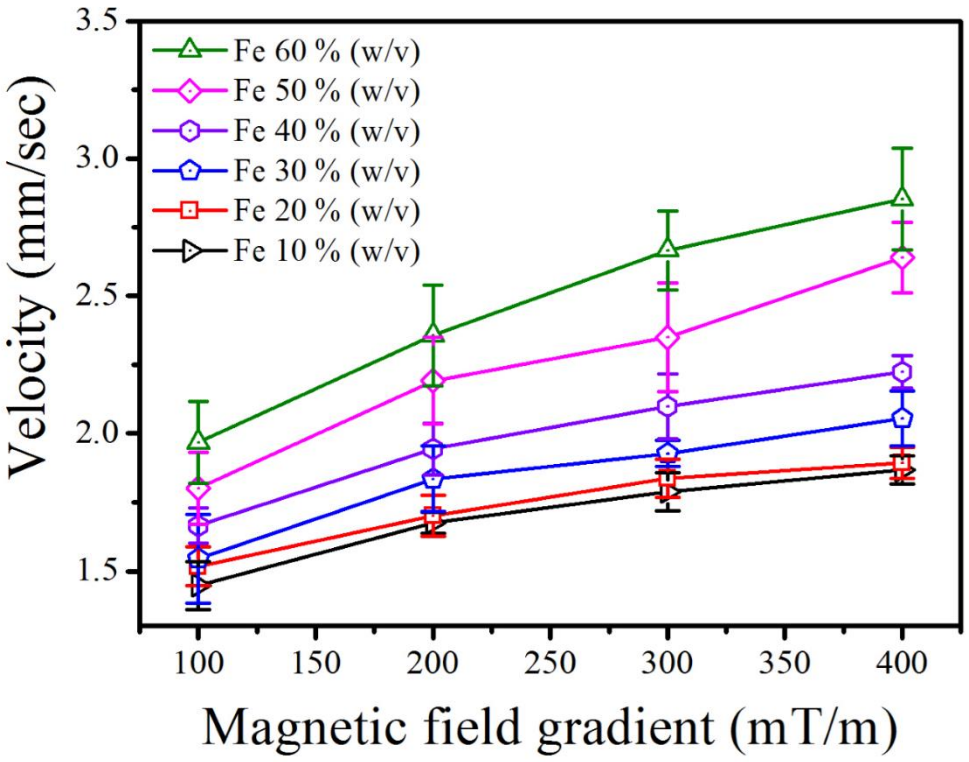

Figure 4.13 Translational velocity of the fabricated 2 dimensional biodegradable microrobot in different concentrations of iron particles and magnetic field gradient (∇B) to X axis and constant magnetic field (B) to Z axis using electromagnetic actuation system.

4.3 Degradation of the fabricated 2 dimensional biodegradable microrobot

4.3.1 Experimental procedure and degradation of the fabricated 2 dimensional biodegradable microrobot

Briefly, the chapter 2.1 introduced degradation and emission mechanism of biodegradable polymer such as poly (D,L-lactide-co-glycolide acid) by hydrolysis reaction in the human body. In this chapter based on the chapter 2.1, the fabricated 2 dimensional biodegradable microrobot was prepared in different concentrations of iron particles for experiments of degradation. It was consisted of 5 % (w/v) of poly (D,L lactide-co-glycolide acid) and 0, 10, 40 and 60 % (w/v) of iron particles in Phosphate buffered saline (PBS; 10mM, 45 mL, around pH 7) solution at 37 °C for 6 weeks.

The fabricated 2 dimensional biodegradable microrobot illustrated was immersed in Phosphate buffered saline (45 mL, around pH 7) solution and then measured every 1 week by using optical microscope and scanning electron microscope for 6 weeks. In addition, Phosphate buffered saline was also constantly changed every week. The fabricated 2 dimensional biodegradable microrobot was fixed on a slide glass shown in Figure 4.15 and 4.16 because it was difficult to re-collect decomposed microrobot from tube due to attached phenomenon on the bottom of a tube.

Figure 4.14 shows the relative degraded area from initial area of the fixed microrobot on a slide glass. The fixed microrobot with 0 % (w/v) of iron particles was sharply faster degraded than others the fixed microrobot with different concentration of iron particles. However, the fixed microrobot with 0 % (w/v) of iron particles was too much degraded to measure degraded area by hydrolysis reaction after 4 weeks approximately 45 % from initial area. In contrast to the fixed microrobot with 0 % (w/v) of iron particles, the fixed microrobot with 10, 40, and 60 % (w/v) of iron particles was degraded up to approximately 45, 30 and 20 %

from respective initial area after 6 weeks. Through the experiment of degradation, we can know that the different concentration of iron particles may affect the degradation of the fabricated microrobot. Figure 4.15 and 4.16 by optical microscope shows that the fixed microrobot, having different concentration of iron particles was degraded for 6 weeks. Figure 4.17 and 4.18 shows scanning electron microscope images for 6 weeks.

Many paper suggested that for complete degradation of biodegradable polymer such as poly (D,L-lactide-co-glycolide acid), molecular weight of polymer should be reduced and also the ratio between poly (lactic) and poly (glycolic) be adjusted [15, 28, 73, 77]. In addition, the size of spherical shape and thickness such as film structure of biodegradable polymer for targeted drug delivery should be reduced. Consequently, degradation of biodegradable polymer is affected by several factors such as concentration of iron particles.

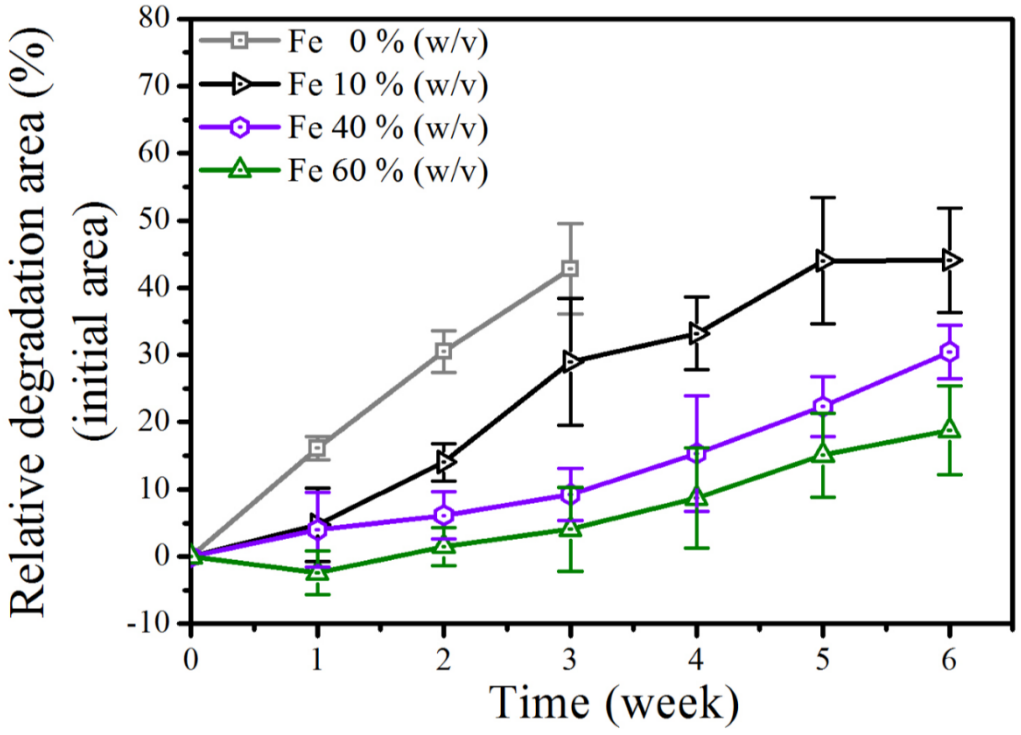

Figure 4.14 Degradation of the fabricated 2 dimensional biodegradable microrobot with 0, 10, 40 and 60% (w/v) of iron particles in PBS solution at 37 ºC for 6 weeks.

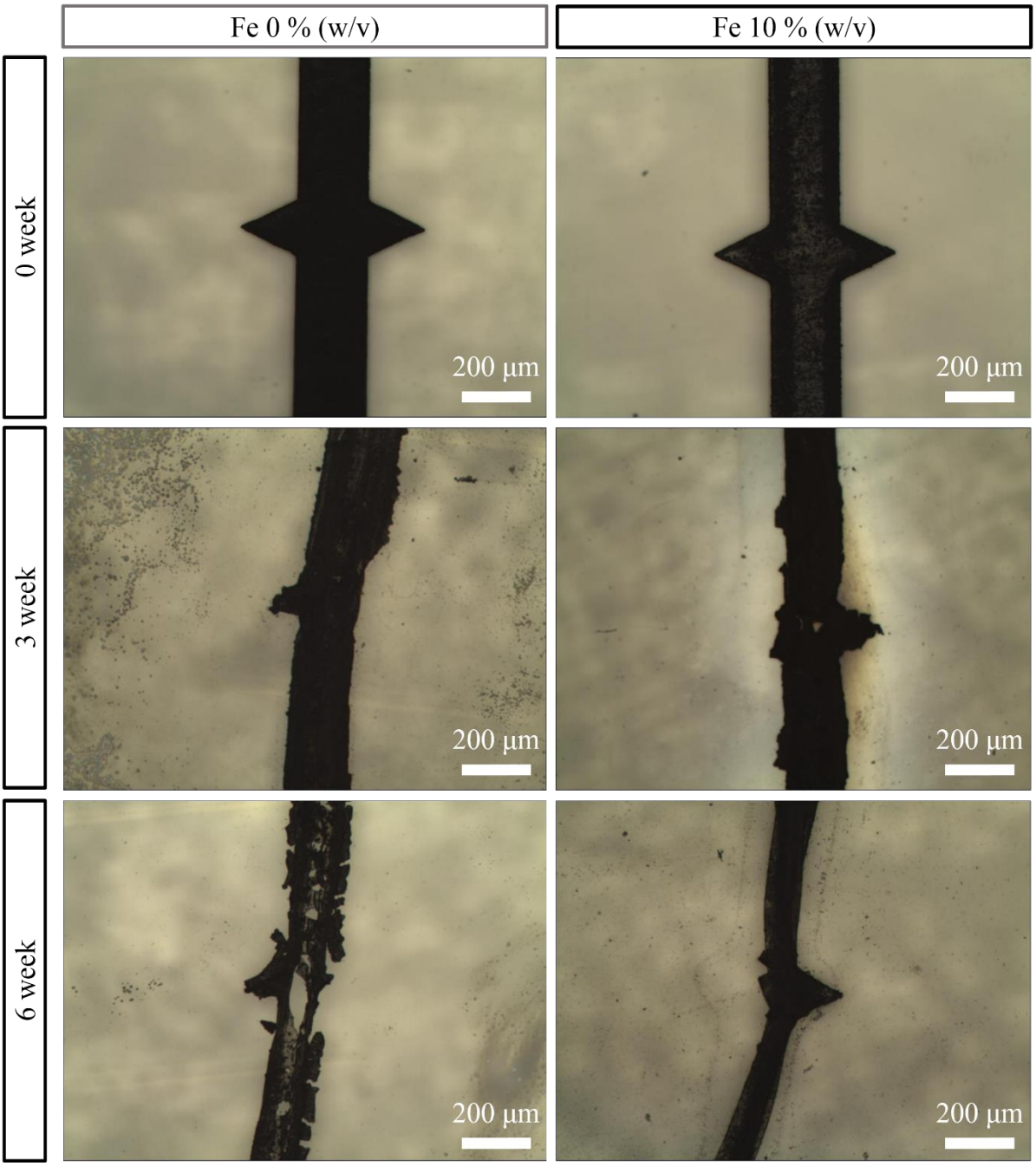

Figure 4.15 Optical images of the fabricated 2 dimensional biodegradable microrobot with 0 and 10 % (w/v) of iron particles after 0, 3 and 6 week.

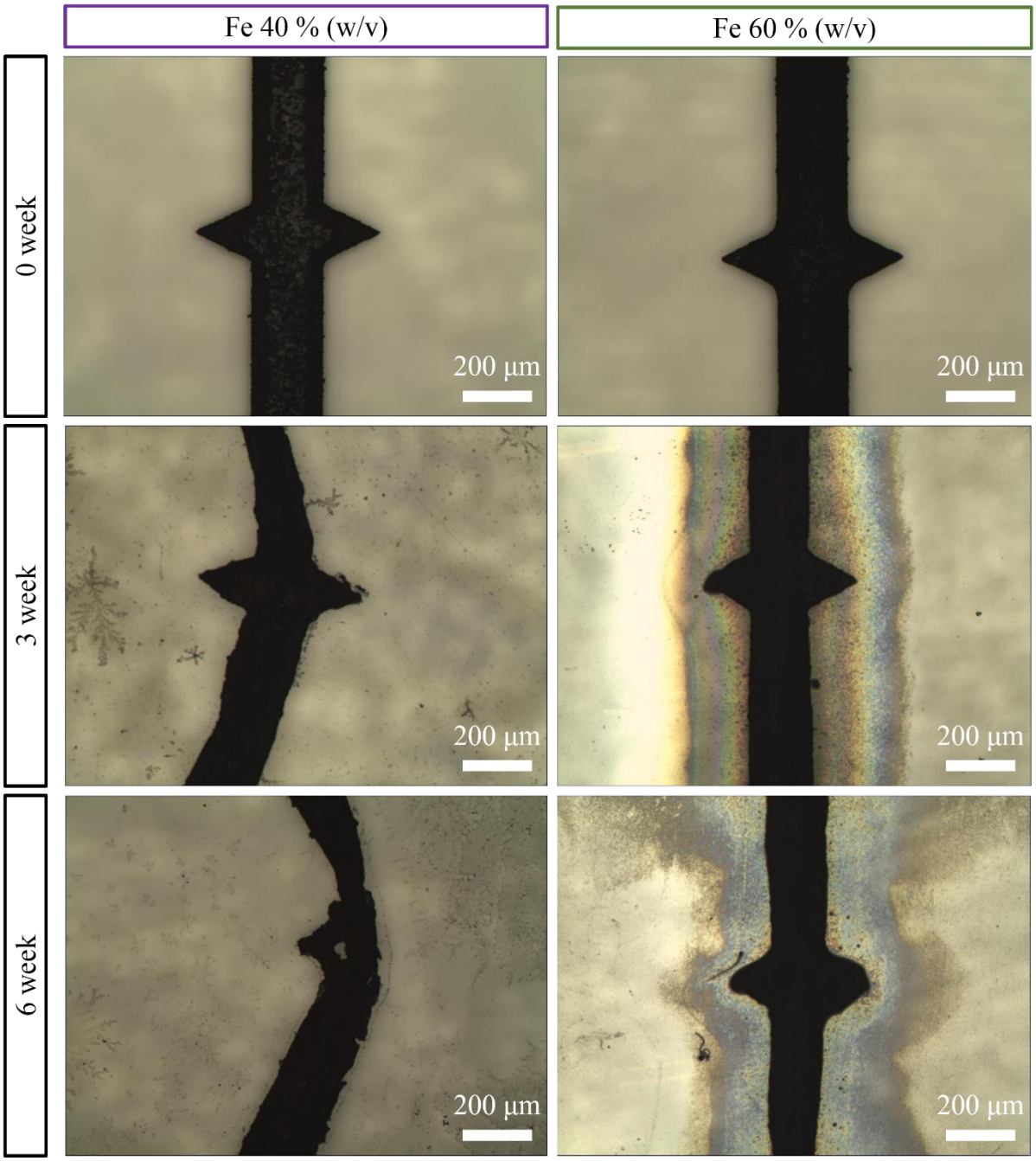

Figure 4.16 Optical images of the fabricated 2 dimensional biodegradable microrobot with 40 and 60 % (w/v) of iron particles after 0, 3 and 6 week.

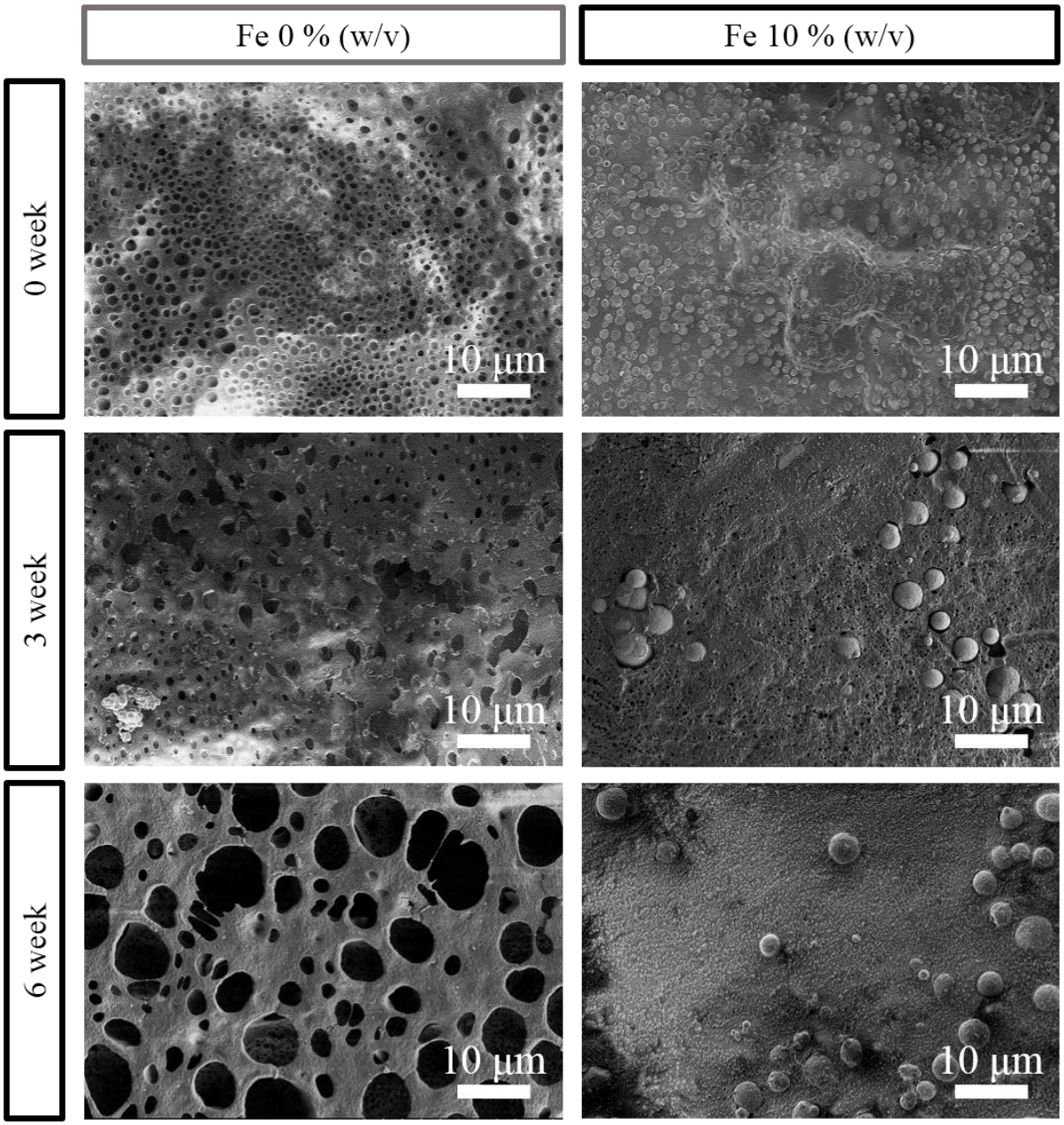

Figure 4.17 Scanning electron microscope images of the fabricated 2 dimensional biodegradable microrobot with 0 and 10 % (w/v) of iron particles after 0, 3 and 6 week.

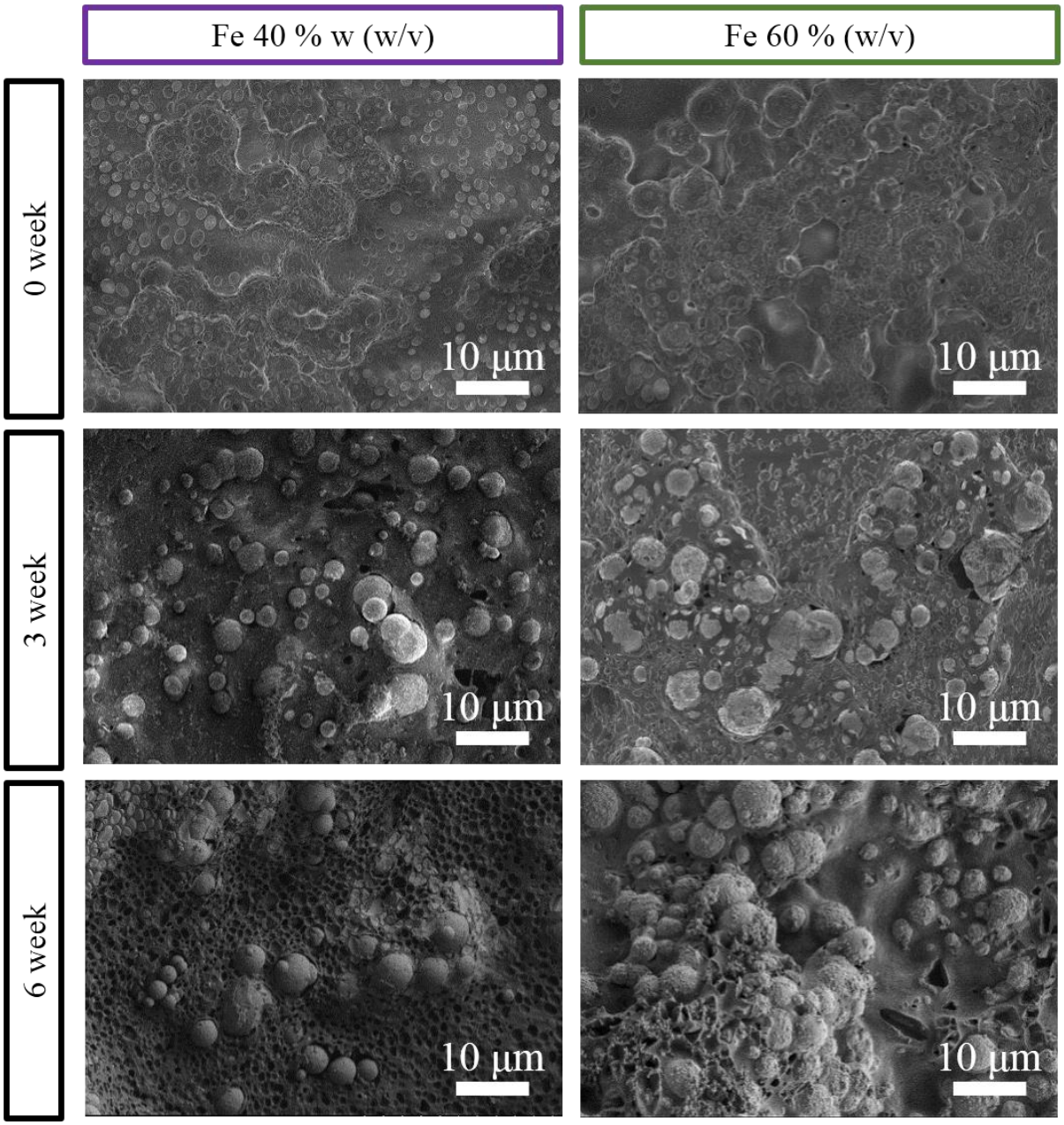

Figure 4.18 Scanning electron microscope images of the fabricated 2 dimensional biodegradable microrobot with 40 and 60 % (w/v) of iron particles after 0, 3 and 6 week.

4.3.2 Relationship between the amount of poly (D,L-lactide-co-glycolide acid) and iron particles in fabricated 2 dimensional biodegradable microrobot

In this chapter 4.3.2, we measured the amount of poly (D,L-lactide-co-glycolide acid) in different concentration of iron particles from the fabricated 2 dimensional biodegradable microrobot using UV-VIS-NIR spectrophotometer to find out the effect on the iron particles. The fabricated 2 dimensional biodegradable microrobot was prepared after fully dissolved poly (D,L-lactide-co-glycolide acid) in different concentration of iron particles in dichloromethane which can dissolve organic polymer.

Before measuring the amount of poly (D,L-lactide-co-glycolide acid) in different concentration of iron particles using UV-VIS-NIR spectrophotometer, we assumed that the amount of iron particles is affected to the amount of poly (D,L-lactide-co-glycolide acid) from the fabricated 2 dimensional biodegradable microrobot. After measurement, however the amount of iron particles was not significantly affected to degradation of the fabricated microrobot because the amount of poly (D,L-lactide-co-glycolide acid) was similar to 0, 10, 20, 50 and 60 % (w/v) of iron particles from measured wavelength (nm). Figure 4.19 shows the relative UV wavelength (nm) of poly (D,L-lactide-co-glycolide acid) in different concentration of iron particles. Figure 4.20 shows the relative percent of poly (D,L-lactide-co-glycolide acid) with respect to control from the Figure 4.19.

Therefore the measured results by UV-VIS-NIR spectrophotometer show that assuming the reason of slow degradation of the fabricated microrobot fail and another reason is contacted area of between poly (D,L-lactide-co-glycolide acid) and water because many references suggested that the degradation of polymer is affected by surface, size and molecular weight. The reason of slow degradation is contracted area because other conditions, size and molecular weight, are the same to experimental procedure[15, 28, 73, 77].

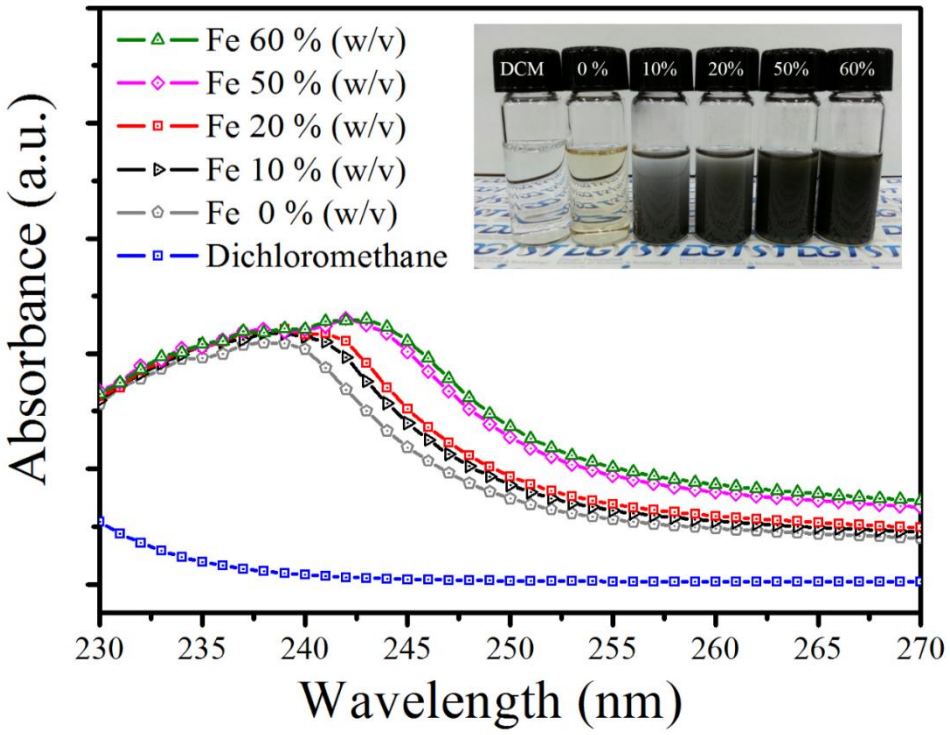

Figure 4.19 Relative UV wavelength of PLGA in the fabricated 2 dimensional biodegradable microrobot prepared in different concentrations of iron particles, 0 – 60 % (w/v) with respect to the control using UV-VIS-NIR spectrophotometer.

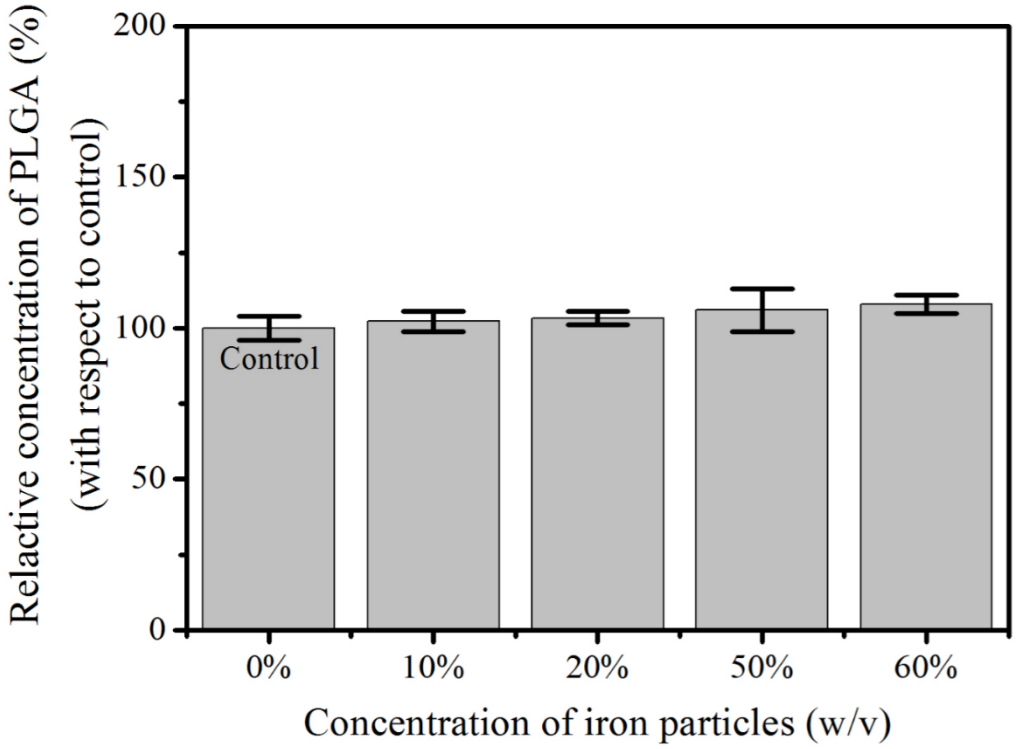

Figure 4.20 Relative concentration of PLGA in the fabricated 2 dimensional biodegradable microrobot prepared in different concentrations of iron particles, 0 – 60 % (w/v) with respect to the control.

4.4 Drug release from the fabricated 2 dimensional biodegradable microrobot with anticancer drug (5 Fluorouracil)

4.4.1 Experimental procedure and calibration curve of anticancer drug (5 Fluorouracil)

The chapter 2.1.2 introduced the fabrication procedure for the developed Fe/PLGA/5-FU microrobot for targeted drug delivery. The chapter 2.2.3 also showed the anticancer drug (5 Fluorouracil) which can prevent cell growth from a growing tumor. In this chapter 4.4.1, we present experimental procedure and calibration curve of anticancer drug (5 Fluorouracil)[166].

For the quantitative analysis of the amount of 5 Fluorouracil from the fabricated 2 dimensional biodegradable microrobot, 5 Fluorouracil was dissolved in PBS solution (10 mL) with ranging from 50 to 500 μM. And then we measured UV wavelength (nm) 5 Fluorouracil (266 nm) by UV-VIS-NIR spectrophotometer. As result of measurement by UV-VIS-NIR spectrophotometer, the UV wavelength (50 - 500 μM) was obtained illustrated Figure 4.21. From the measured UV wavelengths, the each of the UV wavelengths was calculated for calibration curve of 5 Fluorouracil. Figure 4.22 linearly shows the standard curve with the correlation coefficient value, $R^2 = 0.9995$[167].

After making standard curve of 5 Fluorouracil, the microrobot was prepared in different concentration of 5 Fluorouracil with ranging from 50 to 500 μM. It was immersed in PBS solution (10 mL) at 37 °C for 6 weeks. After 6 weeks, the amount of released drug from microrobot was measured by UV-VIS-NIR spectrophotometer illustrated Figure 4.23. We could calculate the standard curve from the fabricated microrobot in different concentration of 5 Fluorouracil. Figure 4.24 shows the standard curve from the fabricated microrobot. Consequently, we could make two calibration curves of 5 Fluorouracil and the amount of released drug from the fabricated microrobot in different concentration of 5 Fluorouracil and know the quantitative amount of drug in the fabricated 2 dimensional biodegradable microrobot.

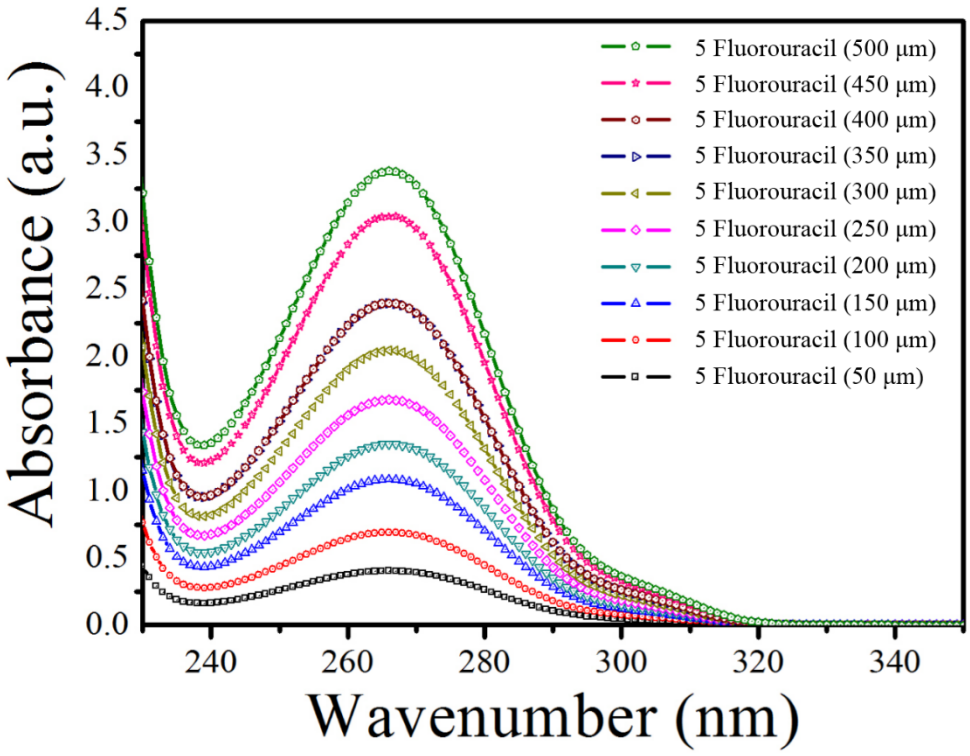

Figure 4.21 UV wavelengths by UV-VIS-NIR spectrophotometer for calibration curve of 5 Fluorouracil with ranging from 0 – 500 µM.

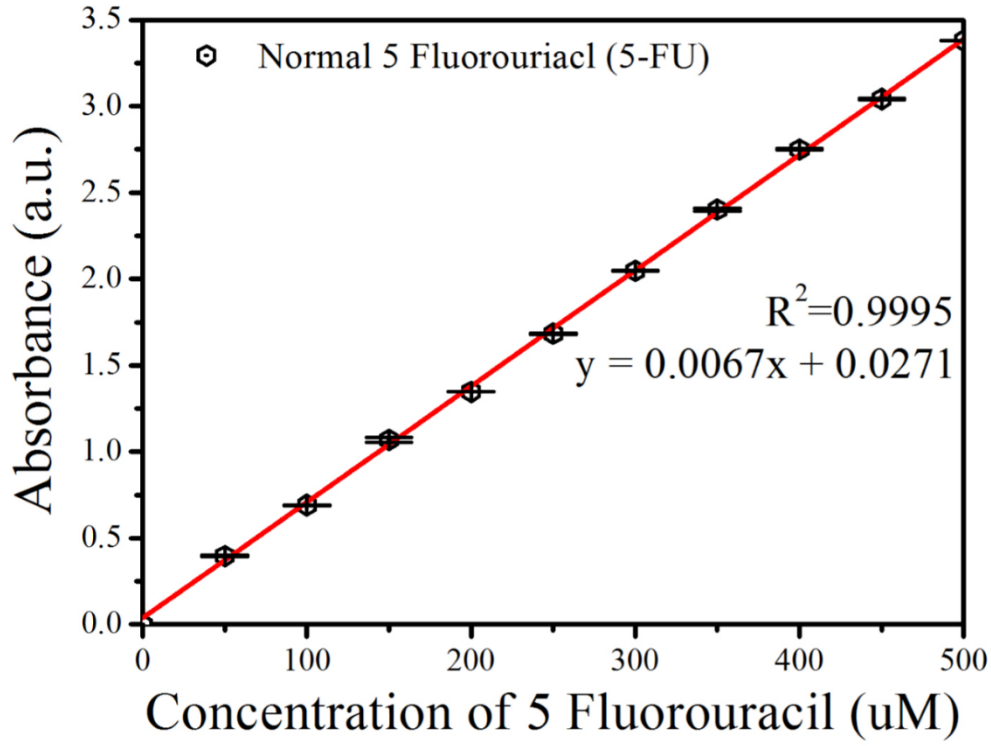

Figure 4.22 Calibration curve of 5 Fluorouracil, having the correlation coefficient value with ranging from 0 – 500 µM.

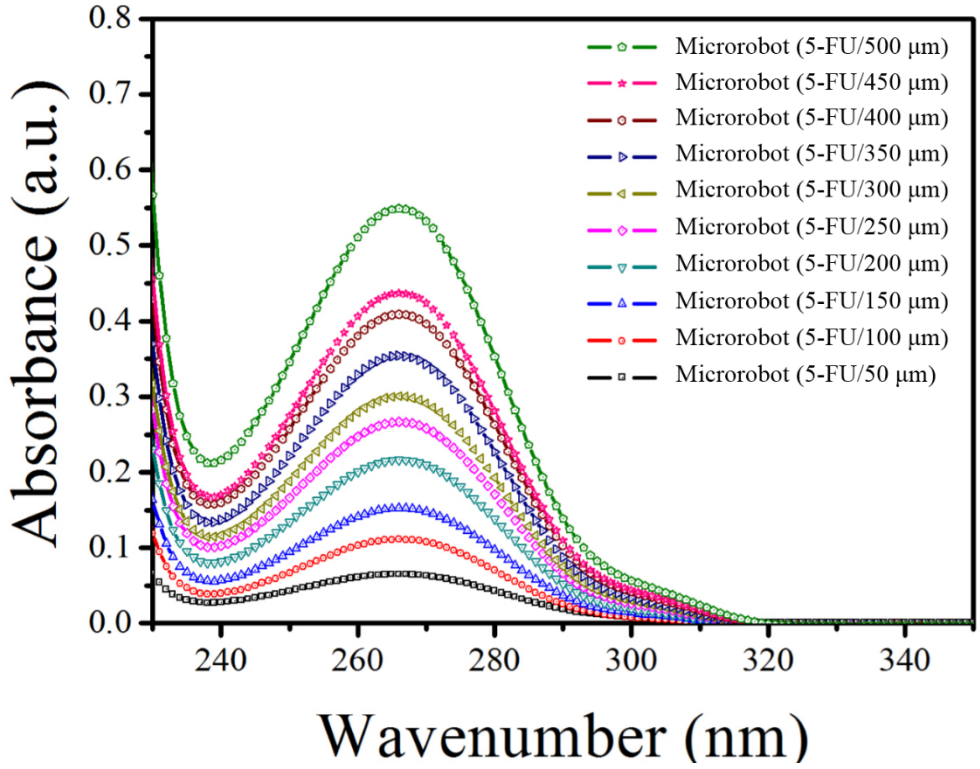

Figure 4.23 UV wavelengths by UV-VIS-NIR spectrophotometer for calibration curve of the fabricated 2 dimensional biodegradable microrobot with ranging from 0 – 500 µM.

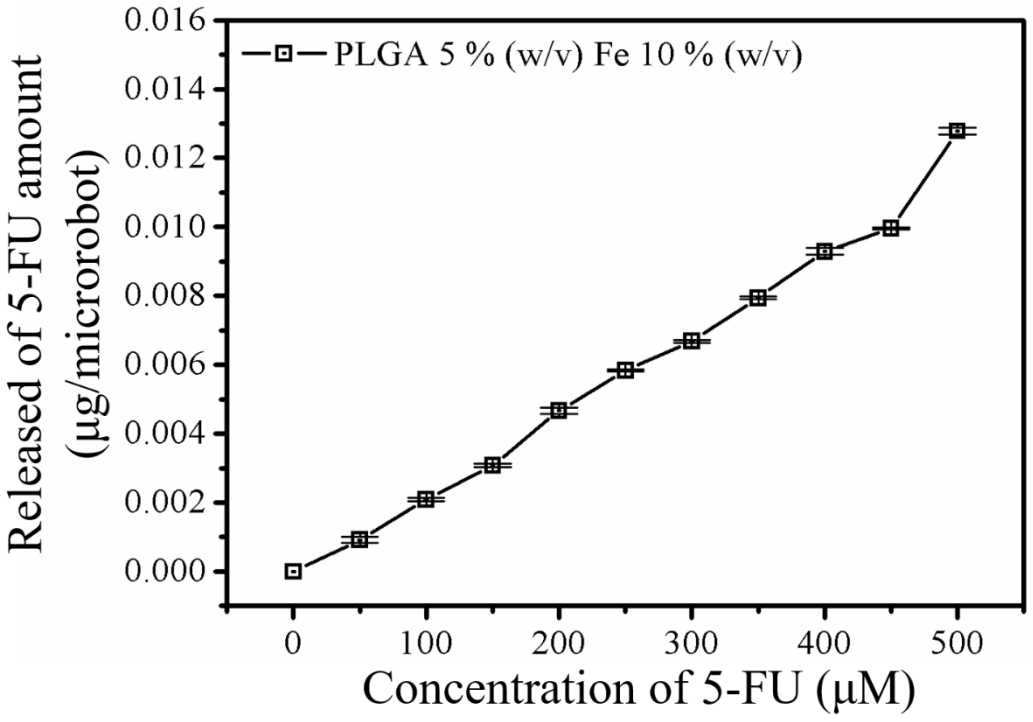

Figure 4.24 Calibration curve of the fabricated 2dimensional biodegradable microrobot with ranging from 0 – 500 µM.

4.4.2 Drug release from the fabricated 2 dimensional biodegradable microrobot

In this chapter 4.4.2 from the chapter 4.4.1, we present the results of the amount of released drug at 37 °C for 6 weeks. For experiment of drug release from the fabricated 2 dimensional biodegradable microrobot, it was fabricated with 5 % (w/v) of poly (D,L-lactide-co-glycolide acid), 10 % (w/v) of iron particles and 500 μM of 5 Fluorouracil. The prepared microrobot was degraded in PBS (10 ml, around pH 7) solution at 37 °C for 6 weeks. 5-FU from the microrobot in PBS (10 ml, around pH 7) solution was monitored using UV-VIS-NIR spectrophotometer after 30 minutes, 1 hour, 3 hour, 6 hour, 12 hour, 24 hour, 2 day, 4 day, 7 day, 14 day, 21 day, 28 day, 35 day and 42 day respectively (n=3). After each of days, the released amount of 5 Fluorouracil in the prepared microrobot was measured and calculated based on standard curve of the Figure 4.24.

The fabricated 2 dimensional biodegradable microrobot contained approximately 0 to 0.013 μg/microrobot. It was important that the amount of released drug from the fabricated microrobot can be controlled by adjusting different concentration of 5 Fluorouracil, fabricating the microrobot. The drug from the fabricated microrobot was released approximately 50 % and 90 % within 2 days and 3 weeks illustrated Figure 4.25. Figure 4.26 shows also that the drug is sharply burst within 2 days approximately 50 % due to wide surface of the fabricated microrobot and high solubility of 5 Fluorouracil in water[141, 144-146, 166].

Consequently, the chapter 4.4.2 shows experimental procedure and results of released drug from the fabricated microrobot. The fabricated 2 dimensional biodegradable microrobot also successfully encapsulated and released anticancer drug (5 Fluorouracil) for targeted drug delivery to a specific area.

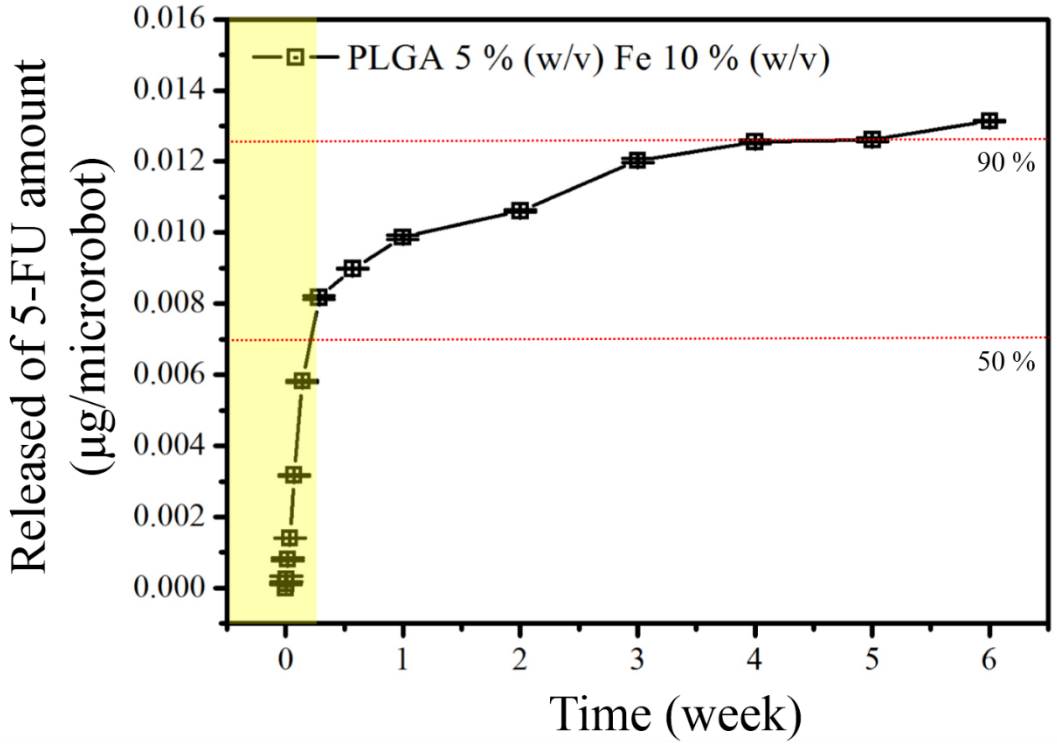

Figure 4.25 Drug release profile of a fabricated 2 dimensional biodegradable microrobot with 5 % (w/v) of poly (D,L-lactide-co-glycolide acid), 10% (w/v) of iron particles and 500 µM of 5 Fluroruracil for 6 weeks.

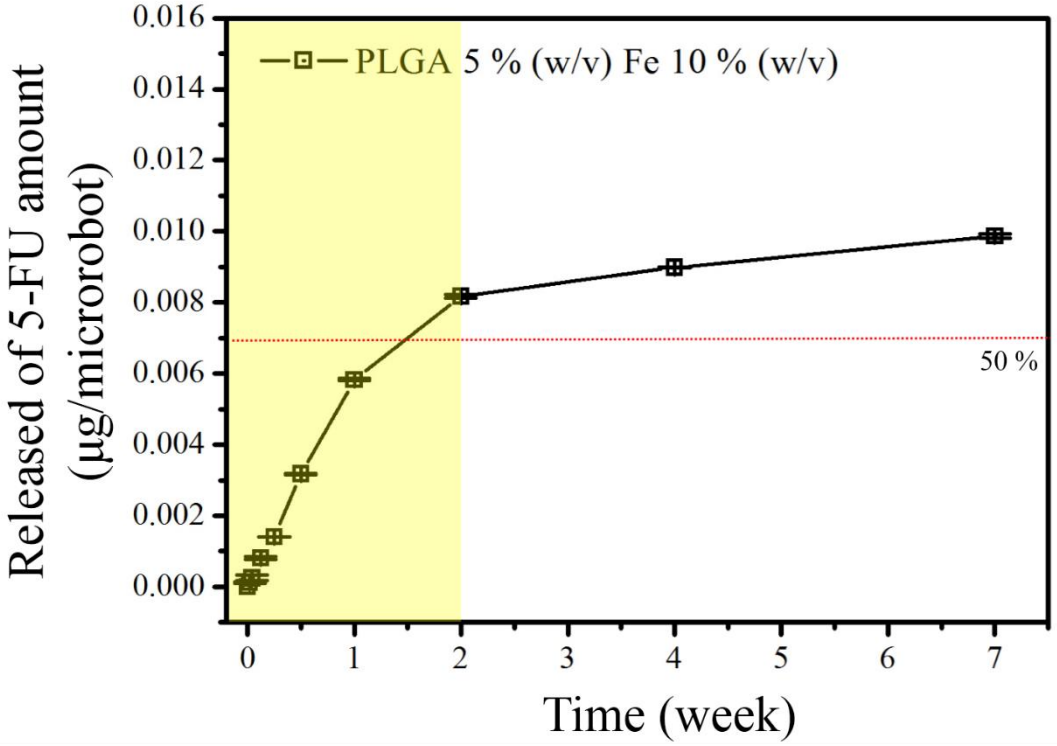

Figure 4.26 Burst drug release profile of a fabricated 2 dimensional biodegradable microrobot with 5 % (w/v) of poly (D,L-lactide-co-glycolide acid), 10% (w/v) of iron particles and 500 µM of 5 Fluroruracil for 1 weeks.

4.5 Discussion

In recent, developed microrobot coated and small particles encapsulated anticancer drug for targeted drug delivery was introduced to substitute and improve for existing therapies because it has gradually been developed to reduce adverse effects and improve the efficiency of drug. However above introduced study showed several problems to be applied in the human body, which cannot be degraded from microrobot and is low efficiency from small particles due to blood circulation[2-4, 25, 27, 158].

In this thesis, the developed 2 dimensional biodegradable microrobot was fabricated with biodegradable polymer (poly (D,L-lactide-co-glycolide acid)), magnetic particles (iron average < 10μm) and anticancer drug (5 Fluorouracil) to improve efficiency of drug release and overcome specific issues of degradation. The chemical structure of the fabricated microrobot was measured by Fourier transform infrared spectroscopy and precisely controlled using external magnetic field by electromagnetic actuation system and then it could be decomposed in similar to blood environment such as PBS solution at 37 ˚C for 6 weeks. For targeted drug delivery, the fabricated microrobot could contain different concentration of anticancer drug using dipping method and release drug from itself. Therefore, the developed 2 dimensional biodegradable microrobot was successfully fabricated and characterized.

However, in this thesis the developed 2 dimensional biodegradable microrobot with anticancer drug (5 Fluorouracil) was not conducted with experiments about cytotoxicity of biodegradable polymer (poly (D,L-lactide-co-glycolide acid)) and magnetic particles (iron average < 10μm) also and compared with drug delivery efficiency of the conventional microrobot. In the future, for *in vivo* experiment after *in vitro* experiment using the developed microrobot, I should take care that many paper refer to that magnetic particles can leave the blood vessel through metabolic pathway, when particles are smaller than 100 nm[168-173].

Consequently, in this thesis, I did not conduct some experiments about cytotoxicity of biodegradable polymer and magnetic particles also affect the actual cancer cells from the developed 2 dimensional biodegradable microrobot with anticancer drug (5 Fluorouracil) [174, 175]. Therefore, in the future, I will conduct experiments to prove targeted drug delivery efficiency of the developed 2 dimensional biodegradable microrobot.

5. CONCLUSIONS

In this thesis, these experiments have demonstrated facile and simple dipping method to fabricate the magnetically actuated and biodegradable 2 dimensional microrobots with various shape for biomedical application such as targeted drug delivery. They can encapsulate different concentration of anticancer drugs within itself with poly (D,L-lactide-co-glycolide acid), magnetic particles (average size < 10 μm), and anticancer drug (5 Fluorouracil) without the need for an additional drug loading procedure. Anticancer drug was able to be simultaneously contained in the fabricated microrobot (thickness: 30 μm, width: 200 μm, length: 600 μm), forming a micro body with various 2 dimensional shapes by using UV-laser micro machining.

Movements of the developed and fabricated 2 dimensional biodegradable microrobot was remotely and accurately controlled by external power source such as magnetic field manipulated by an electromagnetic actuation(EMA) system. The fastest translational velocity of the fabricated 2 dimensional microrobot with 60 % (w/v) of magnetic particles was approximately 3 mm/s (≈1/5 body length per second). They have successfully loaded anticancer drug (5-FU) from 0 to 0.013 μg/microrobot and released drug in biological environment such as PBS solution (around pH 7.4). Drug content, drug release time, and complete degraded time can be modified by adjusting several conditions such as the size and thickness of microrobot, molecular weight of polymer and drug types.

In the future, magnetic particles in the fabricated microrobot will be changed from iron (Fe) micro- particles to iron oxide (Fe_3O_4) nano- particles because of cytotoxicity and biocompatibility of the microrobot with various shape to be applied for *in vivo* application. Additionally, it also will compare the results of changing degradation time according to the

molecular weight of polymer or types of drug such as hydrophobic and hydrophilic chemical property. Consequently, the developed and fabricated 2 dimensional biodegradable microrobot can contribute to *in vivo* application for targeted drug delivery to specific area and, eventually, advance of targeted therapies.

REFERENCES

[1] J. Yang, C. H. Lee, H. J. Ko, J. S. Suh, H. G. Yoon, K. Lee*, et al.*, "Multifunctional magneto-polymeric nanohybrids for targeted detection and synergistic therapeutic effects on breast cancer," *Angewandte Chemie International Edition,* vol. 46, pp. 8836-8839, 2007.

[2] J. Yang, C.-H. Lee, J. Park, S. Seo, E.-K. Lim, Y. J. Song*, et al.*, "Antibody conjugated magnetic PLGA nanoparticles for diagnosis and treatment of breast cancer," *Journal of Materials Chemistry,* vol. 17, pp. 2695-2699, 2007.

[3] R. Mhanna, F. Qiu, L. Zhang, Y. Ding, K. Sugihara, M. Zenobi-Wong*, et al.*, "Artificial Bacterial Flagella for Remote-Controlled Targeted Single-Cell Drug Delivery," *Small,* vol. 10, pp. 1953-1957, 2014.

[4] F. Qiu, R. Mhanna, L. Zhang, Y. Ding, K. Sugihara, M. Zenobi-Wong*, et al.*, "Artificial bacterial flagella functionalized with temperature-sensitive liposomes for biomedical applications," in *2013 Transducers & Eurosensors XXVII: The 17th International Conference on Solid-State Sensors, Actuators and Microsystems (TRANSDUCERS & EUROSENSORS XXVII)*, 2013, pp. 2130-2133.

[5] A. Göpferich, "Polymer bulk erosion," *Macromolecules,* vol. 30, pp. 2598-2604, 1997.

[6] A. Göpferich, "Mechanisms of polymer degradation and erosion," *Biomaterials,* vol. 17, pp. 103-114, 1996.

[7] J. Tamada and R. Langer, "Erosion kinetics of hydrolytically degradable polymers," *Proceedings of the National Academy of Sciences,* vol. 90, pp. 552-556, 1993.

[8] F. von Burkersroda, L. Schedl, and A. Göpferich, "Why degradable polymers undergo surface erosion or bulk erosion," *Biomaterials,* vol. 23, pp. 4221-4231, 2002.

[9] K. KODA, H. MIYAUCHI, C. KOSUGI, T. KAIHO, N. TAKIGUCHI, S. KOBAYASHI*, et al.*, "Tumor 5-FU-related mRNA Expression and Efficacy of Oral Fluoropyrimidines in Adjuvant Chemotherapy of Colorectal Cancer," *Anticancer Research,* vol. 36, pp. 5325-5331, 2016.

[10] V.-G. Roullin, J.-R. Deverre, L. Lemaire, F. Hindré, M.-C. Venier-Julienne, R. Vienet*, et al.*, "Anti-cancer drug diffusion within living rat brain tissue: an experimental study using [3 H](6)-5-fluorouracil-loaded PLGA microspheres," *European Journal of Pharmaceutics and Biopharmaceutics,* vol. 53, pp. 293-299, 2002.

[11] G. Winocur, J. Vardy, M. A. Binns, L. Kerr, and I. Tannock, "The effects of the anti-cancer drugs, methotrexate and 5-fluorouracil, on cognitive function in mice," *Pharmacol Biochem Behav,* vol. 85, pp. 66-75, Sep 2006.

[12] M. Chasin, *Biodegradable polymers as drug delivery systems* vol. 45: Informa Health Care, 1990.

[13] A. Dumitru, F. Espinosa, R. Garcia, G. Foschi, S. Tortorella, F. Valle*, et al.*, "In situ nanomechanical characterization of the early stages of swelling and degradation of a biodegradable polymer," *Nanoscale,* vol. 7, pp. 5403-5410, 2015.

[14] A. Kumari, S. K. Yadav, and S. C. Yadav, "Biodegradable polymeric nanoparticles based drug delivery systems," *Colloids and Surfaces B: Biointerfaces,* vol. 75, pp. 1-18, 2010.

[15] H. K. Makadia and S. J. Siegel, "Poly lactic-co-glycolic acid (PLGA) as biodegradable controlled drug delivery carrier," *Polymers,* vol. 3, pp. 1377-1397, 2011.

[16] A. Mohanty, M. Misra, and G. Hinrichsen, "Biofibres, biodegradable polymers and biocomposites: an overview," *Macromolecular materials and Engineering,* vol. 276, pp. 1-24, 2000.

[17] L. S. Nair and C. T. Laurencin, "Biodegradable polymers as biomaterials," *Progress in polymer science,* vol. 32, pp. 762-798, 2007.

[18] S. H. Oh and J. H. Lee, "Hydrophilization of synthetic biodegradable polymer scaffolds for improved cell/tissue compatibility," *Biomedical materials,* vol. 8, p. 014101, 2013.

[19] N. Shah, A. Railkar, F. Chen, R. Tarantino, S. Kumar, M. Murjani*, et al.*, "A biodegradable injectable implant for delivering micro and macromolecules using poly (lactic-co-glycolic) acid (PLGA) copolymers," *Journal of Controlled Release,* vol. 27, pp. 139-147, 1993.

[20] G. Singh, T. Kaur, R. Kaur, and A. Kaur, "Recent biomedical applications and patents on biodegradable polymer-PLGA," *International Journal of Pharmacology and Pharmaceutical Sciences,* vol. 1, pp. 30-42, 2014.

[21] R. Yang, T. Chen, H. Chen, and W. Wang, "Fabrication of biodegradable polymer (PLGA) microstructures and applications in controlled drug delivery," in *Micromachining and Microfabrication*, 2004, pp. 130-137.

[22] J. Han, J. Zhen, G. G. Van Du Nguyen, Y. Choi, S. Y. Ko, J.-O. Park*, et al.*, "Hybrid-Actuating Macrophage-Based Microrobots for Active Cancer Therapy," *Scientific Reports,* vol. 6, 2016.

[23] H. Li, G. Go, S. Y. Ko, J.-O. Park, and S. Park, "Magnetic actuated pH-responsive hydrogel-based soft micro-robot for targeted drug delivery," *Smart Materials and Structures,* vol. 25, p. 027001, 2016.

[24] W. Gao, X. Feng, A. Pei, C. R. Kane, R. Tam, C. Hennessy*, et al.*, "Bioinspired helical microswimmers based on vascular plants," *Nano letters,* vol. 14, pp. 305-310, 2013.

[25] S. Kim, S. Lee, J. Lee, B. J. Nelson, L. Zhang, and H. Choi, "Fabrication and Manipulation of Ciliary Microrobots with Non-reciprocal Magnetic Actuation," *Scientific Reports,* vol. 6, 2016.

[26] W. Zhu, J. Li, Y. J. Leong, I. Rozen, X. Qu, R. Dong*, et al.*, "3D-Printed Artificial Microfish," *Advanced Materials,* vol. 27, pp. 4411-4417, 2015.

[27] S. Kim, F. Qiu, S. Kim, A. Ghanbari, C. Moon, L. Zhang*, et al.*, "Fabrication and Characterization of Magnetic Microrobots for Three-Dimensional Cell Culture and Targeted Transportation," *Advanced Materials,* vol. 25, pp. 5863-5868, 2013.

[28] G. Acharya, C. S. Shin, K. Vedantham, M. McDermott, T. Rish, K. Hansen*, et al.*, "A study of drug release from homogeneous PLGA microstructures," *Journal of Controlled Release,* vol. 146, pp. 201-206, 2010.

[29] B. E. Kratochvil, M. P. Kummer, S. Erni, R. Borer, D. R. Frutiger, S. Schürle*, et al.*, "MiniMag: a hemispherical electromagnetic system for 5-DOF wireless micromanipulation," in *Experimental Robotics*, 2014, pp. 317-329.

[30] W. Gao, Y. Zheng, R. Wang, H. Chen, X. Cai, G. Lu*, et al.*, "A smart, phase transitional and injectable DOX/PLGA-Fe implant for magnetic-hyperthermia-induced synergistic tumor eradication," *Acta biomaterialia,* vol. 29, pp. 298-306, 2016.

[31] C. E. DeSantis, C. C. Lin, A. B. Mariotto, R. L. Siegel, K. D. Stein, J. L. Kramer*, et al.*, "Cancer treatment and survivorship statistics, 2014," *CA: a cancer journal for clinicians,* vol. 64, pp. 252-271, 2014.

[32] R. Siegel, C. DeSantis, K. Virgo, K. Stein, A. Mariotto, T. Smith*, et al.*, "Cancer treatment and survivorship statistics, 2012," *CA: a cancer journal for clinicians,* vol. 62, pp. 220-241, 2012.

[33] C. Peters, M. Hoop, S. Pané, B. J. Nelson, and C. Hierold, "Degradable Magnetic Composites for Minimally Invasive Interventions: Device Fabrication, Targeted Drug Delivery, and Cytotoxicity Tests," *Advanced Materials,* vol. 28, pp. 533-538, 2016.

[34] S. Tottori, L. Zhang, F. Qiu, K. K. Krawczyk, A. Franco-Obregón, and B. J. Nelson, "Magnetic helical micromachines: fabrication, controlled swimming, and cargo transport," *Advanced materials,* vol. 24, pp. 811-816, 2012.

[35] Y. Sadzuka, E. Mochizuki, and Y. Takino, "Caffeine modulates the antitumor activity and toxic side effects of adriamycin," *Japanese journal of cancer research,* vol. 84, pp. 348-353, 1993.

[36] G. Joshi, R. Sultana, J. Tangpong, M. P. Cole, D. K. St Clair, M. Vore*, et al.*, "Free radical mediated oxidative stress and toxic side effects in brain induced by the anti cancer drug adriamycin: insight into chemobrain," *Free Radic Res,* vol. 39, pp. 1147-54, Nov 2005.

[37] I. R. Edwards and J. K. Aronson, "Adverse drug reactions: definitions, diagnosis, and management," *The Lancet,* vol. 356, pp. 1255-1259, 2000.

[38] N. Carelle, E. Piotto, A. Bellanger, J. Germanaud, A. Thuillier, and D. Khayat, "Changing patient perceptions of the side effects of cancer chemotherapy," *Cancer,* vol. 95, pp. 155-163, 2002.

[39] M. M. Gottesman, "Mechanisms of cancer drug resistance," *Annual review of medicine,* vol. 53, pp. 615-627, 2002.

[40] W. E. Evans and H. L. McLeod, "Pharmacogenomics—drug disposition, drug targets, and side effects," *New England Journal of Medicine,* vol. 348, pp. 538-549, 2003.

[41] M. Kobayashi, P. A. Wood, and W. J. Hrushesky, "Circadian chemotherapy for gynecological and genitourinary cancers," *Chronobiology international,* vol. 19, pp. 237-251, 2002.

[42] R. W. Ross and E. J. Small, "Osteoporosis in men treated with androgen deprivation therapy for prostate cancer," *The Journal of urology,* vol. 167, pp. 1952-1956, 2002.

[43] J. Sehouli, D. Stengel, D. Elling, O. Ortmann, J. Blohmer, H. Riess*, et al.*, "First-line chemotherapy with weekly paclitaxel and carboplatin for advanced ovarian cancer: a phase I study," *Gynecologic oncology,* vol. 85, pp. 321-326, 2002.

[44] K.-W. Jung, Y.-J. Won, H.-J. Kong, C.-M. Oh, D. H. Lee, and J. S. Lee, "Cancer statistics in Korea: incidence, mortality, survival, and prevalence in 2011," *Cancer Research and Treatment,* vol. 46, pp. 109-123, 2014.

[45] R. Siegel, C. DeSantis, and A. Jemal, "Colorectal cancer statistics, 2014," *CA: a cancer journal for clinicians,* vol. 64, pp. 104-117, 2014.

[46] E. Ward, C. DeSantis, A. Robbins, B. Kohler, and A. Jemal, "Childhood and adolescent cancer statistics, 2014," *CA: a cancer journal for clinicians,* vol. 64, pp. 83-103, 2014.

[47] S. Fusco, H.-W. Huang, K. E. Peyer, C. Peters, M. Häberli, A. Ulbers*, et al.*, "Shape-switching microrobots for medical applications: The influence of shape in drug delivery and locomotion," *ACS applied materials & interfaces,* vol. 7, pp. 6803-6811, 2015.

[48] S. Jeong, H. Choi, K. Cha, J. Li, J.-o. Park, and S. Park, "Enhanced locomotive and drilling microrobot using precessional and gradient magnetic field," *Sensors and Actuators A: Physical,* vol. 171, pp. 429-435, 2011.

[49] D. Li, H. Choi, S. Cho, S. Jeong, Z. Jin, C. Lee*, et al.*, "A hybrid actuated microrobot using an electromagnetic field and flagellated bacteria for tumor-targeting therapy," *Biotechnology and bioengineering,* vol. 112, pp. 1623-1631, 2015.

[50] S. J. Park, Y. K. Lee, S. Cho, S. Uthaman, I. K. Park, J. J. Min*, et al.*, "Effect of chitosan coating on a bacteria-based alginate microrobot," *Biotechnology and bioengineering,* vol. 112, pp. 769-776, 2015.

[51] F. Qiu and B. J. Nelson, "Magnetic Helical Micro-and Nanorobots: Toward Their Biomedical Applications," *Engineering,* vol. 1, pp. 021-026, 2015.

[52] J. C. Breger, C. Yoon, R. Xiao, H. R. Kwag, M. O. Wang, J. P. Fisher*, et al.*, "Self-folding thermo-magnetically responsive soft microgrippers," *ACS applied materials & interfaces,* vol. 7, pp. 3398-3405, 2015.

[53] A. Servant, F. Qiu, M. Mazza, K. Kostarelos, and B. J. Nelson, "Controlled In Vivo Swimming of a Swarm of Bacteria-Like Microrobotic Flagella," *Advanced Materials,* vol. 27, pp. 2981-2988, 2015.

[54] F. Z. Temel and S. Yesilyurt, "Confined swimming of bio-inspired microrobots in rectangular channels," *Bioinspiration & biomimetics,* vol. 10, p. 016015, 2015.

[55] F. Qiu, S. Fujita, R. Mhanna, L. Zhang, B. R. Simona, and B. J. Nelson, "Magnetic helical microswimmers functionalized with lipoplexes for targeted gene delivery," *Advanced Functional Materials,* vol. 25, pp. 1666-1671, 2015.

[56] K. Peyer, E. Siringil, L. Zhang, and B. Nelson, "Magnetic polymer composite artificial bacterial flagella," *Bioinspiration & biomimetics,* vol. 9, p. 046014, 2014.

[57] B. Jang, E. Gutman, N. Stucki, B. F. Seitz, P. D. Wendel-García, T. Newton*, et al.*, "Undulatory Locomotion of Magnetic Multilink Nanoswimmers," *Nano letters,* vol. 15, pp. 4829-4833, 2015.

[58] F. Qiu, L. Zhang, K. E. Peyer, M. Casarosa, A. Franco-Obregón, H. Choi*, et al.*, "Noncytotoxic artificial bacterial flagella fabricated from biocompatible ORMOCOMP and iron coating," *Journal of Materials Chemistry B,* vol. 2, pp. 357-362, 2014.

[59] Y. Ding, F. Qiu, X. Casadevall i Solvas, F. W. Y. Chiu, B. J. Nelson, and A. deMello, "Microfluidic-Based Droplet and Cell Manipulations Using Artificial Bacterial Flagella," *Micromachines,* vol. 7, p. 25, 2016.

[60] K. E. Peyer, S. Tottori, F. Qiu, L. Zhang, and B. J. Nelson, "Magnetic helical micromachines," *Chemistry–A European Journal,* vol. 19, pp. 28-38, 2013.

[61] S. Schuerle, S. Pané, E. Pellicer, J. Sort, M. D. Baró, and B. J. Nelson, "Helical and tubular lipid microstructures that are electroless-coated with CoNiReP for wireless magnetic manipulation," *small,* vol. 8, pp. 1498-1502, 2012.

[62] C. Peters, O. Ergeneman, P. D. W. García, M. Müller, S. Pané, B. J. Nelson*, et al.*, "Superparamagnetic Twist-Type Actuators with Shape-Independent Magnetic Properties and Surface Functionalization for Advanced Biomedical Applications," *Advanced Functional Materials,* vol. 24, pp. 5269-5276, 2014.

[63] M. Suter, L. Zhang, E. C. Siringil, C. Peters, T. Luehmann, O. Ergeneman*, et al.*, "Superparamagnetic microrobots: fabrication by two-photon polymerization and biocompatibility," *Biomedical microdevices,* vol. 15, pp. 997-1003, 2013.

[64] C. E. Astete and C. M. Sabliov, "Synthesis and characterization of PLGA nanoparticles," *Journal of Biomaterials Science, Polymer Edition,* vol. 17, pp. 247-289, 2006.

[65] M. G. Cascone, Z. Zhu, F. Borselli, and L. Lazzeri, "Poly (vinyl alcohol) hydrogels as hydrophilic matrices for the release of lipophilic drugs loaded in PLGA nanoparticles," *Journal of Materials Science: Materials in Medicine,* vol. 13, pp. 29-32, 2002.

[66] J. A. Champion, Y. K. Katare, and S. Mitragotri, "Making polymeric micro-and nanoparticles of complex shapes," *Proceedings of the National Academy of Sciences,* vol. 104, pp. 11901-11904, 2007.

[67] V. Diz, G. Leyva, R. Zysler, J. Awruch, and L. Dicelio, "Photophysics of an octasubstituted zinc (II) phthalocyanine incorporated into solid polymeric magnetic and non-magnetic PLGA–PVA nanoparticles," *Journal of Photochemistry and Photobiology A: Chemistry,* vol. 316, pp. 44-51, 2016.

[68] Y. Dong and S.-S. Feng, "Poly (D, L-lactide-co-glycolide)(PLGA) nanoparticles prepared by high pressure homogenization for paclitaxel chemotherapy," *International journal of pharmaceutics,* vol. 342, pp. 208-214, 2007.

[69] C. Fonseca, S. Simoes, and R. Gaspar, "Paclitaxel-loaded PLGA nanoparticles: preparation, physicochemical characterization and in vitro anti-tumoral activity," *Journal of Controlled Release,* vol. 83, pp. 273-286, 2002.

[70] J. Guan, N. Ferrell, L. J. Lee, and D. J. Hansford, "Fabrication of polymeric microparticles for drug delivery by soft lithography," *Biomaterials,* vol. 27, pp. 4034-4041, 2006.

[71] M. Hans and A. Lowman, "Biodegradable nanoparticles for drug delivery and targeting," *Current Opinion in Solid State and Materials Science,* vol. 6, pp. 319-327, 2002.

[72] S. Kayal and R. Ramanujan, "Doxorubicin loaded PVA coated iron oxide nanoparticles for targeted drug delivery," *Materials Science and Engineering: C,* vol. 30, pp. 484-490, 2010.

[73] D. Klose, F. Siepmann, K. Elkharraz, S. Krenzlin, and J. Siepmann, "How porosity and size affect the drug release mechanisms from PLGA-based microparticles," *International journal of pharmaceutics,* vol. 314, pp. 198-206, 2006.

[74] Y. Lu, M. Sturek, and K. Park, "Microparticles produced by the hydrogel template method for sustained drug delivery," *International journal of pharmaceutics,* vol. 461, pp. 258-269, 2014.

[75] G. Mittal, D. Sahana, V. Bhardwaj, and M. R. Kumar, "Estradiol loaded PLGA nanoparticles for oral administration: effect of polymer molecular weight and copolymer composition on release behavior in vitro and in vivo," *Journal of Controlled Release,* vol. 119, pp. 77-85, 2007.

[76] Y. Mo and L.-Y. Lim, "Paclitaxel-loaded PLGA nanoparticles: potentiation of anticancer activity by surface conjugation with wheat germ agglutinin," *Journal of controlled release,* vol. 108, pp. 244-262, 2005.

[77] J. Siepmann, N. Faisant, J. Akiki, J. Richard, and J. Benoit, "Effect of the size of biodegradable microparticles on drug release: experiment and theory," *Journal of Controlled Release,* vol. 96, pp. 123-134, 2004.

[78] M. Sturek, K. Park, and Y. Lu, "Microparticles Produced by the Hydrogel Template Method for Sustained Drug Delivery," 2014.

[79] F. Xu, F. Inci, O. Mullick, U. A. Gurkan, Y. Sung, D. Kavaz*, et al.*, "Release of magnetic nanoparticles from cell-encapsulating biodegradable nanobiomaterials," *ACS nano,* vol. 6, pp. 6640-6649, 2012.

[80] J.-W. Yoo and S. Mitragotri, "Polymer particles that switch shape in response to a stimulus," *Proceedings of the National Academy of Sciences,* vol. 107, pp. 11205-11210, 2010.

[81] Y. Chen, L. Jiang, R. Wang, M. Lu, Q. Zhang, Y. Zhou*, et al.*, "Injectable Smart Phase-Transformation Implants for Highly Efficient In Vivo Magnetic-Hyperthermia Regression of Tumors," *Advanced Materials,* vol. 26, pp. 7468-7473, 2014.

[82] T. G. Leong, C. L. Randall, B. R. Benson, A. M. Zarafshar, and D. H. Gracias, "Self-loading lithographically structured microcontainers: 3D patterned, mobile microwells," *Lab on a Chip,* vol. 8, pp. 1621-1624, 2008.

[83] K. Andreas, R. Zehbe, M. Kazubek, K. Grzeschik, N. Sternberg, H. Bäumler*, et al.*, "Biodegradable insulin-loaded PLGA microspheres fabricated by three different emulsification techniques: investigation for cartilage tissue engineering," *Acta biomaterialia,* vol. 7, pp. 1485-1495, 2011.

[84] G. Chen, "Degradation Behavior of Aliphatic Biodegradable Polyester," *Society of Plastics Engineers,* pp. 1-2, 2010.

[85] A. Muvaffak, I. Gurhan, U. Gunduz, and N. Hasirci, "Preparation and characterization of a biodegradable drug targeting system for anticancer drug delivery: Microsphere-antibody conjugate," *Journal of drug targeting,* vol. 13, pp. 151-159, 2005.

[86] R. Yang, T. Chen, H. Chen, and W. Wang, "Microfabrication of biodegradable (PLGA) honeycomb-structures and potential applications in implantable drug delivery," *Sensors and Actuators B: Chemical,* vol. 106, pp. 506-511, 2005.

[87] S. Ali, P. Doherty, and D. Williams, "Mechanisms of polymer degradation in implantable devices. 2. Poly (DL-lactic acid)," *Journal of biomedical materials research,* vol. 27, pp. 1409-1418, 1993.

[88] S. Ali, S.-P. Zhong, P. Doherty, and D. Williams, "Mechanisms of polymer degradation in implantable devices: I. Poly (caprolactone)," *Biomaterials,* vol. 14, pp. 648-656, 1993.

[89] R. Astaneh, M. Erfan, H. Moghimi, and H. Mobedi, "Changes in morphology of in situ forming PLGA implant prepared by different polymer molecular weight and its effect on release behavior," *Journal of pharmaceutical sciences,* vol. 98, pp. 135-145, 2009.

[90] K. A. Athanasiou, G. G. Niederauer, and C. M. Agrawal, "Sterilization, toxicity, biocompatibility and clinical applications of polylactic acid/polyglycolic acid copolymers," *Biomaterials,* vol. 17, pp. 93-102, 1996.

[91] R. De Alteriis, R. Vecchione, C. Attanasio, M. De Gregorio, M. Porzio, E. Battista*, et al.*, "A method to tune the shape of protein-encapsulated polymeric microspheres," *Scientific reports,* vol. 5, 2015.

[92] R. E. Eliaz and J. Kost, "Characterization of a polymeric PLGA-injectable implant delivery system for the controlled release of proteins," *Journal of biomedical materials research,* vol. 50, pp. 388-396, 2000.

[93] J. Key, A. L. Palange, F. Gentile, S. Aryal, C. Stigliano, D. Di Mascolo*, et al.*, "Soft discoidal polymeric nanoconstructs resist macrophage uptake and enhance vascular targeting in tumors," *ACS nano,* vol. 9, pp. 11628-11641, 2015.

[94] S. Lyu, R. Sparer, and D. Untereker, "Analytical solutions to mathematical models of the surface and bulk erosion of solid polymers," *Journal of Polymer Science Part B: Polymer Physics,* vol. 43, pp. 383-397, 2005.

[95] T. G. Park, "Degradation of poly (lactic-co-glycolic acid) microspheres: effect of copolymer composition," *Biomaterials,* vol. 16, pp. 1123-1130, 1995.

[96] S. N. Rothstein, W. J. Federspiel, and S. R. Little, "A unified mathematical model for the prediction of controlled release from surface and bulk eroding polymer matrices," *Biomaterials,* vol. 30, pp. 1657-1664, 2009.

[97] G. Scott, *Mechanisms of polymer degradation and stabilisation*: Springer, 1990.

[98] J.-H. Shim, J. Y. Kim, J. K. Park, S. K. Hahn, J.-W. Rhie, S.-W. Kang*, et al.*, "Effect of thermal degradation of SFF-based PLGA scaffolds fabricated using a multi-head deposition system followed by change of cell growth rate," *Journal of Biomaterials Science, Polymer Edition,* vol. 21, pp. 1069-1080, 2010.

[99] J. Siepmann and A. Göpferich, "Mathematical modeling of bioerodible, polymeric drug delivery systems," *Advanced drug delivery reviews,* vol. 48, pp. 229-247, 2001.

[100] K. E. Uhrich, S. M. Cannizzaro, R. S. Langer, and K. M. Shakesheff, "Polymeric systems for controlled drug release," *Chemical reviews,* vol. 99, pp. 3181-3198, 1999.

[101] J. Arias, V. Gallardo, S. Gomez-Lopera, R. Plaza, and A. Delgado, "Synthesis and characterization of poly (ethyl-2-cyanoacrylate) nanoparticles with a magnetic core," *Journal of Controlled Release,* vol. 77, pp. 309-321, 2001.

[102] A. Ghanbari, P. H. Chang, B. J. Nelson, and H. Choi, "Electromagnetic steering of a magnetic cylindrical microrobot using optical feedback closed-loop control," *International Journal of Optomechatronics,* vol. 8, pp. 129-145, 2014.

[103] A. Banerjee, J. Qi, R. Gogoi, J. Wong, and S. Mitragotri, "Role of nanoparticle size, shape and surface chemistry in oral drug delivery," *Journal of Controlled Release,* vol. 238, pp. 176-185, 2016.

[104] D. Sharma, R. Kumar Sharma, A. Bhatnagar, D. K Nishad, T. Singh, R. Gabrani*, et al.*, "Nose to Brain Delivery of Midazolam Loaded PLGA Nanoparticles: In Vitro and In Vivo Investigations," *Current drug delivery,* vol. 13, pp. 557-564, 2016.

[105] I. Khan, A. Gothwal, A. K. Sharma, P. Kesharwani, L. Gupta, A. K. Iyer*, et al.*, "PLGA nanoparticles and their versatile role in anticancer drug delivery," *Critical Reviews™ in Therapeutic Drug Carrier Systems,* vol. 33, 2016.

[106] P. Basto, F. Alexis, E. Levy-Nissenbaum, R. Langer, and O. Farokzhad, "Targeted aptamer-nanoparticles to diminish drug resistance of cancer cells in vitro study," *Une,* vol. 13, p. 15, 2016.

[107] A. Kumari, R. Singla, A. Guliani, and S. K. Yadav, "Biodegradable Nanoparticles and Their In Vivo Fate," in *Nanoscale Materials in Targeted Drug Delivery, Theragnosis and Tissue Regeneration*, ed: Springer, 2016, pp. 21-39.

[108] K. K. Chereddy, G. Vandermeulen, and V. Préat, "PLGA based drug delivery systems: Promising carriers for wound healing activity," *Wound Repair and Regeneration,* vol. 24, pp. 223-236, 2016.

[109] C. H. Villa, A. C. Anselmo, S. Mitragotri, and V. Muzykantov, "Red blood cells: Supercarriers for drugs, biologicals, and nanoparticles and inspiration for advanced delivery systems," *Advanced drug delivery reviews,* 2016.

[110] G. Sharma, A. Modgil, T. Zhong, C. Sun, and J. Singh, "Influence of short-chain cell-penetrating peptides on transport of doxorubicin encapsulating receptor-targeted liposomes across brain endothelial barrier," *Pharmaceutical research,* vol. 31, pp. 1194-1209, 2014.

[111] Y. Bi, F. Hao, G. Yan, L. Teng, R. J Lee, and J. Xie, "Actively Targeted Nanoparticles for Drug Delivery to Tumor," *Current Drug Metabolism,* vol. 17, pp. 763-782, 2016.

[112] G. Abrego, H. Alvarado, E. B. Souto, B. Guevara, L. H. Bellowa, M. L. Garduño*, et al.*, "Biopharmaceutical profile of hydrogels containing pranoprofen-loaded PLGA nanoparticles for skin administration: In vitro, ex vivo and in vivo characterization," *International journal of pharmaceutics,* vol. 501, pp. 350-361, 2016.

[113] K. G. Neoh, S. Lu, E.-T. Kang, R. Mahendran, and E. Chiong, "Tailoring Soft Nanoparticles for Potential Application as Drug Carriers in Bladder Cancer Chemotherapy," in *Nanotechnology: Delivering on the Promise Volume 2*, ed: ACS Publications, 2016, pp. 167-195.

[114] H. Lin, Y. Yue, D. E. Maidana, P. Bouzika, A. Atik, H. Matsumoto*, et al.*, "Drug Delivery Nanoparticles: Toxicity Comparison in Retinal Pigment Epithelium and Retinal Vascular Endothelial Cells," in *Seminars in ophthalmology*, 2016, pp. 1-9.

[115] S. Jose, B. Juna, T. Cinu, H. Jyoti, and N. Aleykutty, "Carboplatin loaded Surface modified PLGA nanoparticles: Optimization, characterization, and in vivo brain targeting studies," *Colloids and Surfaces B: Biointerfaces,* vol. 142, pp. 307-314, 2016.

[116] G. Ma, C. Zhang, L. Zhang, H. Sun, C. Song, C. Wang*, et al.*, "Doxorubicin-loaded micelles based on multiarm star-shaped PLGA–PEG block copolymers: influence of arm numbers on drug delivery," *Journal of Materials Science: Materials in Medicine,* vol. 27, pp. 1-15, 2016.

[117] C. Saraiva, C. Praça, R. Ferreira, T. Santos, L. Ferreira, and L. Bernardino, "Nanoparticle-mediated brain drug delivery: Overcoming blood–brain barrier to treat neurodegenerative diseases," *Journal of Controlled Release,* vol. 235, pp. 34-47, 2016.

[118] L. Zou, F. Chen, J. Bao, S. Wang, L. Wang, M. Chen*, et al.*, "Preparation, characterization, and anticancer efficacy of evodiamine-loaded PLGA nanoparticles," *Drug delivery,* vol. 23, pp. 898-906, 2016.

[119] J. Trousil, S. K. Filippov, M. Hrubý, T. Mazel, Z. Syrová, D. Cmarko*, et al.*, "System with embedded drug release and nanoparticle degradation sensor showing efficient rifampicin delivery into macrophages," *Nanomedicine: Nanotechnology, Biology and Medicine,* 2016.

[120] R. P. Friedrich, M. Pöttler, I. Cicha, S. Lyer, C. Janko, and C. Alexiou, "Novel nanoparticulate drug delivery systems," *Nanomedicine,* vol. 11, pp. 573-576, 2016.

[121] Y. T. Ho, B. Poinard, and J. C. Y. Kah, "Nanoparticle drug delivery systems and their use in cardiac tissue therapy," *Nanomedicine,* vol. 11, pp. 693-714, 2016.

[122] D. Dehaini, R. H. Fang, B. T. Luk, Z. Pang, C.-M. J. Hu, A. V. Kroll*, et al.*, "Ultra-small lipid–polymer hybrid nanoparticles for tumor-penetrating drug delivery," *Nanoscale,* vol. 8, pp. 14411-14419, 2016.

[123] Q. Zhang, J. Li, W. Gao, and L. Zhang, "Nanoparticles for Ocular Drug Delivery," in *Ophthalmic Disease Mechanisms and Drug Discovery*, ed: World Scientific, 2016, pp. 197-223.

[124] A. D. Kulkarni, H. M. Patel, S. J. Surana, V. S. Belgamwar, and C. V. Pardeshi, "Brain–blood ratio: implications in brain drug delivery," *Expert opinion on drug delivery,* vol. 13, pp. 85-92, 2016.

[125] W. Gao, Y. Zhang, Q. Zhang, and L. Zhang, "Nanoparticle-Hydrogel: A Hybrid Biomaterial System for Localized Drug Delivery," *Annals of biomedical engineering,* pp. 1-13, 2016.

[126] R. Meng, K. Li, Z. Chen, and C. Shi, "Multilayer Coating of Tetrandrine-loaded PLGA nanoparticles: Effect of surface charges on cellular uptake rate and drug release profile," *Journal of Huazhong University of Science and Technology [Medical Sciences],* vol. 36, pp. 14-20, 2016.

[127] I. Posadas, S. Monteagudo, and V. Ceña, "Nanoparticles for brain-specific drug and genetic material delivery, imaging and diagnosis," *Nanomedicine,* vol. 11, pp. 833-849, 2016.

[128] J. Emami, H. Hamishehkar, A. R. Najafabadi, K. Gilani, M. Minaiyan, H. Mahdavi*, et al.*, "Particle size design of PLGA microspheres for potential pulmonary drug delivery using response surface methodology," *Journal of microencapsulation,* vol. 26, pp. 1-8, 2009.

[129] A. S. Lübbe, C. Alexiou, and C. Bergemann, "Clinical applications of magnetic drug targeting," *Journal of Surgical Research,* vol. 95, pp. 200-206, 2001.

[130] S. E. Bae, J. S. Son, K. Park, and D. K. Han, "Fabrication of covered porous PLGA microspheres using hydrogen peroxide for controlled drug delivery and regenerative medicine," *Journal of Controlled Release,* vol. 133, pp. 37-43, 2009.

[131] K. Brodbeck, J. DesNoyer, and A. McHugh, "Phase inversion dynamics of PLGA solutions related to drug delivery: Part II. The role of solution thermodynamics and bath-side mass transfer," *Journal of Controlled Release,* vol. 62, pp. 333-344, 1999.

[132] P. Graham, K. Brodbeck, and A. McHugh, "Phase inversion dynamics of PLGA solutions related to drug delivery," *Journal of Controlled Release,* vol. 58, pp. 233-245, 1999.

[133] K. Iwasaki, Y. Osaka, S. Tachibana, T. Suda, Y. Ota, S. Hoshino*, et al.*, "Phase I Study of Docetaxel, Cisplatin, and 5-Fluorouracil Chemoradiotherapy for Local or Metastatic Esophageal Cancer," *Anticancer research,* vol. 36, pp. 987-994, 2016.

[134] F. Ramazani, C. F. van Nostrum, G. Storm, F. Kiessling, T. Lammers, W. E. Hennink*, et al.*, "Locoregional cancer therapy using polymer-based drug depots," *Drug discovery today,* vol. 21, pp. 640-647, 2016.

[135] F. Ramazani, W. Chen, C. F. van Nostrum, G. Storm, F. Kiessling, T. Lammers*, et al.*, "Strategies for encapsulation of small hydrophilic and amphiphilic drugs in PLGA microspheres: state-of-the-art and challenges," *International journal of pharmaceutics,* vol. 499, pp. 358-367, 2016.

[136] A. C. de Mattos, C. Altmeyer, T. T. Tominaga, N. M. Khalil, and R. M. Mainardes, "Polymeric nanoparticles for oral delivery of 5-fluorouracil: Formulation optimization, cytotoxicity assay and pre-clinical pharmacokinetics study," *European Journal of Pharmaceutical Sciences,* vol. 84, pp. 83-91, 2016.

[137] S. Egodawatte, S. Dominguez, and S. C. Larsen, "Solvent effects in the development of a drug delivery system for 5-fluorouracil using magnetic mesoporous silica nanoparticles," *Microporous and Mesoporous Materials,* vol. 237, pp. 108-116, 2017.

[138] C. Shi, P. Liu, X. Liu, X. Feng, and D. Fu, "The effects of mPEG proportion and LA/GA ratio on degradation and drug release behaviors of PLGA-mPEG microparticles," *Die Pharmazie-An International Journal of Pharmaceutical Sciences,* vol. 71, pp. 243-246, 2016.

[139] G. Amasya, U. Badilli, B. Aksu, and N. Tarimci, "Quality by design case study 1: Design of 5-fluorouracil loaded lipid nanoparticles by the W/O/W double emulsion—Solvent evaporation method," *European Journal of Pharmaceutical Sciences,* vol. 84, pp. 92-102, 2016.

[140] R. S. Gelman and S. Taylor, "Cyclophosphamide, methotrexate, and 5-fluorouracil chemotherapy in women more than 65 years old with advanced breast cancer: the

elimination of age trends in toxicity by using doses based on creatinine clearance," *Journal of Clinical Oncology,* vol. 2, pp. 1404-1413, 1984.

[141] D. B. Longley, D. P. Harkin, and P. G. Johnston, "5-fluorouracil: mechanisms of action and clinical strategies," *Nature Reviews Cancer,* vol. 3, pp. 330-338, 2003.

[142] P. Menei, M. Boisdron-Celle, A. Croué, G. Guy, and J.-P. Benoit, "Effect of stereotactic implantation of biodegradable 5-fluorouracil-loaded microspheres in healthy and C6 glioma-bearing rats," *Neurosurgery,* vol. 39, pp. 117-123, 1996.

[143] P. Menei, E. Jadaud, N. Faisant, M. Boisdron-Celle, S. Michalak, D. Fournier*, et al.*, "Stereotaxic implantation of 5-fluorouracil-releasing microspheres in malignant glioma," *Cancer,* vol. 100, pp. 405-410, 2004.

[144] P. Menei, M. C. Venier, E. Gamelin, J. P. Saint-André, G. Hayek, E. Jadaud*, et al.*, "Local and sustained delivery of 5-fluorouracil from biodegradable microspheres for the radiosensitization of glioblastoma," *Cancer,* vol. 86, pp. 325-330, 1999.

[145] L. Nair, S. Jagadeeshan, S. A. Nair, and G. V. Kumar, "Biological evaluation of 5-fluorouracil nanoparticles for cancer chemotherapy and its dependence on the carrier, PLGA," *International journal of nanomedicine,* vol. 6, p. 1685, 2011.

[146] G. Winocur, J. Vardy, M. A. Binns, L. Kerr, and I. Tannock, "The effects of the anti-cancer drugs, methotrexate and 5-fluorouracil, on cognitive function in mice," *Pharmacology Biochemistry and Behavior,* vol. 85, pp. 66-75, 2006.

[147] A. K. Yadav, A. Agarwal, G. Rai, P. Mishra, S. Jain, A. K. Mishra*, et al.*, "Development and characterization of hyaluronic acid decorated PLGA nanoparticles for delivery of 5-fluorouracil," *Drug delivery,* vol. 17, pp. 561-572, 2010.

[148] T. R. Groves, R. Farris, J. E. Anderson, T. C. Alexander, F. Kiffer, G. Carter*, et al.*, "5-Fluorouracil chemotherapy upregulates cytokines and alters hippocampal dendritic complexity in aged mice," *Behavioural Brain Research,* vol. 316, pp. 215-224, 2017.

[149] L. Theodoro, M. Longo, E. Ervolino, C. Duque, M. Ferro-Alves, N. Assem*, et al.*, "Effect of low-level laser therapy as an adjuvant in the treatment of periodontitis induced in rats subjected to 5-fluorouracil chemotherapy," *Journal of periodontal research,* 2016.

[150] X. Wu, C. He, Y. Wu, and X. Chen, "Synergistic therapeutic effects of Schiff's base cross-linked injectable hydrogels for local co-delivery of metformin and 5-fluorouracil in a mouse colon carcinoma model," *Biomaterials,* vol. 75, pp. 148-162, 2016.

[151] R. Han, Y. Sun, C. Kang, H. Sun, and W. Wei, "Amphiphilic dendritic nanomicelle-mediated co-delivery of 5-fluorouracil and doxorubicin for enhanced therapeutic efficacy," *Journal of Drug Targeting,* pp. 1-9, 2016.

[152] H. Luo, D. Ji, C. Li, Y. Zhu, G. Xiong, and Y. Wan, "Layered nanohydroxyapatite as a novel nanocarrier for controlled delivery of 5-fluorouracil," *International Journal of Pharmaceutics,* vol. 513, pp. 17-25, 2016.

[153] H. Hashemi-Moghaddam, S. Kazemi-Bagsangani, M. Jamili, and S. Zavareh, "Evaluation of magnetic nanoparticles coated by 5-fluorouracil imprinted polymer for controlled drug delivery in mouse breast cancer model," *International journal of pharmaceutics,* vol. 497, pp. 228-238, 2016.

[154] S. De Luca, P. Seal, D. Ouyang, H. S. Parekh, S. K. Kannam, and S. C. Smith, "Dynamical Interactions of 5-Fluorouracil Drug with Dendritic Peptide Vectors: The Impact of Dendrimer Generation, Charge, Counter-Ions and Structured Water," *The Journal of Physical Chemistry B,* 2016.

[155] S. Kumar and V. R. Sinha, "Design, Development and Characterization of Topical Microemulsions of 5-Fluorouracil for the Treatment of Non Melanoma Skin Cancer and its Precursor Lesions," *Anti-Cancer Agents in Medicinal Chemistry (Formerly Current Medicinal Chemistry-Anti-Cancer Agents),* vol. 16, pp. 259-268, 2016.

[156] S. Liu, J. Zhang, X. Cui, Y. Guo, X. Zhang, and W. Hongyan, "Synthesis of chitosan-based nanohydrogels for loading and release of 5-fluorouracil," *Colloids and Surfaces A: Physicochemical and Engineering Aspects,* vol. 490, pp. 91-97, 2016.

[157] E. Catıker, M. Gümüşderelioğlu, and A. Güner, "Degradation of PLA, PLGA homo- and copolymers in the presence of serum albumin: a spectroscopic investigation," *Polymer international,* vol. 49, pp. 728-734, 2000.

[158] F.-Y. Cheng, C.-H. Su, P.-C. Wu, and C.-S. Yeh, "Multifunctional polymeric nanoparticles for combined chemotherapeutic and near-infrared photothermal cancer therapy in vitro and in vivo," *Chemical communications,* vol. 46, pp. 3167-3169, 2010.

[159] Q. Cheng, M.-O. Blais, G. Harris, and E. Jabbarzadeh, "PLGA-carbon nanotube conjugates for intercellular delivery of caspase-3 into osteosarcoma cells," *PloS one,* vol. 8, p. e81947, 2013.

[160] H. S. Yoo, K. H. Lee, J. E. Oh, and T. G. Park, "In vitro and in vivo anti-tumor activities of nanoparticles based on doxorubicin–PLGA conjugates," *Journal of Controlled Release,* vol. 68, pp. 419-431, 2000.

[161] M. Stevanović, A. Radulović, B. Jordović, and D. Uskoković, "Poly (DL-lactide-co-glycolide) nanospheres for the sustained release of folic acid," *Journal of Biomedical Nanotechnology,* vol. 4, pp. 349-358, 2008.

[162] C. D. A. C. Erbetta, R. J. Alves, J. M. Resende, R. F. de Souza Freitas, and R. G. de Sousa, "Synthesis and characterization of poly (D, L-lactide-co-glycolide) copolymer," *Journal of Biomaterials and Nanobiotechnology,* vol. 3, p. 208, 2012.

[163] P. Blasi, A. Schoubben, S. Giovagnoli, L. Perioli, M. Ricci, and C. Rossi, "Ketoprofen poly (lactide-co-glycolide) physical interaction," *AAPS PharmSciTech,* vol. 8, pp. E78-E85, 2007.

[164] K. Fu, K. Griebenow, L. Hsieh, A. M. Klibanov, and R. Langera, "FTIR characterization of the secondary structure of proteins encapsulated within PLGA microspheres," *Journal of Controlled Release,* vol. 58, pp. 357-366, 1999.

[165] D. Edith and J.-L. Six, "Surface characteristics of PLA and PLGA films," *Applied Surface Science,* vol. 253, pp. 2758-2764, 2006.

[166] W. B. Parker and Y. C. Cheng, "Metabolism and mechanism of action of 5-fluorouracil," *Pharmacology & therapeutics,* vol. 48, pp. 381-395, 1990.

[167] I. C. Cojocaru, L. Ochiuz, A. Spac, G. Popa, L. Palade, and I. Popovici, "The validation of the UV spectrophotometric method for the assay of 5 fluorouracil," *FARMACIA,* vol. 60, pp. 379-385, 2012.

[168] S. Mitragotri and J. Lahann, "Physical approaches to biomaterial design," *Nature materials,* vol. 8, pp. 15-23, 2009.

[169] Y. Tabata and Y. Ikada, "Phagocytosis of polymer microspheres by macrophages," in *New Polymer Materials*, ed: Springer, 1990, pp. 107-141.

[170] S. Stolnik, L. Illum, and S. Davis, "Long circulating microparticulate drug carriers," *Advanced Drug Delivery Reviews,* vol. 16, pp. 195-214, 1995.

[171] H. Goldsmith and V. Turitto, "Rheological aspects of thrombosis and haemostasis: basic principles and applications. ICTH-Report-Subcommittee on Rheology of the International Committee on Thrombosis and Haemostasis," *Thrombosis and haemostasis,* vol. 55, pp. 415-435, 1986.

[172] V. R. S. Patil, C. J. Campbell, Y. H. Yun, S. M. Slack, and D. J. Goetz, "Particle diameter influences adhesion under flow," *Biophysical Journal,* vol. 80, pp. 1733-1743, 2001.

[173] A. Lamprecht, U. Schäfer, and C.-M. Lehr, "Size-dependent bioadhesion of micro-and nanoparticulate carriers to the inflamed colonic mucosa," *Pharmaceutical research,* vol. 18, pp. 788-793, 2001.

[174] S. M. Masloub, M. H. Elmalahy, D. Sabry, W. S. Mohamed, and S. H. Ahmed, "Comparative evaluation of PLGA nanoparticle delivery system for 5-fluorouracil and curcumin on squamous cell carcinoma," *Archives of oral biology,* vol. 64, pp. 1-10, 2016.

[175] E. Tawfik, M. Ahamed, A. Almalik, M. Alfaqeeh, and A. Alshamsan, "Prolonged exposure of colon cancer cells to 5-fluorouracil nanoparticles improves its anticancer activity," *Saudi Pharmaceutical Journal,* 2016.

요 약 문

표적 지향성 약물 전달을 위한 5 Fluorouracil 함유된 2 차원 생분해성 마이크로로봇의 제작 및 성능평가

표적 지향성 약물 전달을 위한 의료용 체내 삽입형 마이크로로봇에 관한 연구는 기존의 절개 방식을 사용한 수술에 비해 비침습적이며 국소 부위 접근의 용이성 등의 장점을 보여주었다. 하지만 현재 체내 삽입형 마이크로로봇에 관한 연구는 국내외적으로 정밀 제어 및 이동에 관한 연구에 초점을 맞추고 있으며, 실제 암과 같은 병들을 진단 및 치료를 하기 위해서는 특정 재료의 연구 및 추가 기능들의 연구가 시급하다. 그러나 지금까지 개발된 표적 지향성 약물 전달을 위한 마이크로로봇은 공정 및 재료의 한계점으로 인해 특정 부위의 약물을 전달하기 위한 역할로서 마이크로로봇의 연구는 미미한 상태이다.

본 연구에서 표적 지향성 약물 전달을 위한 마이크로로봇을 개발하기 위해 미국 식품의약국(FDA) 에서 승인 받은 생분해성 고분자(PLGA)와 DNA 의 합성 저해 및 RNA 의 기능 장애를 유도하는 항암제(5 Fluorouracil)가 사용되었다. 본 공정에서는 폴리비닐알코올(PVA) 분말을 정제수와 함께 일정 비율(2 % (w/v))로 혼합하여 얇은 필름(30 μm)을 제작하였으며, 이 필름을 마이크로 UV 레이저 기계 가공 기술을 사용하여 마이크로 크기의 다양한 2 차원 패턴을 제조하였다. 제조된 다양한 2 차원 생분해성 마이크로 패턴(두께: 30 μm, 폭: 200 μm, 길이: 600 μm)은 유기용매제에 녹인 생분해성 고분자(PLGA), 항암제(5 Fluorouracil) 그리고 자성을 위한 다양한 농도의 철(Fe) 분말의 혼합물에 짧은 시간 코팅이 진행된다. 코팅된 마이크로로봇은 최종적으로 정제수에서 폴리비닐알코올(PVA)을 제거하는 과정을 거치며 완성된다.

제조가 완성된 표적 지향성 약물 전달을 위한 다양한 2 차원 마이크로로봇은 생분해성 고분자와 철 분말의 화학적 결합 및 구조를 측정하기 위한 실험이 진행되었으며, 또한 인체의 환경과 유사한 수용액 (Phosphate buffer saline; pH 7.4) 속에서 다양한 철 농도에 따른 병진 운동 실험 및 분해 실험을 진행하였다. 다양한 철의 농도는 마이크로로봇의 속도와 분해 실험에 영향을 미쳤으며, 그 결과 철의 농도 증가로 인해 빨라지는 속도와 늦어지는 분해 속도를 확인할 수 있었다.

표적 지향성 약물 전달을 위한 약물 방출 실험은 5 % (w/v)의 생분해성 고분자와 10 % (w/v)의 철 분말의 기반으로 제조된 마이크로로봇에 500 μM 농도의 항암제를 혼합하여 진행하였다. 본 실험은 6 주의 기간 동안 총 13 구간의 약물 방출 특성을 측정하며 정략적인 분석 결과를 보여주었다. 또한 약물 방출 실험이 진행된 2 일 구간에서 대략 50 %의 급격한 방출 결과를 보였으며 5 주 구간에서는 대략 90 %의 약물 방출을 확인할 수 있었다.

본 연구를 통하여 표적 지향성 약물 전달을 위한 의료용 마이크로 크기의 다양한 2 차원 생분해성 마이크로로봇의 제작이 성공적으로 가능하였으며, 생분해성 고분자(PLGA)와 항암제(5-FU)를 함께 혼합함으로써 추가적인 공정이 필요 없다는 것을 보였다. 또한 생분해성 고분자로 인해 체내에서 분해가 가능하며 자성으로 인해 외부의 자기장으로 정밀 제어가 성공적으로 가능함을 보였다. 그러므로 제조된 2 차원 생분해성 마이크로로봇은 국소 부위에 정확하게 접근하여, 장시간 지속적으로 체내에 약물을 전달할 수 있는 표적 지향성 약물 전달 시스템으로 응용할 수 있는 가능성을 보였다.

핵심어: Targeted drug delivery, Biodegradable microrobot, Electromagnetic actuation system, UV Laser micro machining, Poly (lactic-co-glycolic acid)

APPENDIX

Micro patterns using UV laser micro machine (ALM100; Sejoong Information Technology, Korea)

(1) Run Lantek's CAD / CAM program (Lantek Export, line).

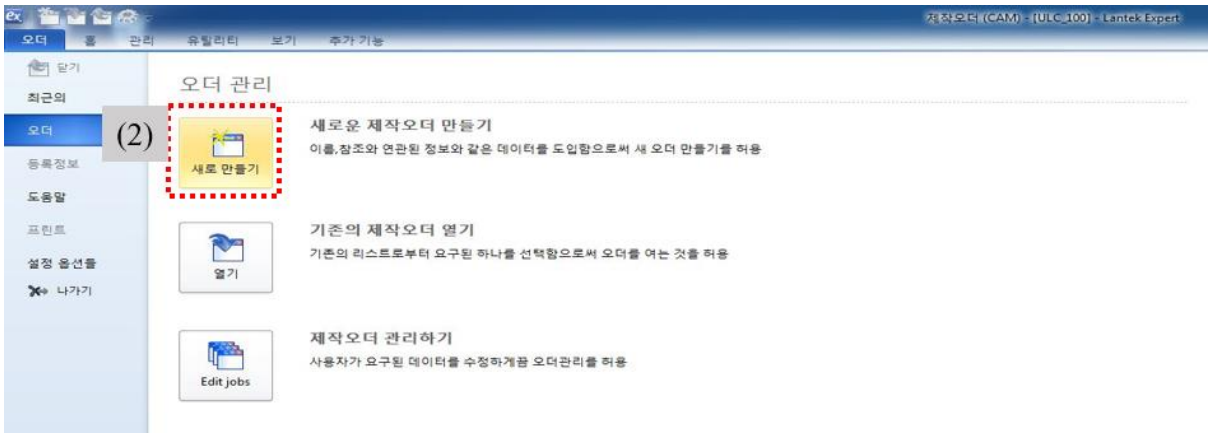

(2) Click create new order (line).

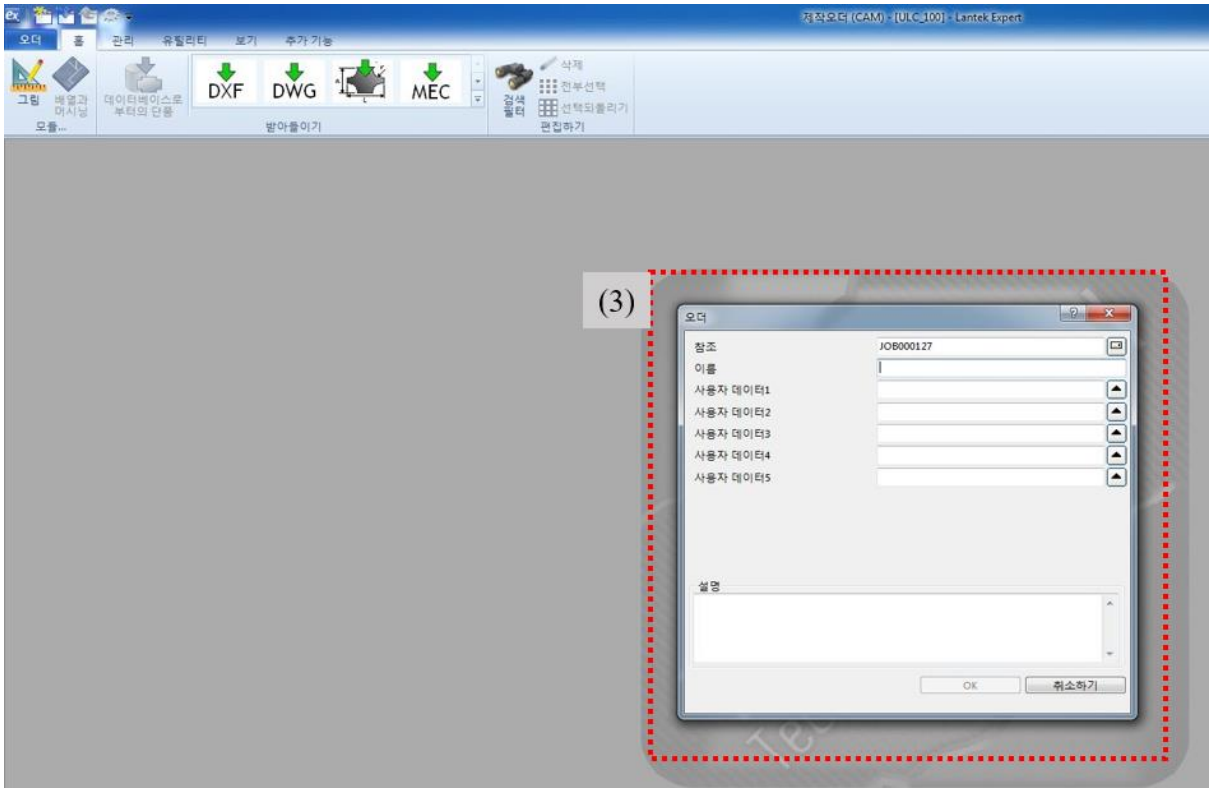

(3) Create new order (line).

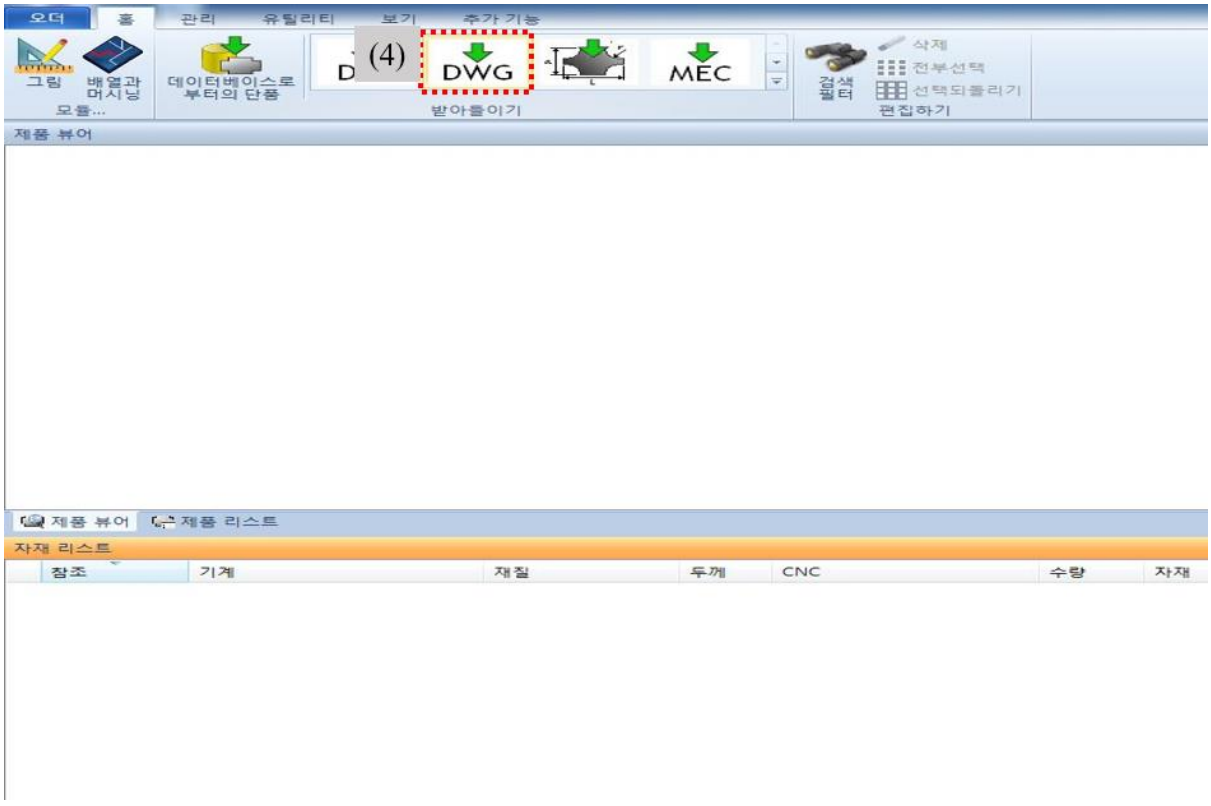

(4) Load your processing drawing (2D CAD file, line).

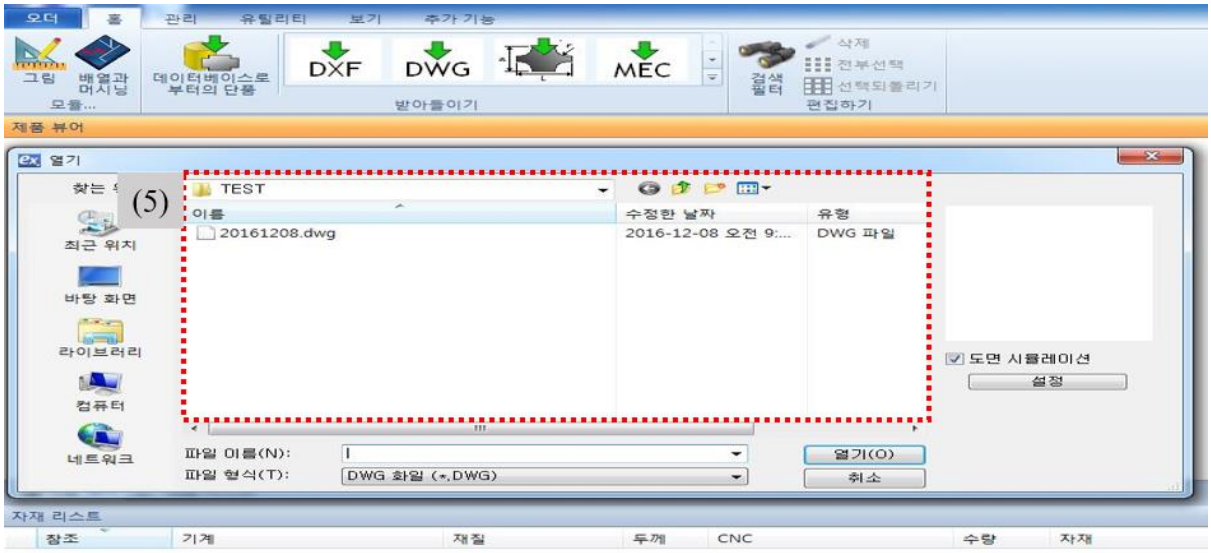

(5) Enter your drawing information (line).

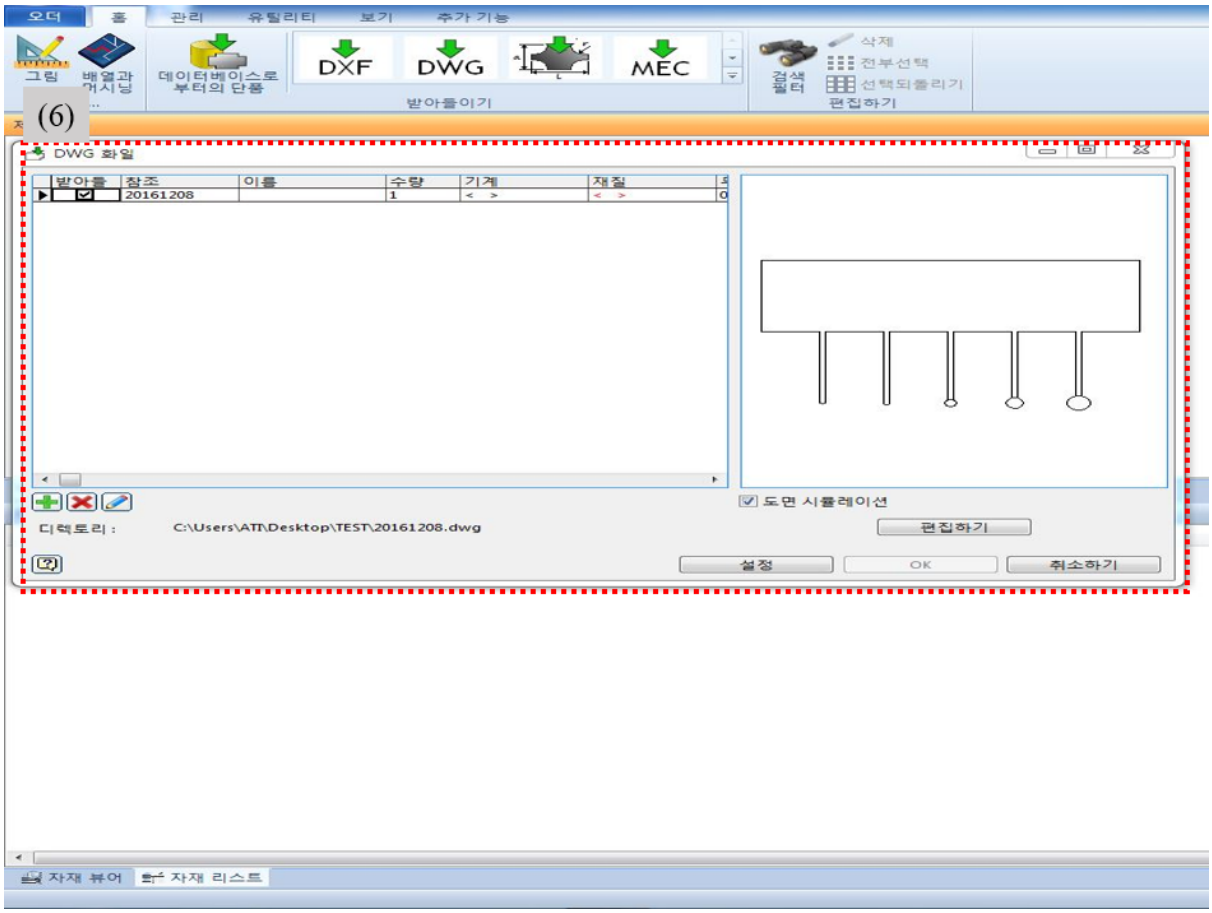

(6) Edit your drawing basic information (Name, Quantity, Material, Thickness) (line).

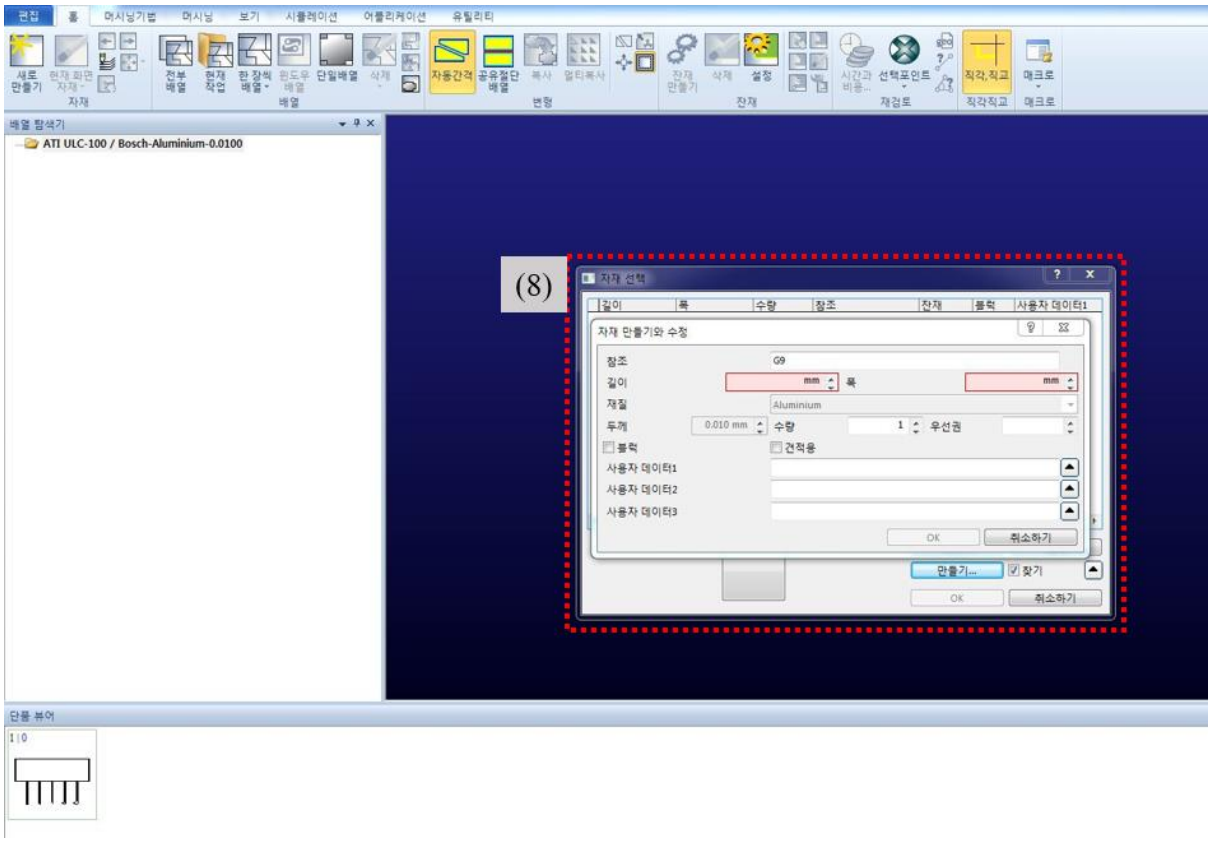

(7-8) Create material and create your new template (line).

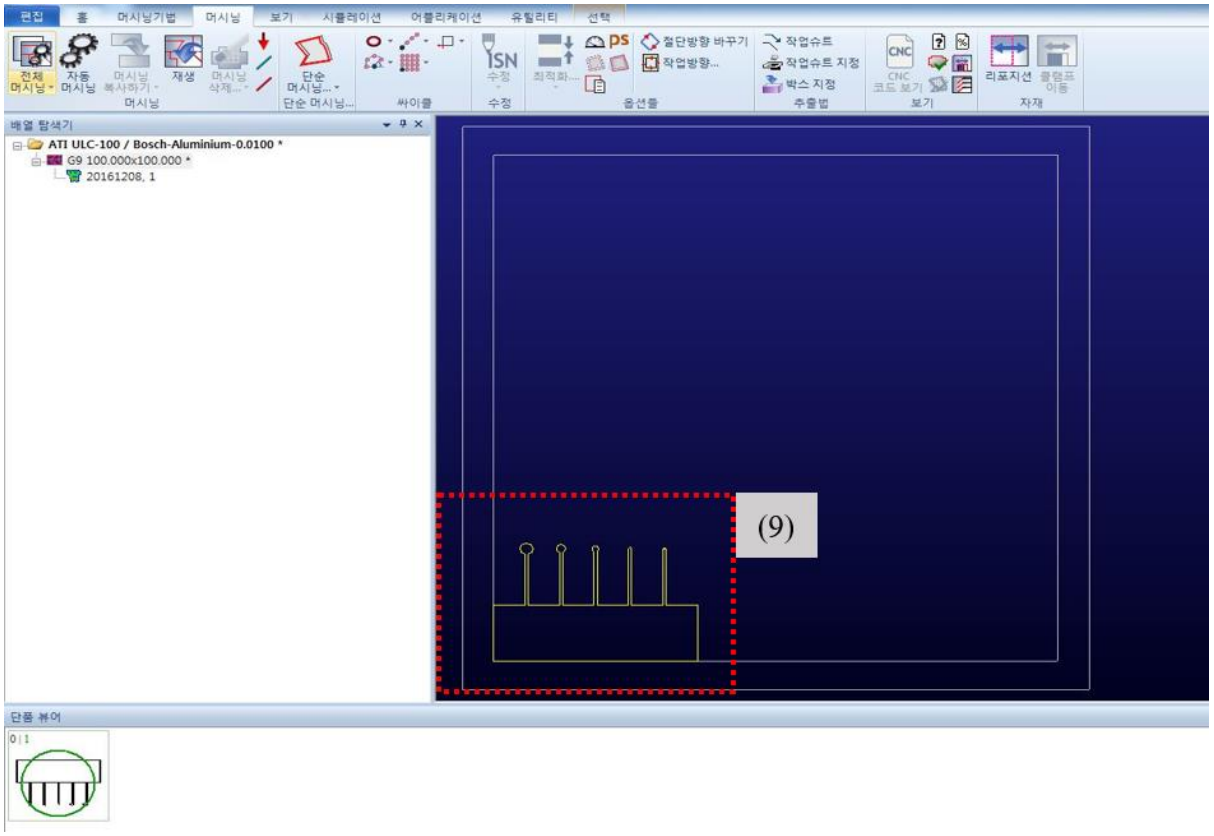

(9) Load the processing drawing on the created template (line).

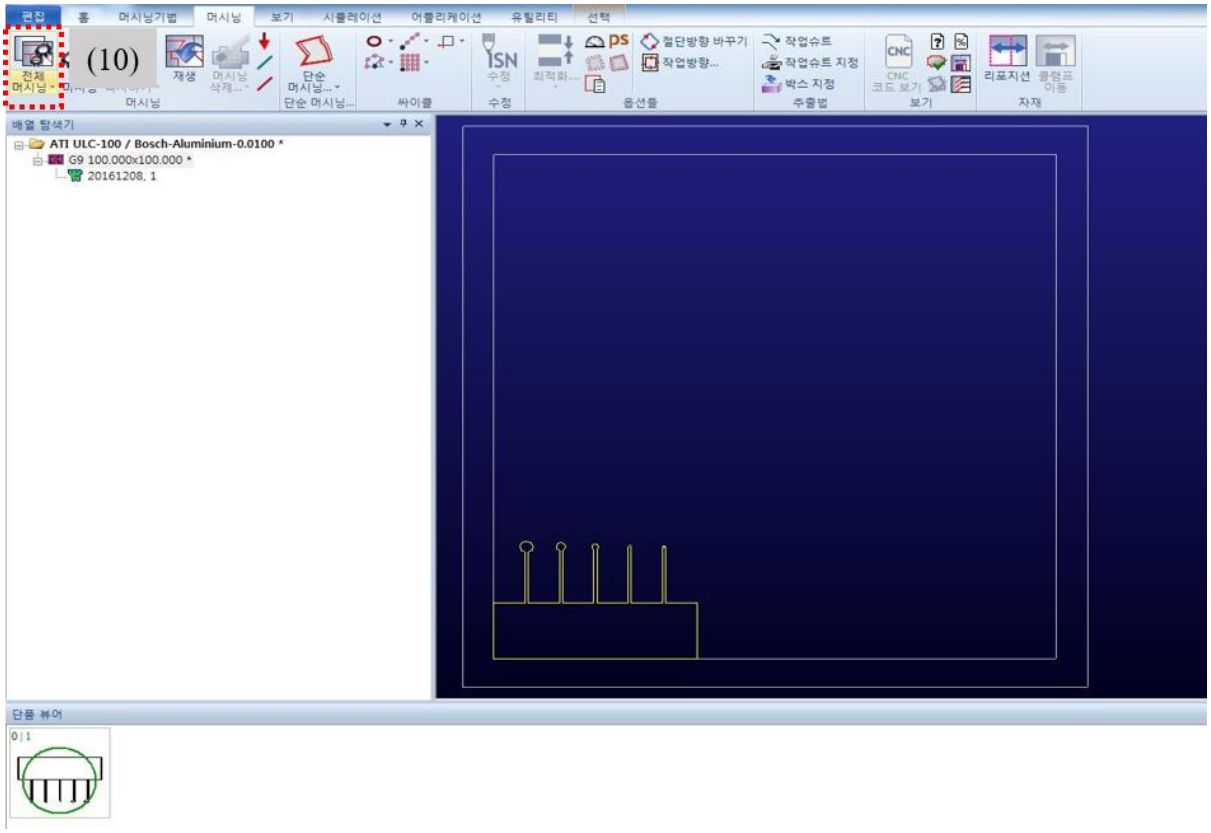

(10) Separate - Simple Machining (line).

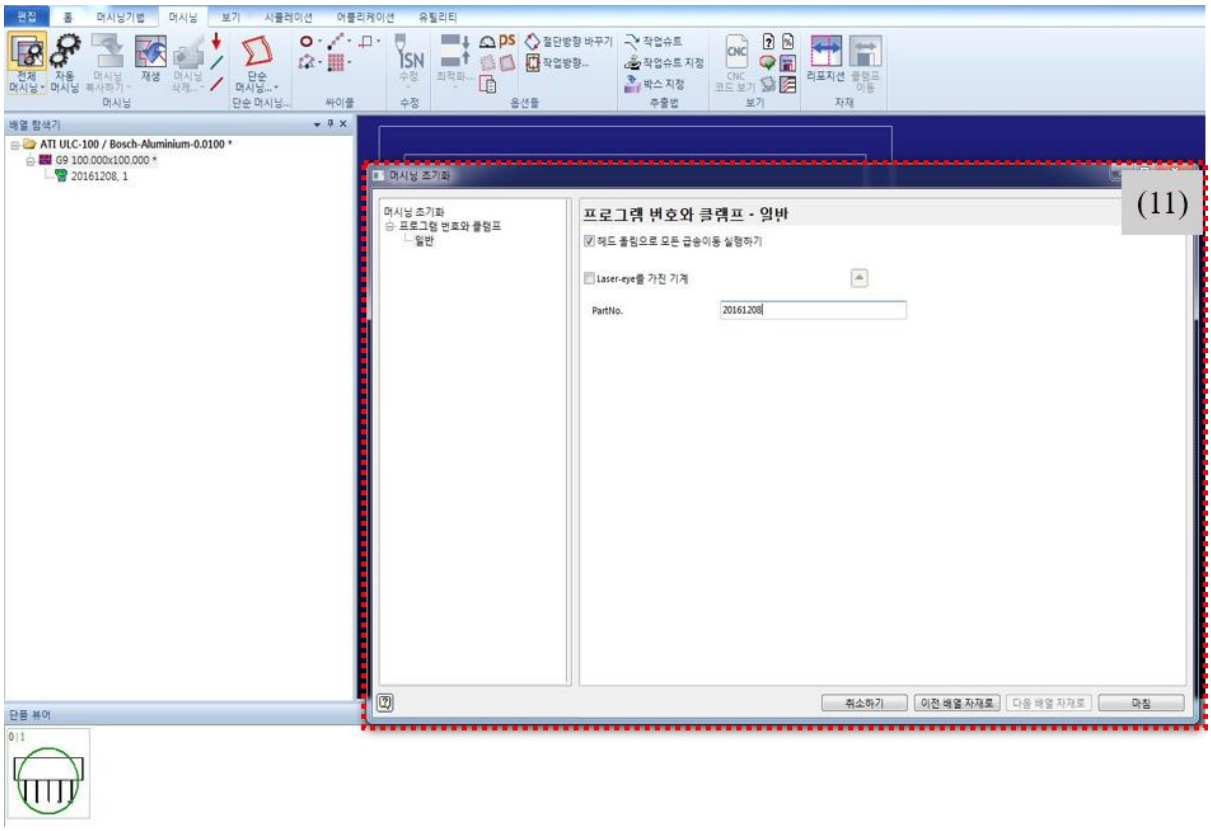

(11) Create your G-code name (line).

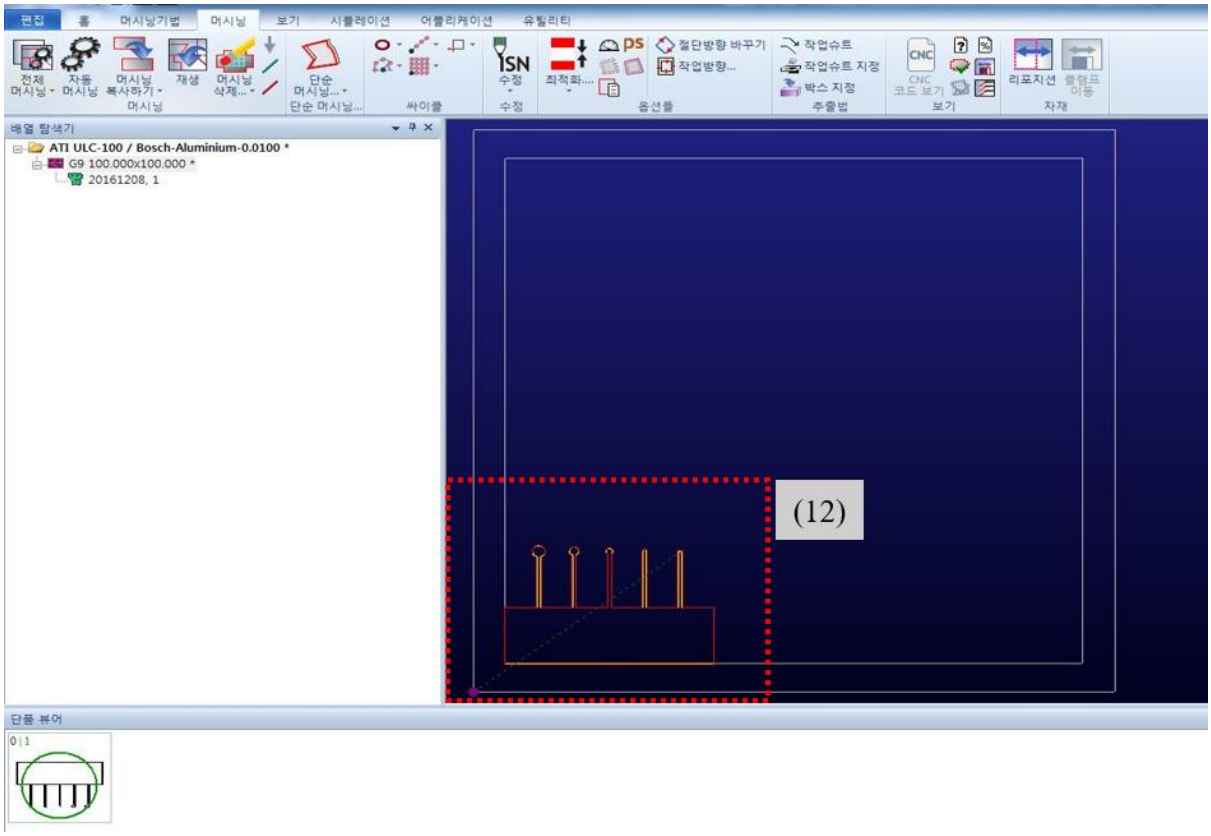

(12) Single piece machining selection (line)

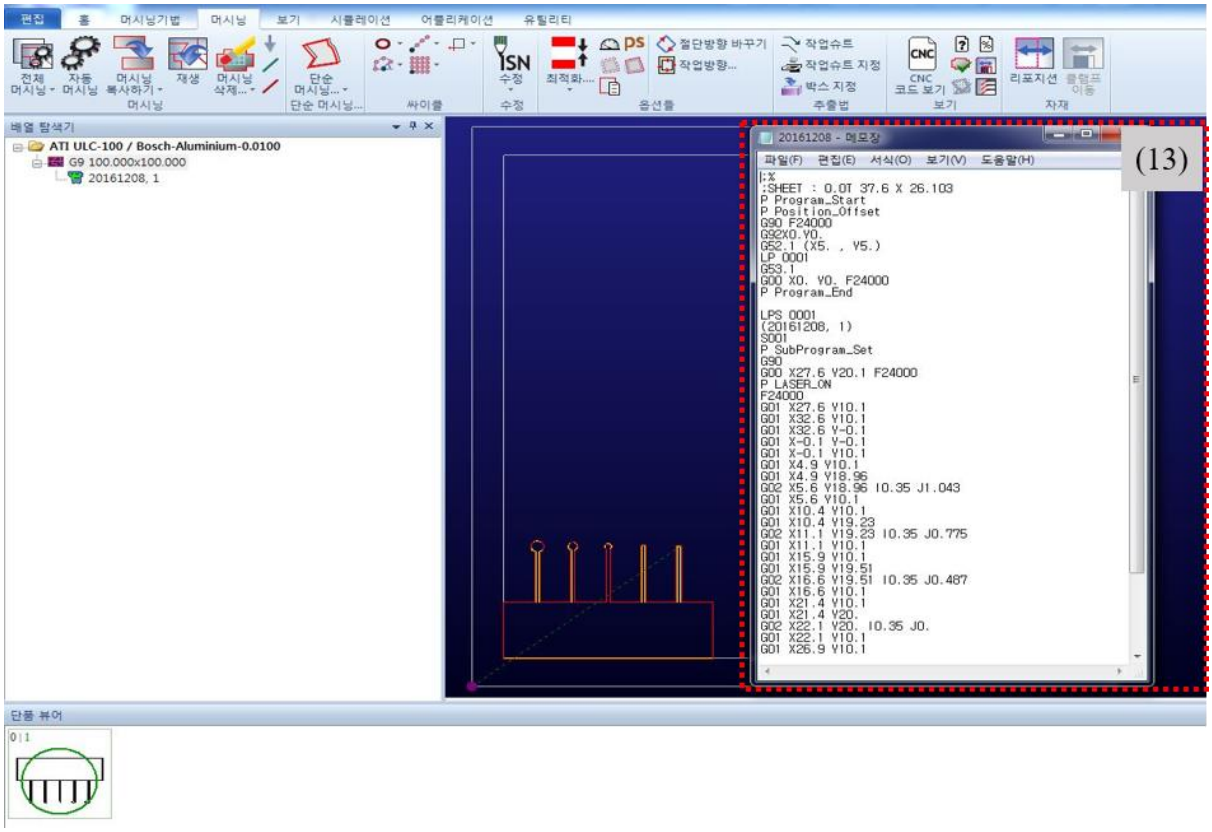

(13) Save file and check CNC G-code (line).

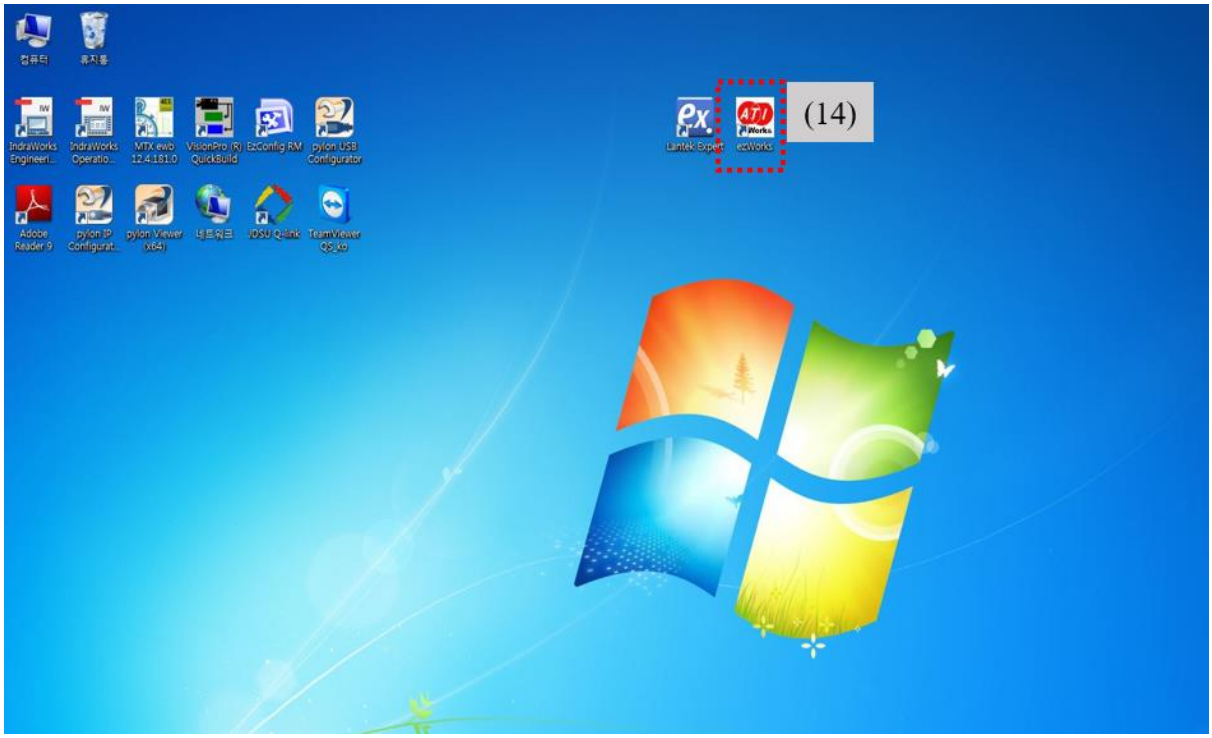

(14) Run ezWorks program (line).

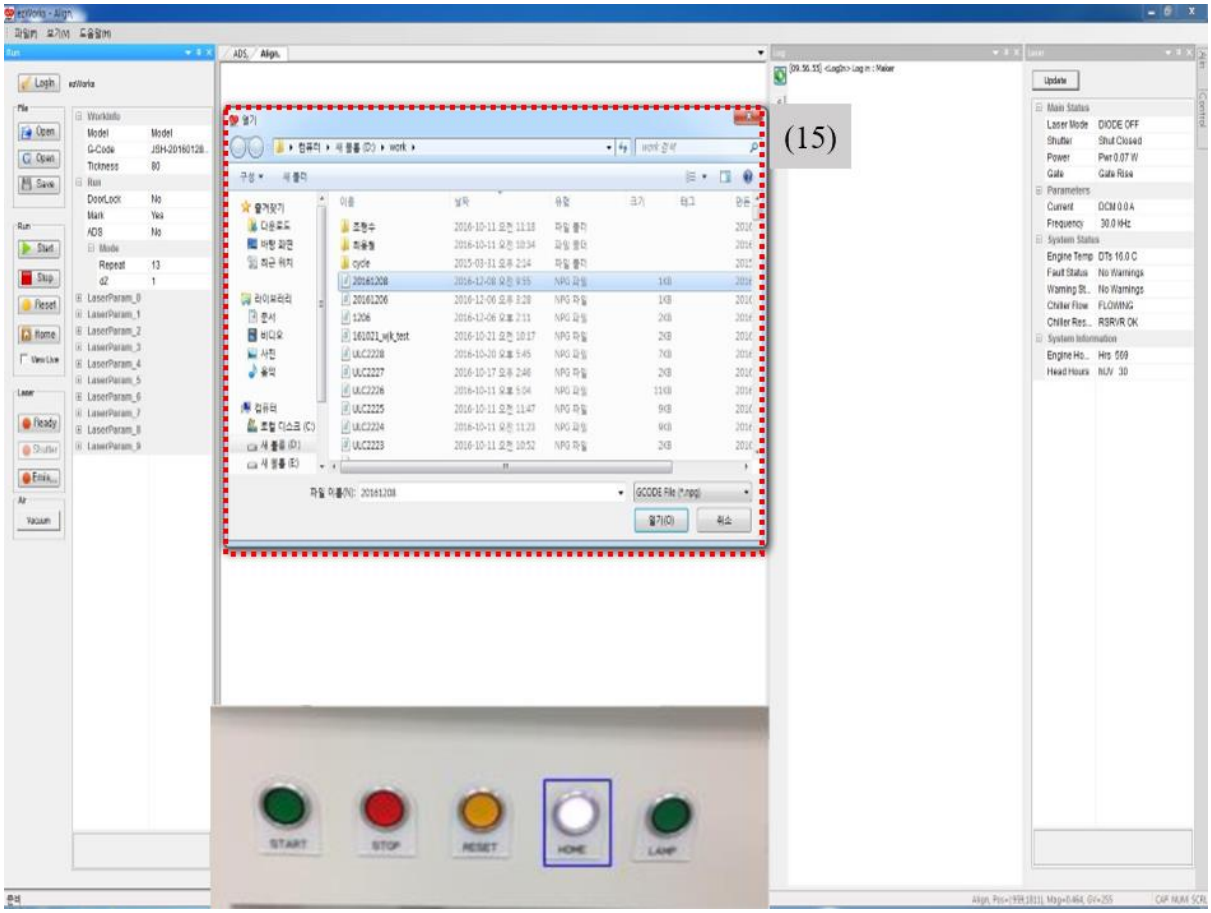

(15) Open master file and created G-Code (line).

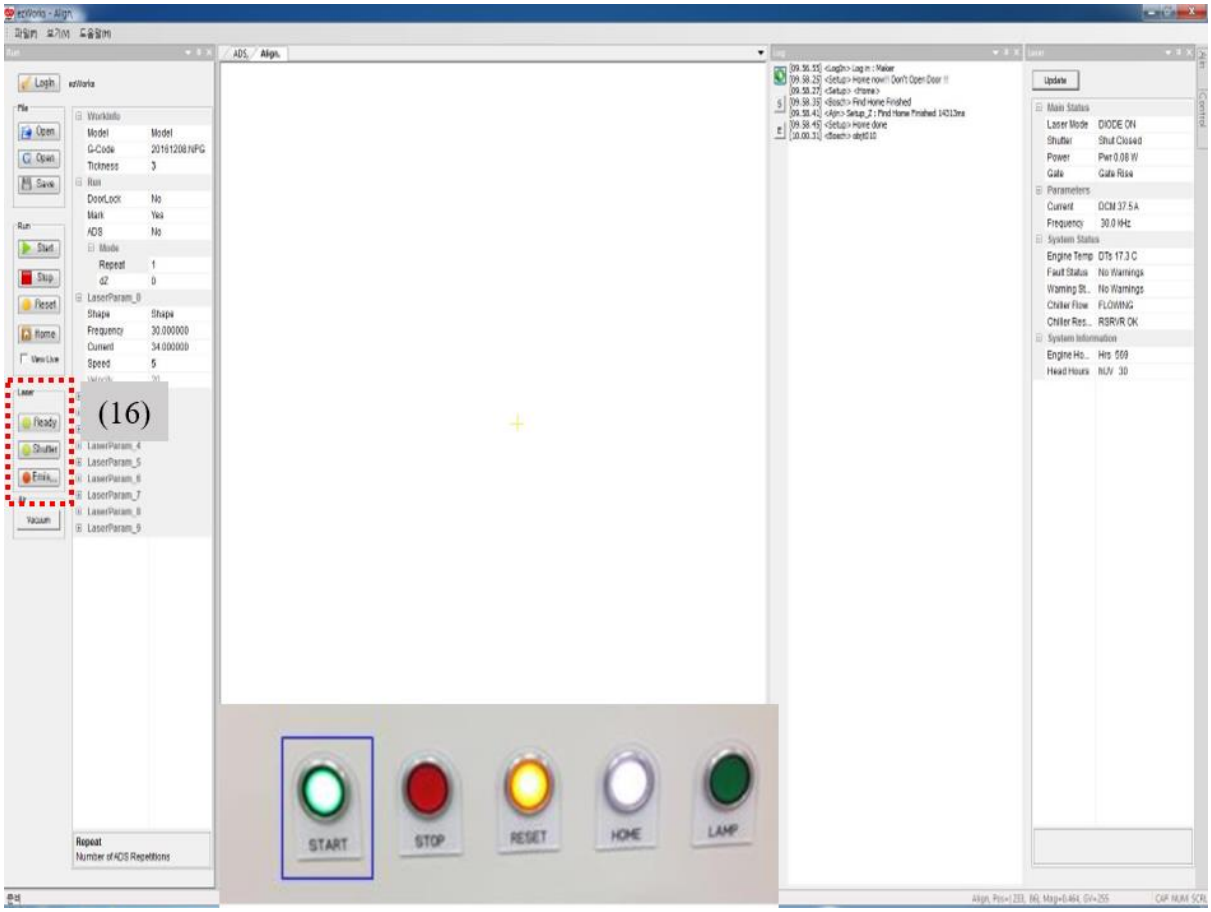

(16) Check laser status & start (line).